# Design of Communication Systems with Energy Harvesting Transmitters and Receivers

A Thesis

Submitted for the Degree of

## Doctor of Philosophy

in the Faculty of Engineering

by

## Mohit Kumar Sharma

Electrical Communication Engineering
Indian Institute of Science, Bangalore
Bangalore – 560 012 (INDIA)

May 2018

To

the memory of my Grandparents

*Smt. Barfi Devi and Sri. Natthi Lal Goswami*

# Acknowledgements

I consider myself lucky to have *Prof. Chandra R. Murthy* as my thesis advisor, whose commitment and dedication to work has been a great source of inspiration for me. He has been a very patient listener to all of my ideas. He was very kind in accommodating my impromptu meeting requests which were almost always met on the same day. I can't thank him enough for his constant support and guidance all throughout my formative years as a Ph.D. student. I am also highly grateful to my teachers in IISc for their excellent lectures which made it easy for me to understand complicated topics. I was very fortunate to have collaborations with *Prof. Rahul Vaze* from TIFR, Bombay, and *Prof. Marceau Coupechoux*, from Telecom ParisTech. I had several insightful discussions with *Prof. Vaze* on energy harvesting systems, and I am thankful to him for introducing me to the concept of uncoordinated communication between nodes. I would also like to thank *Prof. Coupechoux* for our discussions on device-to-device communication networks, and for providing me with the opportunity to work in his lab.

I would like to thank my colleagues *Adithya* and *Bala* for our collaborations. I had several interesting discussions with Adithya, even after he moved to University of Florida. He introduced me to new ideas which helped me immensely in my research work.

My lab-mates *Saurabh, Geethu, Parthajit, Venu, Abhay, Bharath, Ranjitha, Sireesha, Lekshmi, Sai, Ramu, Chethan, Ribhu, Akshay, Bala, Mohan, Sanjeev, Arun, Ashok, Gana* and *Suma* made my journey as a Ph. D. student highly enjoyable. I have learned a lot from each one of them. I greatly benefited from our Saturday group meetings and enjoyed the follow up coffee sessions. Also, I would like to thank *Shilpa, Jobin, Tirupathaiah, Bala, Sarvendra and Praveen* from Next Gen. Wireless lab for a variety of both technical as well as non-technical discussions. I would like to thank *Tarun* and *Karthik* for their help. I

# Abstract

An energy harvesting node (EHN) operates using the energy harvested from the environment, e.g., solar, piezoelectric and radio frequency, which presents the tantalizing possibility of perpetually operating of sensor nodes. However, the operation of an EHN is governed by the *energy neutrality constraint* (ENC), which makes it mandatory that, at any point in time, the total cumulative energy consumed by a node must not exceed the total cumulative energy harvested by it. Due to the random and sporadic nature of the harvested energy, energy management becomes the central issue in the optimization of energy harvesting (EH) communication systems. The design of energy management policies for the systems where only the transmitter is an EHN has been considered extensively in the literature. On the other hand, designing the policies for the networks where both the transmitter and receiver use harvested energy to operate is significantly more challenging, as aspects of coordination of the transmission attempts as well as nonzero decoding cost come into play. In this thesis, we present the design of energy management policies for a variety of scenarios where all nodes in a network are energy harvesting. The main contributions of this thesis are as follows:

- In the initial part of the thesis (Chapters 2-5), we present the design of packet drop probability (PDP)-optimal power control policies for retransmission-based multi-hop EH links where all the nodes are EHNs and the cost of decoding the data at the receiver is nonzero. In order to design the policies, we first derive *closed-form* PDP expressions for multi-hop EH links employing retransmission index based policies (RIPs) that are unaware of the state-of-charge (SoC) of the batteries at the nodes. Since the transmit power prescribed by an SoC-unaware RIP is independent of the current battery state, the RIPs obviate the need to measure the SoC of the battery. In practice, it is difficult to accurately measure the SoC of the battery,

and therefore this is an added benefit of the proposed policy.

- Using the derived PDP expressions, we formulate and solve a PDP optimization problem to obtain near-optimal RIPs. To design the SoC-unaware RIPs we use the notion of *energy unconstrained regime* (EUR), in which, the average energy consumed is less than the average energy harvested. We show that policies designed to operate in the EUR are near-optimal, even with finite sized energy buffers. This, in turn, allows us to replace the ENC in the PDP optimization problem with a single EUR constraint. This significantly simplifies the complexity of designing the optimal policies. We show that the RIPs obtained under EUR constraints are near-optimal and achieve the lower bound on the PDP. Moreover, these policies can be implemented in a distributed fashion.

- In the later part of the thesis (Chapter 6), we investigate impact of lack of coordination between the transmitter and receiver, i.e., when the transmitter (receiver) does not have the information about the SoC of the battery at the receiver (transmitter). The lack of coordination leads to the wastage of energy when, in a slot, only the transmitter (or receiver) is on. The goal here is to maximize the throughput between a transmitter and receiver without any explicit coordination, and only using the statistical information about the energy arrivals at both the nodes. We derive a genie-aided upper bound on the throughput achievable, by analyzing a system that has non-causal knowledge of energy arrivals. Next, we present an online, distributed energy management policy which achieves the throughput within a gap of one bit from the upper bound and requires an occasional one bit feedback. The above policy is modified to obtain a time-dilated policy which achieves the upper bound asymptotically, with the battery size at both the nodes. We also propose a near-optimal, deterministic, fully uncoordinated policy which requires no feedback from the receiver. Our simulation results confirm the theoretical findings and illustrate the trade-offs between system parameters. The policies presented here not only achieve the upper bound but are also simple to implement. Our policies allow the nodes to operate in a truly uncoordinated fashion which, in turn, completely removes the overhead in the feedback.

# Glossary

| | | |
|------|---|------|
| ACK | : | Acknowledgment |
| ARQ | : | Automatic Repeat Request |
| AWGN | : | Additive White Gaussian Noise |
| CGP | : | Complementary GP |
| CSI | : | Channel State Information |
| CSWP | : | Coordinated Sleep-Wake Protocol |
| DTMC | : | Discrete Time Markov Chain |
| EC | : | End Communication |
| EH | : | Energy Harvesting |
| EHN | : | Energy Harvesting Node |
| ENC | : | Energy Neutrality Constraint |
| EPP | : | Equal Power Policy |
| EUR | : | Energy Unconstrained Regime |
| GP | : | Geometric Program |
| HARQ-CC | : | Hybrid ARQ with Chase Combining |
| HARQ-IR | : | Hybrid ARQ with Incremental Redundancy |
| IPM | : | Interior Point Method |
| JTBP | : | Joint Threshold based Policy |
| KKT | : | Karush-Kuhn-Tucker |
| LHS | : | Left Hand Side |
| MDP | : | Markov Decision Process |
| MGF | : | Moment Generating Function |
| MRC | : | Maximal Ratio Combining |
| NMINLP | : | Nonconvex Mixed Integer Nonlinear Program |
| NACK | : | Negative Acknowledgment |
| PDP | : | Packet Drop Probability |
| POMDP | : | Partially Observable MDP |
| RIP | : | Retransmission-index based Policy |
| SC | : | Start Communication |
| SoC | : | State-of-charge |
| RHS | : | Right Hand Side |
| SNR | : | Signal-to-Noise Ratio |
| TPM | : | Transition Probability Matrix |

# Contents

# List of Figures

ix

# List of Tables

# Chapter 1

# Introduction

The next generation wireless networks aim to provide connectivity to massive number of low power sensors deployed to collect the data for monitoring and surveillance. Often, these nodes operate with a *pre-charged* battery which needs to be charged or replaced periodically. Several applications, such as structural health monitoring, require the sensors to be deployed at places that are not easily accessible. Hence, the lifetime of a sensor is limited by the battery attached to it which, in turn, also limits the lifespan of the entire network [3]. The energy harvesting (EH) technology circumvents this problem, as an EH sensor can harvest the energy from the environment, e.g., from a solar, wind, piezoelectric or radio frequency source [4,5], and can operate perpetually. In contrast to conventional communication systems where the energy available is constant yet limited, the energy harvested from the environment is generally time-varying. Hence, the performance guarantees and the design methods developed for the conventional communication systems are not be directly applicable to the network with EH nodes (EHNs), which poses a unique design challenge. Using a battery or super-capacitor to store the harvested energy an EHN can mitigate the time-variations of the EH process.

The operation of an EHN, powered using harvested energy only, is governed by the energy conservation principle which requires that, at any time, the cumulative energy consumed by a node can not exceed the total amount of energy harvested by it up to that time. This fundamental constraint is termed as the *energy neutrality constraint* (ENC), and can be mathematically expressed as follows, for a time-slotted system:

$$\sum_{n=1}^{N} e_n \leq \sum_{n=1}^{N} \mathcal{E}_n, \tag{1.1}$$

for all $N$, where $n$ is the slot index. In the above, $e_n$ and $\mathcal{E}_n$ denote the amount of energy consumed and harvested in the $n^{\text{th}}$ slot, respectively. Moreover, the maximum amount of energy an EHN can use is equal to the energy stored in the battery, and the maximum stored energy is limited by the size of the battery. Hence, the battery evolution over time is governed by

$$B_{n+1} = \min\{\{B_n + \mathcal{E}_n - e_n\}^+, B_{\max}\}, \tag{1.2}$$

where $B_n$ and $B_{\max}$ denote the amount of energy stored and the size of the battery, respectively, and $\{x\}^+ \triangleq \max\{0, x\}$. In the light of the above constraints, to realize the design of EH networks the following challenges need to be addressed:

1. *Design of energy management policies*: Due to the temporal variations of the harvested energy, and constraints (1.1) and (1.2), the design of an energy management policy (a decision rule which determines the value $e_n$ for each $n$) is important in the design of EH communication systems. For example, a policy with aggressive energy consumption will lead to frequent energy outages, i.e., the battery gets empty, which results in missed transmission opportunities. On the other hand, a

conservative policy may lead to frequent energy overflows, due to battery being full, and wastage of harvested energy. In addition to the time-variations in the EH process, an energy management policy need to deal with the time-variations of the wireless channel also, which makes the design challenging.

2. *Determining fundamental limits*: Since the design of communication among energy harvesting nodes represents a fundamental paradigm shift, the fundamental performance limits for EH communication systems are not known and need to be determined. Hence, another important issue is to derive the performance limits of the EH communication systems, and understand the trade-offs between different system parameters such as the harvesting statistics, battery capacity, channel fading characteristics, information available about the state of the battery and channel, etc.

In the literature, the above two issues have been studied under a variety of network settings and performance objectives. In the following paragraphs, we briefly review the literature, while also pointing out the key factors that affect the design of EH networks.

## 1.1 Factors affecting the design of EH networks

### 1.1.1 Battery size

In general, the performance of an EH system improves with increase in the battery size. Hence, the performance of an EH communication system where the nodes are equipped with ideal, infinite capacity batteries is an upper bound on the performance of a system finite capacity battery nodes. The finiteness of the battery capacity makes

the design and analysis of EH systems significantly more challenging. For instance, for a point-to-point link with an EH transmitter equipped with an infinite capacity battery communicating with a non-EH receiver, termed as mono-T EH links, over an AWGN channel, it is known that the information-theoretic capacity is equal to the capacity of a conventional AWGN channel operating under an average power constraint equal to the average rate of energy harvesting [6]. In contrast, determining the information-theoretic capacity of mono-T EH links with finite size battery is quite difficult hence only the approximate expressions and upper bounds for the capacity are available [7–9]. The design of energy management policies for an EH node equipped with an infinite sized battery also simplifies, e.g., the design of throughput and delay optimal policies [10]. This happens because the energy neutrality constraints, given in (1.1), can be replaced by the simpler average energy constraint, which requires the rate of energy consumption to be $\epsilon$ less than the harvesting rate, with $\epsilon > 0$ being arbitrarily small. The energy in the battery of a node operating under such an average energy constraint gradually builds up to infinity, thus making it possible to always satisfy the energy neutrality constraint. This greatly simplifies the design of energy management policies by circumventing the problem of dealing with potentially infinite number of constraints over time.

When an EHN is equipped with a finite capacity battery, it is sub-optimal to operate under an average energy constraint. The battery of a node operating under the average energy constraint eventually hits the full state, and energy that is harvested when the battery is full is wasted. In such a scenario, one way to design energy management

policies is to use a dynamic programming based approach such as the Markov deci-
sion process (MDP) [2, 11]. However, the computational complexity of the dynamic
programming based approaches increases quickly with the size of the state space. This
makes it unsuitable for the design of large networks. Thus, it is pertinent to character-
ize the performance loss of a network of nodes with finite size batteries, resulting from
the use of policies designed under the average power constraint.

### 1.1.2 Information available about the EH process

The energy management policy should, among other things, account for the random-
ness of the harvesting process. Depending on the nature of the harvesting mechanism,
an EHN may either have non-causal information about the (future) energy arrivals
[12–15] or it may only have information about the statistics of the EH process [16–18].
An energy management policy designed using non-causal information about the har-
vested energy is called an offline policy; otherwise it is termed as an online policy. Since
an offline energy management policy can exploit the information about the future en-
ergy arrivals to determine the transmit power at the current slot, an offline policy typ-
ically outperforms online policy [19]. Generally, the design of an offline policy can be
expressed as an static optimization problem [20, 21]. In contrast, due the randomness
of the harvested energy, the design of online policies is often formulated as a dynamic
program, which makes the design of an online policy more complex [11, 22]. Thus, it
is desirable to come up with a design procedure for online policies which entails low
complexity.

### 1.1.3   Energy cost to receive and decode data

For short distance communications, the energy consumed in transmission and reception of the data are typically of same order of magnitude [23]. Therefore, when the receiver is an EHN, the availability of harvested energy determines the amount of data that can be received successfully [24]. Moreover, if the transmitter is also an EHN, the transmission parameters (transmit power or rate) need to be adapted depending on energy availability at the receiver [25], as data transmitted in a slot when the receiver does not have sufficient energy to receive data will result energy wastage at the transmitter. Thus, the design of energy management policies for the EH links where both transmitter and receiver are EHNs needs to account for the statistics of the EH process at the transmitter and receiver, the energy cost for receiving data, and the spatio-temporal correlation in the EH processes at the nodes.

A related issue in the design of links where both the transmitter and receiver are EHNs is the lack of information about the battery state (or energy state) of the other node [26]. This may result in sub-optimal performance due to wastage of energy when one node attempts to transmit/receive when the other node has run out of energy. One possible approach to tackle this problem is to develop a protocol for communicating the battery state [27]. However, in such protocols, the control signals used to communicate the battery state may result in excessive energy overhead for low power sensors. This necessitates the development of energy management policies which can achieve the optimal performance using only the local information available at each node for their operation. However, the design of an optimal policy for *uncoordinated* EH links is quite challenging, and the fundamental limits of their performance are known only in very

few special cases, e.g., for links with unit-sized batteries [28].

### 1.1.4 Measurement of state-of-charge of the battery

A majority of the energy management policies proposed in the existing literature adapts the transmit power based on current state-of-charge (SoC) of the battery which requires availability of perfect information about battery's SoC. However, the estimation of SoC could be energy-expensive [29, 30]. The authors in [31] show that the knowledge of the EH statistics can partially compensate for the lack of SoC information. In [32, 33], the authors present policies that achieve near-optimal utility with 1-bit quantized SoC information. These considerations have lead to the concept of SoC-unaware policies, which operate independent of SoC information, e.g., fixed power policies [34] and linear power policies [1, 2]. However, the performance of such policies has not been studied systematically and needs to be benchmarked. Also, a systematic procedure for designing SoC-independent policies is not available in the literature.

An important component of low power communications standards such as IEEE $802.15.4$ [35] or bluetooth low energy specifications [36] is packet retransmissions. Further, in EH networks, retransmission protocols extenuate the impact of both small scale fading and the randomness of energy availability [34]. In the following section, we discuss the background on retransmission protocols.

## 1.2 Retransmission protocols

In a retransmission protocol, each packet transmission attempt is followed by an acknowledgment (ACK) or negative ACK (NACK) signal, which indicates the success

and failure of the attempt, respectively. After receiving a NACK the packet is retransmitted, provided the node has energy to do so and the packet delay has not yet exceeded the maximum allowed limit. Retransmission protocols come in various flavors. In the basic automatic repeat request (ARQ) protocol, a packet received in an attempt is decoded independently of the copies of the packet received in previous failed attempts, and unsuccessfully decoded packets are discarded. On the other hand, hybrid ARQ (HARQ) protocols, such as HARQ with chase combining (HARQ-CC) and HARQ with incremental redundancy (HARQ-IR), use all the copies of the packet received in the previous failed attempts to decode the packet received in current attempt, thereby improving the spectral efficiency [37]. For HARQ-CC, all copies of the packet received in the previous attempts are maximal-ratio combined with the current packet, and decoding is performed on the combined output [38], while for HARQ-IR the retransmissions contain extra parity bits which are suitably combined with the ones received in the previous rounds. For systems with low signal-to-noise ratio (SNR), HARQ-CC outperforms HARQ-IR. In addition, the HARQ-CC offers lower computational complexity than the HARQ-IR [39]. The design of optimal power control policies for conventional communication systems with both ARQ and HARQ-CC protocols has been studied extensively in the literature [38, 40–44].

## 1.2.1 Retransmission-based EH networks

In a conventional communication system, HARQ protocols offer an improvement in performance over the ARQ protocol. However, it is not known if the performance improvement provided by the HARQ protocols carries over to EH networks also. For

example, if the energy cost of maximal ratio combining is high, and ARQ could outperform HARQ. Moreover, both ARQ and HARQ protocols need to be optimized for EH networks. The authors in [45] and [46] proposed selectively sampling the packet and adjusting the ACK/NACK feedback, respectively, depending on the energy available at the receiver. In [2], the authors designed optimal policies for mono-T links, using partially observable MDP (POMDP). The computational complexity of the POMDP based design increases exponentially with the size of the battery. On the other hand, in [1] and [34], the authors considered ARQ based EH links and analyze their delay-limited throughput and packet drop probability (PDP), respectively. In [1], the authors proposed throughput maximizing policies for EH links where both the transmitter and receiver are EHNs. The optimal policy is obtained using a global search over the space of affine policies. However, the restriction of the search to affine policies may be sub-optimal in general. Also, the computational complexity of global search methods is prohibitively large, even for moderate sized batteries. Hence, it is desirable to come up with design procedures whose complexity does not scale with the battery size and other system parameters.

In light of the above discussion, we are now ready to summarize the main contributions of this thesis.

## 1.3   Outline of the thesis and summary of contributions

In this thesis, we consider the design and analysis of EH links where both transmitter and receiver are energy harvesting, and the energy cost of receiving a packet is comparable to the packet transmission cost.
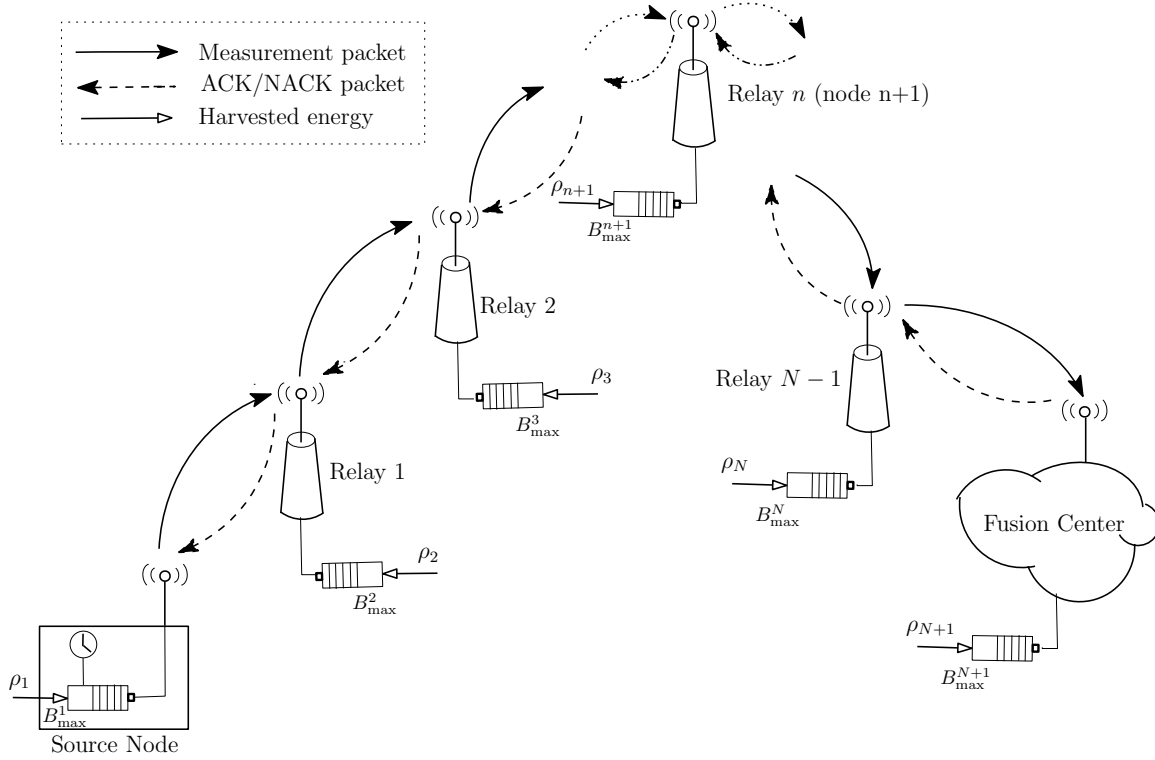
Figure 1.1: System model. Each node transmits and receives in its assigned sub-frame.

We consider a monitoring system, shown in Fig. 1.1, where a sensor node takes periodic measurements which are to be delivered to a destination over a multi-hop link formed between EHNs. Each relay node in the multi-hop link operates in a decode-and-forward manner. In addition, the packet transmission over each hop follows the ARQ protocol to deliver a given packet to the next node, within a fixed but predetermined number of slots allocated to it. For each attempt of the packet, the receiving node sends an acknowledgment (ACK) or negative ACK (NACK) to indicate the success or failure of the previous attempt, respectively. Once the transmitter receives an ACK for the current packet, it stops the transmission and goes to sleep, till it is time for it to receive

the next packet from the preceding node. A node in the sleep mode does not consume energy, but continues to harvest energy from the environment. Packets that are not delivered to the destination before the next measurement is taken are *dropped*. Thus, a packet is dropped if and only if any node fails to deliver it to the next node within its allocated number of slots. A packet failure may happen either due to the energy outage at the transmitter or receiver, or due to channel fading/noise at the receiver. For ARQ-based links with periodic transmission of fixed-size measurement packets, the PDP is used as a metric for reliability [2, 34]. For this system, the PDP is defined as the fraction of packets that are dropped.

We present a PDP-optimal retransmission-index based policy (RIP) for each node when the actions of transmitter and the receiver are *coordinated*, i.e., when both nodes are aware of whether or not the other node has run out of energy. An RIP specifies the transmit energy schedule for each attempt of a packet. For ease of discussion, consider a two hop path, where a source transmits a packet to a relay, which then forwards it to the destination. When the receiver consumes a fixed amount of energy for each reception attempt, the RIP of source-relay hop determines the average amount of energy consumed by the relay in receiving the packet. This, in turn, determines the amount of energy left at the relay for transmitting the packet to the destination. Thus, the RIP of the source node and the RIP of the relay node are coupled together. This coupling between the RIPs of the EHNs calls for joint optimization of the RIPs. Furthermore, the time-varying wireless channel and the EH process along with finite sized energy buffers renders this joint optimization even more challenging. For example, a single transmission attempt at high power saves the energy consumed in the reception, and

leaves more energy at the receiver for transmitting the packet to the next node. On the other hand, a single attempt prohibits the node from exploiting the diversity gain due to retransmissions, and thereby reduces the odds of successful packet delivery to the destination. Thus, there exists a trade-off between the diversity and the power consumption at the receiver, that needs to be accounted for in the design of RIPs.

In the above, coordination between the transmitter and receiver can be achieved if the receiver sends an ACK for a successfully received packet. However, sending an ACK signal is not necessary, e.g., when successful packet reception can be ensured with high probability provided it is transmitted at sufficiently high power, and is an additional overhead for energy-starved sensors. In this context, we analyze the impact of lack of coordination between the communicating nodes on the system performance. We consider a point-to-point link between an energy harvesting transmitter and receiver, where neither node has the information about the battery state or energy availability at the other node. We consider a model where data is successfully delivered only in slots where both nodes are active. Energy loss occurs whenever one node turns on while the other node is in sleep mode. In each slot, based on their own energy availability, the transmitter and receiver need to independently decide whether or not to turn on, with the aim of maximizing the long-term time-average throughput.

The organization and the major contributions of the thesis are as follows:

Chapter 2 of this thesis proposes a general framework to analyze the PDP of point-to-point retransmission based dual EH links where both transmitter and receiver are EHNs. In particular, it presents a rigorous analysis of the PDP of dual EH links, for

both ARQ and HARQ-CC. The analysis can be directly extended to other retransmission protocols such as HARQ-IR. The recursive, exact expressions for the PDP are derived by modeling the system evolution as a discrete-time Markov chain. Furthermore, we derive the approximate *closed-form* expressions which are *exact* when (i) the batteries at the transmitter and receiver are large enough to store the energy required to support all the attempts in a frame, and (ii) the energy used for each attempt exceeds the energy harvested in a single slot. In other cases, the closed-form expression provides an upper bound on the actual PDP. The expressions to compute the PDP for the links in the special case of zero and infinite batteries are also derived. The accuracy of the closed-form PDP expressions in a wide range of scenarios is demonstrated through simulations. The obtained closed-form PDP expressions not only highlight the trade-off between different system parameters but also aid in formulating an optimization problem to find the optimal energy management policies.

In Chapter 3, using the closed-form expressions of the PDP, an optimization problem to obtain the PDP-optimal RIPs is formulated. Since the original optimization problem is intractable, we reformulate it by deriving an upper bound and lower bound on the PDP of dual EH links with finite batteries. The bounds are obtained in terms of the PDP achieved with ideal (infinite capacity) batteries. The gap between the upper and lower bounds is analyzed, and it is shown that for policies operating in the so called *energy unconstrained regime* the gap goes to zero exponentially fast with the battery size at the transmitter and receiver. The optimization problem is reformulated using the EUR constraints. The problem formulation is a non-convex mixed integer program, which is known to be strongly NP hard. It is solved in a computationally efficient and provably

convergent manner using techniques from geometric programming. This provides a systematic procedure to design near-optimal RIPs for dual EH links with retransmission. Through simulations, it is observed that the SoC-unaware RIPs, obtained using the proposed method, can even outperform the SoC-aware policies. In addition, the complexity of the design procedure is independent of the size of the battery at the transmitter and receiver.

The focus of Chapters 4 and 5 is the retransmission-based multi-hop EH links, where we extend the results presented in previous chapters. In particular, the DTMC based framework to analyze the PDP of dual EH links is extended to obtain the PDP of multi-hop EH links. Moreover, we provide the upper and lower bounds on the PDP of multi-hop EH links, in terms of the PDP of multi-hop EH links with infinite batteries. Chapter 5 addresses the issue of designing near-optimal RIPs for multi-hop EH links in the two scenarios. In the first case, when the energy required for receiving and decoding a packet is negligible compared to that required for transmitting a packet, we present closed-form expressions for the optimal transmit power policy in both slow and fast fading scenarios. Furthermore, when there is a peak transmit power constraint at the transmitter, we provide a provably convergent algorithm to determine the optimal transmit power control policy. The presented closed-form expressions not only reveal the inter-dependence among the transmit power levels of the RIPs, but also on the system parameters, e.g., harvesting rate, number of retransmissions etc. For example, when the channel is slow fading and the energy required to receive and decode a packet is negligible, we show that the optimal transmit power is geometrically increasing. In contrast, for fast fading links, the transmit power levels have a polynomial

relationship. In the other case, when the energy required for receiving and decoding a packet is non-negligible, the problem becomes a mixed-integer nonlinear program. Using tools from GP, we obtain near-optimal policies in the general case. The obtained policies in both the scenarios can be easily implemented in a distributed fashion without requiring any additional control overhead.

In Chapter 6, the impact of lack of coordination between the EHNs of dual EH links is studied. First, an upper bound on the throughput achievable is derived by analyzing a genie-aided system that has noncausal knowledge of the energy arrivals at both the nodes. Next, an online policy is proposed which requires an occasional one-bit feedback whose throughput is within one bit of the upper bound, asymptotically in the battery size. In order to further reduce the feedback required, a time-dilated version of the online policy is proposed. As the time dilation gets large, this policy does not require any feedback and achieves the upper bound asymptotically in the battery size. Inspired by this, a near-optimal fully uncoordinated policy is proposed. Monte Carlo simulations validate our theoretical results and illustrate the performance of the proposed policies.

A pictorial overview of the thesis is provided in Fig. 1.2. In summary, this thesis studies the performance of EH communication systems, with emphasis on the case when the cost of decoding at the receiver is not negligible. The impact of the decoding cost on the performance is characterized which is further used to obtain energy management policies that achieve optimal/near-optimal performance.
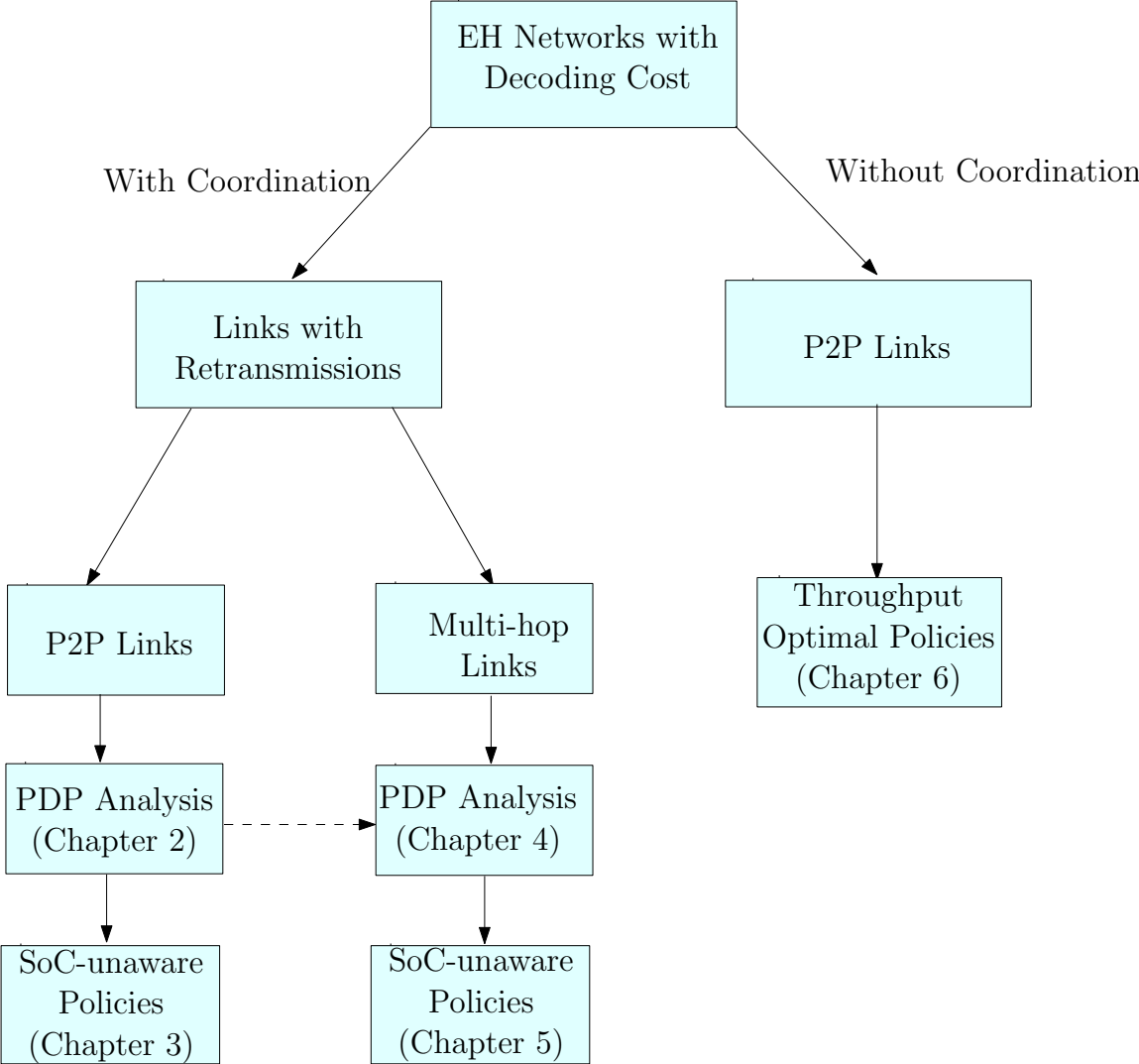
Figure 1.2: Thesis Outline.

# List of Publications from this Thesis

**Journal Papers**

1. **M. Sharma** and C. R. Murthy, "Packet Drop Probability Analysis of Dual Energy Harvesting Links with Retransmission," *IEEE Journal on Selected Areas in Communications*, vol. 34, no. 12, pp. 3646 - 3660, Dec. 2016.

2. **M. Sharma** and C. R. Murthy, "On Design of Dual Energy Harvesting Communication Links with Retransmission," *IEEE Transactions on Wireless Communications*, vol. 16, no. 6, pp. 4079 - 4093, Jun. 2017.

3. **M. Sharma** and C. R. Murthy, "Distributed Power Control for Multi-hop Energy Harvesting Links with Retransmission," to appear in *IEEE Transactions on Wireless Communications*, Mar. 2018.

4. **M. Sharma**, C. R. Murthy and R. Vaze, "Asymptotically Optimal Uncoordinated Power Control Policies for Energy Harvesting Multiple Access Channels with Decoding Costs," *submitted to IEEE Transactions on Communications*, Apr. 2018.

## Conference Papers

1. **M. Sharma** and C. R. Murthy, "Packet Drop Probability Analysis of ARQ and HARQ-CC with Energy Harvesting Transmitters and Receivers," *IEEE Global Conference on Signal and Information Processing (GlobalSIP)*, Atlanta, USA, Dec. 2014

2. A. Devraj, **M. Sharma** and C. R. Murthy, "Power Allocation in Energy Harvesting Sensors with ARQ: A Convex Optimization Approach," *IEEE Global Conference on Signal and Information Processing (GlobalSIP)*, Atlanta, USA, Dec. 2014

3. **M. Sharma**, C. R. Murthy and R. Vaze, "On Distributed Power Control for Uncoordinated Dual Energy Harvesting Links: Performance Bounds and Near-Optimal Policies," *15th International Symposium on Modeling and Optimization in Mobile, Ad Hoc, and Wireless Networks (WiOpt)*, Paris, France, May 2017.

4. **M. Sharma** and C. R. Murthy, "Near-Optimal Distributed Power Control for ARQ Based Multihop Links with Decoding Costs," *IEEE International Conference on Communications (ICC)*, Paris, France, May 2017.

# Chapter 2

# Packet Drop Probability Analysis of Dual Energy Harvesting Links with Retransmission

In this chapter, we derive the packet drop probability of dual energy harvesting links, i.e., where both the transmitter and receiver are EHNs, with retransmission. Our goal is to develop a general framework to analyze and understand the impact of various physical layer parameters, e.g., the energy harvesting profiles, size of the energy buffer, power management policy (at both the transmitter and receiver), channel statistics, and coherence time, on the PDP of dual EH links over block fading channels. Also, considering an EH receiver makes it pertinent to study the impact of data processing at the receiver. To this end, in addition to the automatic-repeat-request (ARQ) protocol, we also analyze the PDP of dual EH links that employ hybrid ARQ with chase combining (HARQ-CC).

The presented framework naturally extends to obtain the PDP of mono EH links also, i.e., links whose only one node is the EHN. The PDP of ARQ based mono-T EH links

for both slow and fast fading channels, when a fixed (constant) power is used for all attempts, is analyzed in [34]. The work in [2] generalized the analysis of [34], for policies where the transmit power is an affine function of the attempt index. The PDP expressions obtained in [2, 34] are recursive in nature hence not amenable for optimization. Moreover, the PDP analysis of dual EH links requires one to consider the interaction between the EH processes at both nodes, which makes it fundamentally different from the analysis of mono EH links in [2, 34]. The PDP analysis presented in this chapter generalizes that in [2, 34] by considering EH at the receiver, spatio-temporal correlation of EH processes at both the EHNs, as well as the impact of data processing at the receiver. Finally, the framework developed in this chapter will facilitate the development of PDP-optimal SoC-unaware policies for multi-hop EH links with retransmissions in the later chapters.

In the next section, we describe the system model.

## 2.1   System Model

We consider an EHN which needs to deliver a data packet once in a *frame* of $T_m$ s. to a receiving EHN. Each transmission attempt takes $T_p$ s., including the time the transmitting EHN waits to receive the ACK or NACK. Thus, a frame contains $K \triangleq \lfloor T_m/T_p \rfloor$ slots, which is also the maximum number of possible attempts for a packet, where $\lfloor \cdot \rfloor$ denotes the floor function. A packet is retransmitted until the transmitting EHN receives an ACK, or the frame duration expires. If an ACK is received, the EHNs do not attempt to communicate and accumulate the harvested energy in a finite capacity but

otherwise perfectly efficient battery for the rest of the frame. The ACK/NACK messages are assumed to be received without error at the transmitter.

We analyze the packet drop performance with two different retransmission protocols at the link layer: the basic ARQ and the HARQ-CC. In the basic ARQ, for decoding, the receiver uses the packet received in the current attempt only, and discards all the erroneously received copies of the packet. In HARQ-CC, the receiver tries to decode the packet received in the current attempt by maximal ratio combining it with all the previously received copies of the same packet. For basic ARQ, we say that the packet is received in *outage*, if the signal-to-noise ratio (SNR), $\gamma_\ell$, of the packet received in the $\ell^{\text{th}}$ *attempt* is less than the minimum SNR, $\gamma_0$, required for successful decoding. For HARQ-CC, under this outage model, the packet remains in outage if the *accumulated* SNR, $\gamma_{ac,\ell}$, up to and including the SNR of the packet received in $\ell^{\text{th}}$ attempt, is less than $\gamma_0$. In addition, for both schemes, the packet remains in outage if either the transmitting or receiving EHN does not have sufficient energy to communicate. A packet is *dropped* if it remains in outage till the end of the frame, i.e., if the EHN fails to deliver it successfully within the $K$ transmission opportunities.

To ensure better rendezvous between the EHNs, and for improved energy efficiency, we consider a *coordinated sleep-wake protocol* (CSWP) [27] with the following control signals:

$$\text{SC} \quad : \text{Start-Communication,}$$

$$\text{EC} \quad : \text{End-Communication.}$$

As shown in Fig. 2.1, the transmitter or receiver sends the end-communication signal
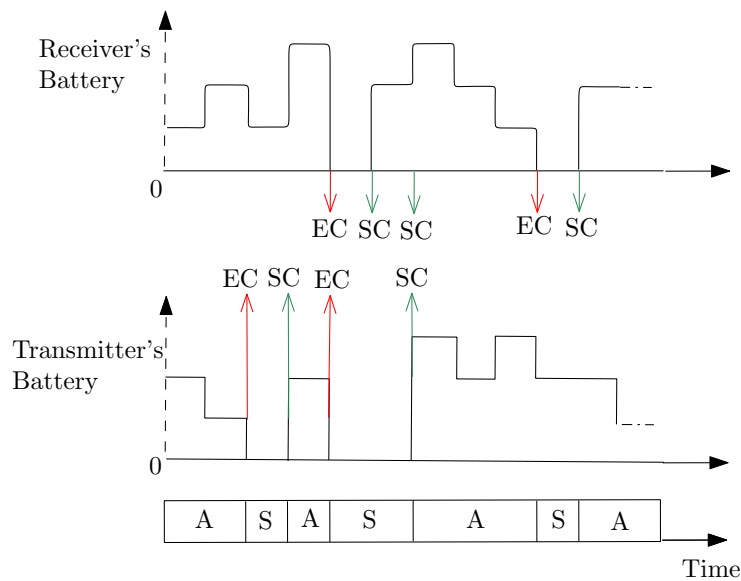
Figure 2.1: The coordinated sleep-wake protocol for dual EH links. The (↓) and (↑) arrows indicate that node is sending a control signal, i.e., a end-communication or start-communication signal. The time intervals during which both nodes are active and in the sleep mode are represented as "A" and "S", respectively.

if it does not have sufficient energy to participate in communication. For a transmitter, the phrase 'sufficient energy' means having adequate energy to transmit a packet and receive the ACK/NACK message, while for a receiver it means having enough energy to receive and decode a packet, and transmit the ACK/NACK message. If a node receives the end-communication signal in a slot, it goes into sleep mode, as successful communication is not possible. In the sleep mode, a node incurs a very low (effectively zero) energy cost, while it could continue to harvest energy. If a node receives a start-communication signal while in sleep mode, and if it has sufficient energy, it turns on and prepares itself to participate in communication from the start of the next slot. We assume that, for both nodes, the end-communication and start-communication signals are received error free.[1] Under the coordinated sleep-wake protocol, an attempt is

---

[1]The EH-WISP-Mote and REACH-Mote employ a wake-up receiver with an energy harvesting circuit. Node wakeup is feasible at a range of up to 37 ft [27], using wake-up transmitter devices such as an RFID

made only if both nodes have sufficient energy. Hence, the CSWP completely avoids

the energy wastage that happens if one node tries to communicate when the other node

has run out of energy. Alternatively, for retransmission based links, the CSWP can be

implemented, with a lesser signaling overhead, by using an implicit signaling scheme

in which the receiver abstains from sending the ACK/NACK message for the current

attempt until it has sufficient energy to receive the next attempt. Further, upon receiv-

ing an ACK/NACK message, the transmitter wakes up once it has sufficient energy to

make the next attempt. After sending the ACK/NACK message, the receiver senses

the channel at the beginning of each slot, and goes to sleep if no transmission is de-

tected. In contrast to CSWP, this scheme does not require explicit control signaling to

communicate the energy availability to the other node.

   We model the EH process at both nodes as a stationary, independent and identically

distributed (i.i.d.) Bernoulli process, i.e., at the beginning of every slot, the transmitter

harvests energy $E_s$ with probability $\rho_t$, and with probability $1 - \rho_t$, it does not har-

vest [34] [2] [49]. The harvesting probability at the receiver is denoted by $\rho_r$. The

Bernoulli model, while simple, captures the sporadic and random nature of the EH pro-

cess and also simplifies the exposition of the key ideas presented in this chapter. How-

ever, as will be shown later in the chapter, the framework presented here can be easily

extended to more sophisticated models, such as the stationary Markov model [49, 50]

(see Section 2.6.1) and the generalized Markov model [51], which are appropriate mod-

els for solar harvested energy and piezoelectric energy [20, 51], respectively.

---

reader [47] or a powercast transmitter [48].
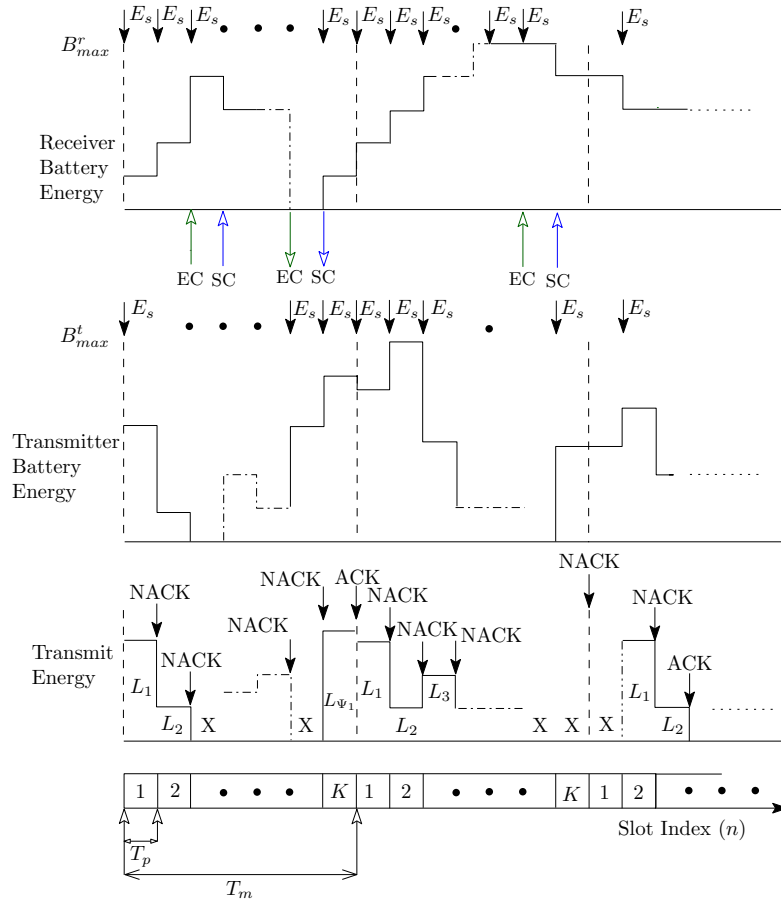
Figure 2.2: Communication time-line of the EHN, showing the random energy harvesting moments and periodic data arrivals. The marker "X" denotes the slots where the EHN does not communicate due to insufficient energy, and $L_{\Psi_1}$ denotes the power level of the last attempt, i.e., there are $\Psi_1$ feasible attempts in the frame.

The EHNs are equipped with a perfectly efficient but finite capacity buffer (e.g., a battery) to store the harvested energy. We consider an RIP, where the transmitting EHN, in the $K$ attempts, transmits at predetermined power levels given as $\mathcal{P} = \{P_1 \triangleq \frac{L_1 E_s}{T_p}, P_2 \triangleq \frac{L_2 E_s}{T_p}, \ldots, P_K \triangleq \frac{L_K E_s}{T_p}\}$, where $L_\ell \in \mathcal{R}^+$ is the amount of energy used and $P_\ell$ is transmit power level in the $\ell^{\text{th}}$ transmission attempt[2] of a given packet. Since the prescribed power levels are independent of the instantaneous state-of-charge (SoC) of the battery,

---

[2]Note: we consider an attempt-based power prescription in this work, not a slot-based prescription. Hence, $P_\ell$ is the power used in the $\ell^{\text{th}}$ attempt, not the $\ell^{\text{th}}$ slot within a frame.

the RIPs are suitable for use in scenarios where it is energy-expensive or technologically challenging to accurately estimate the SoC [29, 30, 52]. Moreover, as will be demonstrated in the sequel, a well designed RIP can even outperform a policy obtained using the MDP which uses quantized SoC information (see Fig. 3.7). The details related to the design of optimal RIPs along with theoretical guarantees on the performance of optimal RIPs are provided in Chapter 3.

For the receive energy consumption, since the size as well as the modulation and coding scheme for each packet is fixed, i.e., the data rate remains fixed, we adopt a simple model where the node consumes $R$ units of energy to receive a packet and send an ACK/NACK message [1, 53–55].

The RIPs conform to the energy neutrality constraint through the battery evolution, at the transmitter, given by[3]

$$
B_{n+1}^t =
\begin{cases}
\min(B_n^t + 1 - L_\ell \mathbb{1}_{\{L_\ell \leq B_n^t, R \leq B_n^r, U_n \neq -1\}}, B_{\max}^t), \\
\qquad\qquad \text{if energy is harvested in the } n^{\text{th}} \text{ slot,} \\
B_n^t - L_\ell \mathbb{1}_{\{L_\ell \leq B_n^t, R \leq B_n^r, U_n \neq -1\}}, \\
\qquad\qquad \text{if no energy is harvested in the } n^{\text{th}} \text{ slot,}
\end{cases}
$$

$$(2.1)$$

where $B_{\max}^t$ is the capacity of the battery at the transmitter, $B_n^t$ and $B_n^r$ denote the battery level in the $n^{\text{th}}$ slot at the transmitter and receiver, respectively, and $U_n \in \{-1, 1 \ldots, K\}$ denotes the packet attempt index. Starting from $U_n = 1$ at the beginning of the frame, it is incremented by $1$ after each unsuccessful attempt, and set to $-1$ for the rest of the

---

[3]Throughout the chapter, the battery levels such as $B_n^t$, $B_n^r$, $B_{\max}^t$, $B_{\max}^r$, are normalized with respect to $E_s$. Further, for the foregoing Markov chain formulation, we require that the power levels such as $L_\ell$ and $R$ are integer or fractional-valued.

frame, once an ACK is received. Thus, (2.1) is written using the fact that, under the coordinated sleep-wake protocol, if the transmitter has not yet received an ACK for the current packet, the $\ell^{\text{th}}$ attempt is made in the $n^{\text{th}}$ slot if and only if $B_n^t \geq L_\ell$ and $B_n^r \geq R$. At the receiver, the battery evolves in a similar fashion, and the evolution is given by

$$
B_{n+1}^r = \begin{cases}
\min(B_n^r + 1 - R\mathbb{1}_{\{L_\ell \leq B_n^t, R \leq B_n^r, U_n \neq -1\}}, B_{\max}^r), \\
\qquad \text{if energy is harvested in } n^{\text{th}} \text{ slot,} \\
B_n^r - R\mathbb{1}_{\{L_\ell \leq B_n^t, R \leq B_n^r, U_n \neq -1\}}, \\
\qquad \text{if no energy is harvested in } n^{\text{th}} \text{ slot,}
\end{cases}
$$

After an ACK is received, both nodes accumulate the harvested energy for the rest of the frame. Fig. 2.2 illustrates the battery evolution of the EHN with random energy injections.

We consider a *block* fading wireless channel between the transmitter and receiver in both slow and fast fading cases. The *slow* fading channel remains constant for the duration of a frame, and changes in an i.i.d. fashion from one frame to the next, while the *fast* fading channel stays constant for a slot, and varies in an i.i.d. fashion from slot to slot. The transmitter only has access to implicit channel state information (CSI), obtained from the ACK/NACK messages. In both cases, the channel is assumed to be Rayleigh distributed, with the complex baseband channel distributed as $\mathcal{CN}(0, \sigma_c^2)$. As described earlier, for the basic ARQ protocol, a packet remains in outage in the $\ell^{\text{th}}$ attempt, if $\gamma_\ell = \frac{P_\ell |h_\ell|^2}{\mathcal{N}_0} < \gamma_0$, where $|h_\ell|^2$ represents the channel gain during the $\ell^{\text{th}}$ attempt and $\mathcal{N}_0$ denotes the power spectral density of the additive white Gaussian noise at the receiver. Hence, for the Rayleigh fading channel, the probability that the $\ell^{\text{th}}$ attempt

results in an outage is given as

$$p_{\text{out},\ell} \triangleq \Pr[\gamma_\ell < \gamma_0] = 1 - e^{-\frac{\gamma_0 \mathcal{N}_0 T_p}{L_\ell E_s \sigma_c^2}}, \tag{2.2}$$

In HARQ-CC, a packet received in a given attempt is decoded by maximal ratio combining it with the copies of the packet received in all previous attempts. Since maximal-ratio-combinig (MRC) corresponds to weighing each copy of the received packet with the complex conjugate of the overall gain applied to the data symbols (including the effect of the power level prescribed by the RIP), the output SNR of MRC is simply the accumulated SNR of the packets received so far. Hence, for HARQ-CC, in the $\ell^{\text{th}}$ attempt, the packet remains in outage if the accumulated SNR, $\gamma_{ac,\ell}$, up to and including the SNR of the packet received in the current round, is less than $\gamma_0$. As a result, for the EH link with a chase combining receiver, the probability that the packet remains in outage is written as

$$p_{\text{out},1\to\ell} \triangleq \Pr[\gamma_{ac,\ell} < \gamma_0], \text{ where } \gamma_{ac,\ell} = \sum_{i=1}^{\ell} \frac{P_i |h_i|^2}{\mathcal{N}_0}. \tag{2.3}$$

Note that, $p_{\text{out},0} = 1$ and $p_{\text{out},1\to0} = 1$.

A packet is dropped if all the attempts result in outage. For ARQ, informally, the PDP is $P_{\text{D}} = \Pr\left[\cap_{\ell=1}^{\ell_m} (\gamma_\ell < \gamma_0)\right]$, while for HARQ-CC it is $P_{\text{D}} = \Pr[\gamma_{ac,\ell_m} < \gamma_0]$, where $\ell_m$ denotes the index of the *last* attempt in the frame. The PDP depends on $\ell_m$, whose distribution is difficult to characterize, as it has a complex dependence on the energy harvesting and channel dynamics, the battery capacities at the transmitter and receiver, etc. In the next section, using a Markov chain formulation, we analyze the PDP of the above described system, which is the main result of this chapter.

## 2.2 PDP Analysis of Dual EH Links

In this section, we analyze the PDP of dual EH links with ARQ and HARQ-CC. Since the battery states at both nodes evolve in a Markovian fashion, the system evolution within a frame is modeled as a discrete time Markov chain (DTMC). The state of the system consists of the battery states at the EHNs and the packet attempt index. The PDP can be obtained by averaging the PDP conditioned on the system state over its stationary distribution. To this end, we derive the conditional PDP and stationary distribution, for both ARQ and HARQ-CC, and for both slow and fast fading channels. We proceed by describing the formulation of the DTMC in the following.

As shown in Fig. 2.3, the state of this DTMC is represented by a tuple $(B_n^t, B_n^r, U_n)$, where $B_n^t$ and $B_n^r$ are the battery state at the transmitter and receiver, respectively, and $U_n \in \{-1, 1, \ldots, K\}$ represents the *packet attempt index* in the $n^{\text{th}}$ slot, defined as

$$U_n \triangleq \begin{cases} -1 & \text{ACK received,} \\ \ell & \ell - 1 \text{ NACKs received, } \ell \in \{1, \ldots, K\}. \end{cases} \tag{2.4}$$

A packet is dropped if and only if $U_K \neq -1$, i.e., if the transmitter does not receive an ACK by the end of the frame.

The state transition probability matrix (TPM) of the DTMC is denoted by $\boldsymbol{G}$. The elements of $\boldsymbol{G}$ represent the probability of a transition from state $(i_1, j_1, \ell_1)$ to state $(i_2, j_2, \ell_2)$ in a single slot, and are defined as

$$G_{i_1,j_1,\ell_1}^{i_2,j_2,\ell_2} \triangleq \Pr\Big[(B_{n+1}^t = i_2, B_{n+1}^r = j_2, U_{n+1} = \ell_2)\,\big|\,(B_n^t = i_1, B_n^r = j_1, U_n = \ell_1)\Big]. \tag{2.5}$$
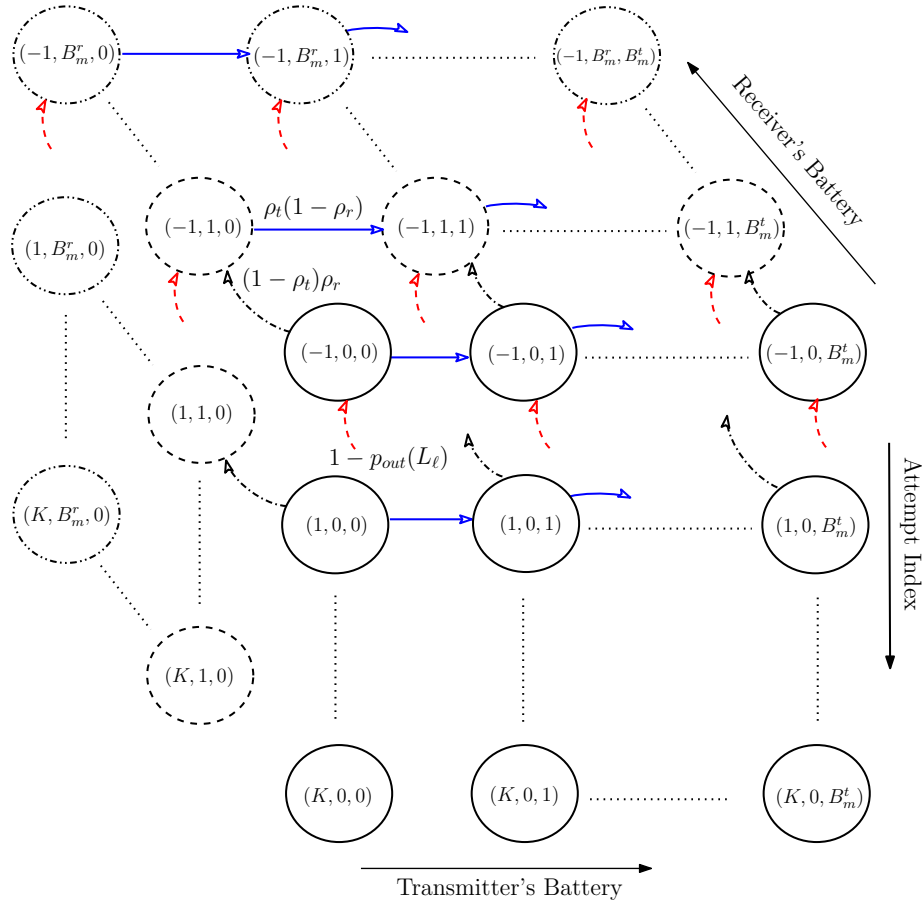
Figure 2.3: DTMC for an RIP. The energy states are normalized with respect to $E_s$. $B_m^t$ and $B_m^r$ denote the capacity of the battery at the transmitter and receiver, respectively. In the above figure, only feasible transitions are depicted. For example, $(K, 0, 0) \rightarrow (K, 1, 1)$ and $(1, 0, 0) \rightarrow (-1, 0, 0)$ are not feasible transitions. The transition probabilities of this DTMC are given in Appendix A.1.

The transition probabilities are determined by the RIP $\mathcal{P}$, and the statistics of the channel and the EH processes at the EHNs. In contrast to mono EH links [2, 34], the transition probabilities of dual EH links need to account for the possible correlation of the EH processes and the coupled evolution of the batteries at the nodes. The transition probabilities are provided in Appendix A.1.

*Remark* 1. The events that a node sends an start-communication or end-communication signal are implicitly accounted for in the transition probabilities. For example, when

$i_1 < L_\ell$ (or $j_1 < R$), the transition probabilities do not include a $p_{\text{out},\ell}$ term, thus accounting for an end-communication signal sent by the transmitter (or receiver).

Now, for any given RIP $\mathcal{P}$, the average packet drop probability is given by

$$P_{\text{D}}(K) = \sum_{i,j} \pi(i,j) P_{\text{D}}(K|i,j,\ell=1). \tag{2.6}$$

Thus, to compute the PDP, we average the conditional PDP, $P_{\text{D}}(K|i,j,\ell=1)$, over the stationary distribution, $\boldsymbol{\pi}$, of the Markov chain, where $\pi(i,j)$ denotes the stationary probability that the transmitter and receiver have $(iE_s, jE_s)$ energy at the start of the frame. The conditional probability, $P_{\text{D}}(K|i,j,\ell=1)$, denotes the probability that the packet is dropped given that the battery states of the transmitter and receiver at the beginning of the frame are $i$ and $j$, respectively, where $(i,j) \in \{(i_t, j_r) \mid 0 \le i_t \le B_{\max}^t, 0 \le j_r \le B_{\max}^r\}$, and conditioning on the attempt index $\ell = 1$ indicates the start of the frame.

To obtain the PDP using (2.6), we need to find the stationary distribution, $\boldsymbol{\pi}$, and the conditional PDP, $P_{\text{D}}(K|i,j,\ell=1)$. Existence of the stationary distribution is ensured by the fact that the number of states is finite, since both the EHNs have finite capacity batteries, and therefore the DTMC is positive recurrent. Next, we derive the stationary distribution for both ARQ and HARQ-CC, with both slow and fast fading channels.

## 2.2.1 Derivation of the Stationary Distribution

The stationary probabilities, $\pi(i,j)$, that the transmitter and receiver have $(iE_s, jE_s)$ units of energy at the *start* of the frame is given by [56, Lemma 1]

$$\boldsymbol{\pi} = (\boldsymbol{G}' - \boldsymbol{I} + \boldsymbol{B})^{-1}\boldsymbol{b} \tag{2.7}$$

where $\boldsymbol{b} = (1, \ldots, 1)^T \in \mathbb{R}^{(B_{\max}^t+1)(B_{\max}^r+1)}$, $\boldsymbol{B}_{i,j} = 1 \, \forall \, i, j$, and $\boldsymbol{G}'$ is the $K$-step TPM of battery states with its entries $\Pr\left[ \left( B_{(M+1)K}^t = i_2, B_{(M+1)K}^r = j_2 \right) \middle| \left( B_{MK}^t = i_1, B_{MK}^r = j_1 \right) \right]$, where $M$ denotes the frame index, for all $(i_1, i_2, j_1, j_2)$. We use the TPM, $\boldsymbol{G}$, to compute $\boldsymbol{G}^K$. The entries of $\boldsymbol{G}^K$ are in turn used to compute the entries of $\boldsymbol{G}'$ as:

$$\sum_{u \in \{-1, 1, \ldots, K\}} \Pr\left[ \left( B_{(M+1)K}^t = i_2, B_{(M+1)K}^r = j_2, U_{(M+1)K} = u \right) \middle| \left( B_{MK}^t = i_1, B_{MK}^r = j_1, U_{MK} = 1 \right) \right].$$

(2.8)

In next subsection, we derive the expressions for the conditional PDP of dual EH links.

## 2.2.2 Exact Conditional PDP of Dual EH Links with ARQ

The key technical challenge in deriving the conditional PDP of dual EH links is that for a given RIP $\mathcal{P}$ and battery states $(i, j)$ at the beginning of the frame, the conditional PDP, $P_D(K|i, j, \ell = 1)$, depends on the evolution of the battery at the transmitter and receiver, which, in turn, depends on the harvesting instances at both EHNs and their battery states. In the following, we derive an exact expression for the conditional PDP. For the clarity of exposition, the conditional PDP is derived for mutually i.i.d. harvesting processes. However, the result can be extended to incorporate both the spatial and temporal correlation of the harvesting processes (see Sec. 2.6).

**Lemma 1.** *For ARQ-based dual EH links with i.i.d. Bernoulli harvesting processes at the transmitter and receiver with harvesting probabilities $\rho_t$ and $\rho_r$, the conditional PDP, $P_D(K|i, j, \ell)$,*

*for all $\ell \geq 1$ and $K \geq 1$, is given by the recursive expression in* (2.9)

$$
P_D\left(K|i,j,\ell\right) = \begin{cases}
p_{out,\ell}\left[\rho_t\rho_r P_D\left(K-1|i-L_\ell+1, j-R+1, \ell+1\right)\right. \\
+\rho_t(1-\rho_r)P_D\left(K-1|i-L_\ell+1, j-R, \ell+1\right) \\
+(1-\rho_t)\rho_r P_D\left(K-1|i-L_\ell, j-R+1, \ell+1\right) \\
\left.+ (1-\rho_t)(1-\rho_r)P_D\left(K-1|i-L_\ell, j-R, \ell+1\right)\right], \quad i \geq L_\ell, j \geq R, \\
\rho_t\rho_r P_D\left(K-1|i+1, j+1, \ell\right) \\
+\rho_t(1-\rho_r)P_D\left(K-1|i+1, j, \ell\right) \\
+(1-\rho_t)\rho_r P_D\left(K-1|i, j+1, \ell\right) \\
+(1-\rho_t)(1-\rho_r)P_D\left(K-1|i, j, \ell\right), \qquad\qquad i < L_\ell \text{ or } j < R, \\
\end{cases}
$$

$$(2.9)$$

*Proof.* When $i \geq L_\ell, j \geq R$, both the transmitter and receiver have sufficient energy to make $\ell^{\text{th}}$ transmission attempt. Depending on the four mutually exclusive cases where the transmitter, receiver, both, or neither harvest energy in the first slot, we get the four terms in the expression for the case $i \geq L_\ell, j \geq R$, with $P_D\left(0|i,j,\ell\right) = 1$ for all values of $i, j$ and $\ell$. Specifically, the first term denotes the probability that the packet is dropped after $K$ slots given that the $\ell^{\text{th}}$ attempt is feasible and both transmitter and receiver harvest energy in the first slot. It is written as a product of three terms: the probability of outage in $\ell^{\text{th}}$ attempt, the probability that both transmitter and receiver harvest energy in the first slot, and the conditional PDP, $P_D\left(K-1|i-L_\ell+1, j-R+1, \ell\right)$. The conditional PDP, $P_D\left(K-1|i-L_\ell+1, j-R+1, \ell\right)$, is the probability that the packet is dropped after the remaining $K-1$ slots given that the batteries of the transmitter and receiver have evolved to $i-L_\ell+1$ and $j-R+1$, respectively. Other three terms in the sum are written similarly. Also, the cases $i < L_\ell$ and $j < R$ are handled by a similar

reasoning, by observing the fact that, in these cases, the packet cannot be attempted in

the first slot. □

A similar expression for $P_\text{D}(K|i,j,\ell)$ of dual EH links with HARQ-CC can be ob-

tained, by replacing $p_{\text{out},\ell}$ in (2.9) by $p_{\text{out},1\to\ell}$ given by (2.3). This completes the charac-

terization of the exact conditional PDP and stationary distribution, which can in turn

be used to compute the PDP of dual EH links using (2.6), (2.7) and (2.9). In the next

subsection, we summarize the procedure to compute the PDP.

### 2.2.3  Procedure to Compute the PDP

The procedure to compute the PDP is summarized in Algorithm 1. We note that the

algorithm provides an easy-to-compute recipe for finding the exact PDP of dual EH

links.

---
**Algorithm 1** Procedure to compute the PDP.

---

1: Compute $\boldsymbol{G}$ from (A.1) in Appendix A.1, and the $K$-step TPM, $\boldsymbol{G}^K$.
2: Using the entries of $\boldsymbol{G}^K$, compute $\boldsymbol{G}'$ in (2.7) using (4.7).
3: Calculate the stationary probabilities, $\pi(i,j)$, using (2.7).
4: Calculate the conditional probabilities $P_\text{D}(K|i,j,\ell=1)$ using (2.9).
5: Calculate the PDP $P_\text{D}(K)$ by substituting the results from steps 3 and 4 in (2.6).

---

The PDP obtained using the conditional PDP in (2.9) is in recursive form, which does

not offer insights into the effect of various system parameters on the PDP. In the next

section, we derive closed-form expressions for the conditional PDP of dual EH links.

## 2.3 Closed Form Expressions for the PDP of Dual EH Links

As can be observed from (2.9), for a given initial state $(i, j)$ of the battery at the transmitter and receiver, the exact conditional PDP $P_{\mathrm{D}}(K|i, j, \ell = 1)$ depends not only on the number of slots but also on the slot index in which energy is harvested. Due to this, it is required to keep track of the battery state to compute the exact PDP, which, in turn, results in the recursive expression in (2.9). However, the following key observations allow us to obtain a closed-form expression which is exact in a wide range of practical scenarios:

1. The conditional PDP depends only on the number of feasible attempts in the frame, and not on the slot indices when the attempts are made.

2. In general, for a given battery state tuple, $(i, j)$, the number of feasible attempts is determined by the exact slot indices in which energy is harvested and depleted. However, for a system with sufficiently large battery at the EHNs (such that the energy overflow can be neglected), the number of feasible attempts depends only on the *number* of slots in which energy is harvested, and not on the precise energy arrival and departure instants. This observation is also valid for any RIP for which $L_\ell \geq 1$ for all $1 \leq \ell \leq K$.

Using these observations, we can write the conditional PDP as a function of the initial battery state tuple $(i, j)$ and the number of slots in which energy is harvested. Let $p_{\mathrm{D}}(i, j, m_t, m_r)$ denote the PDP of dual EH links when the transmitter and receiver have $i$ and $j$ units of energy at the start of the frame and harvest $m_t$ and $m_r$ units of energy

during the frame, respectively. The following Lemma provides a closed form expression for the conditional PDP of dual EH links in terms of $p_D(i, j, m_t, m_r)$. We omit the proof as it is straightforward.

**Lemma 2.** *For dual EH links with mutually i.i.d. Bernoulli harvesting processes at the transmitter and receiver with harvesting probabilities $\rho_t$ and $\rho_r$, the conditional PDP, $P_D(K|i, j, \ell = 1)$, can be written as*

$$P_D(K|i, j, \ell = 1) = \sum_{m_t=0}^{K} \sum_{m_r=0}^{K} \binom{K}{m_t} \binom{K}{m_r} \rho_t^{m_t} \rho_r^{m_r} (1 - \rho_t)^{K-m_t} (1 - \rho_r)^{K-m_r} p_D(i, j, m_t, m_r),$$

(2.10)

In the above, the calculation of $p_D(i, j, m_t, m_r)$ depends on the type of retransmission protocol and whether the channel is slow or fast fading. In next subsection, we derive expressions for $p_D(i, j, m_t, m_r)$ for ARQ-based dual EH links over both slow and fast fading channels.

## 2.3.1 Dual EH Links with ARQ

First, we discuss the case of slow fading channels. For slow fading channels, since the channel is constant over the frame, if the packet remains in outage at a particular power level, all future attempts of the packet at the same or lower power level will also remain in outage. Hence, without loss of generality, we can assume that $P_1 < P_2 < \cdots < P_K$. For such policies, $p_D(i, j, m_t, m_r)$ depends on the power level of the *last feasible* attempt (which, in turn, is determined by the tuple $(i, j, m_t, m_r)$). This is stated in the next Lemma.

**Lemma 3.** *For dual EH links with ARQ and slow fading channels, $p_D(i, j, m_t, m_r) = p_{out, \Psi_1}$,*

*where $p_{out,\Psi_1}$ is given by (2.2), and for a given policy $\mathcal{P}$ such that $P_1 < P_2 < \cdots < P_K$, $0 \leq \Psi_1 \leq K$ denotes the number of feasible attempts for the tuple $(i, j, m_t, m_r)$.*

*Proof.* Since $P_1 < P_2 < \cdots < P_K$, we write

$$
\begin{aligned}
p_{\text{D}}(i, j, m_t, m_r) &= \Pr\left\{ \bigcap_{\ell=1}^{\Psi_1} \left( |h|^2 < \frac{\gamma_0 \mathcal{N}_0}{P_\ell} \right) \right\}, \\
&= \Pr\left\{ \left( |h|^2 < \frac{\gamma_0 \mathcal{N}_0}{P_{\Psi_1}} \right) \right\} = p_{\text{out},\Psi_1}.
\end{aligned}
\tag{2.11}
$$

$\square$

In the above Lemma, the outage probability depends on $\Psi_1$, the number of feasible transmission attempts (or $L_{\Psi_1}$) in a frame. This, in turn, depends on the energy available in the frame, which is a function of the battery states at the beginning of the frame, $(i, j)$, as well as on the number of slots in which the energy is harvested and stored in the battery. In general, the available energy depends on the order in which energy arrives and is used. Let the total energy available at the transmitter and receiver in a frame be denoted by $E_{\text{avl}}^t$ and $E_{\text{avl}}^r$, respectively. The following Lemma provides an expression for the number of attempts, $\Psi_1$, in terms of $E_{\text{avl}}^t$ and $E_{\text{avl}}^r$.

**Lemma 4.** *For a given policy $\mathcal{P} = \{P_1, P_2, \ldots, P_K\}$,*

$$
\Psi_1 = \min\{\kappa_t, \kappa_r\},
\tag{2.12}
$$

$$
\text{where } \kappa_t \triangleq \max\{\ell | 1 \leq \ell \leq K, E_{\text{avl}}^t - \sum_{k=1}^{\ell} P_k T_p \geq 0\},
\tag{2.13}
$$

$$
\kappa_r \triangleq \max\{\ell | 1 \leq \ell \leq K, E_{\text{avl}}^r - \ell R \geq 0\}.
\tag{2.14}
$$

*Here, $\kappa_t$ and $\kappa_r$ denote the number of feasible attempts in the current frame at the transmitter and receiver, respectively.*

*Proof.* Equation (2.12) follows from the operation of the coordinated sleep-wake protocol, while (2.13) and (2.14) follow from the energy neutrality constraint. □

Next, for a given initial battery level and amount of energy harvested at the transmitter and receiver, we propose an approximation for $E_{\text{avl}}^t$ and $E_{\text{avl}}^r$. Due to the randomness in the energy arrivals and uses, $E_{\text{avl}}^t(i, m_t)$ and $E_{\text{avl}}^r(j, m_r)$ are random variables, taking values $i \leq E_{\text{avl}}^t(i, m_t) \leq i + m_t$ and $j \leq E_{\text{avl}}^r(j, m_r) \leq j + m_r$. We approximate the $E_{\text{avl}}^t$ and $E_{\text{avl}}^r$ as $\min\{i + m_t, B_{\text{max}}^t\}$ and $\min\{j + m_r, B_{\text{max}}^r\}$, respectively. In general, this approximation provides a lower bound on $E_{\text{avl}}^t$ and $E_{\text{avl}}^r$, which can potentially result in underestimation of number of feasible attempts, $\Psi_1$. However, the next Lemma asserts that, in a scenario when the size of the battery at the EHNs is sufficient to store the energy needed to support all $K$ attempts in a frame, there is no error in the above approximation. It also provides an exact expression for $E_{\text{avl}}^t$ and $E_{\text{avl}}^r$ in a scenario when $R \geq 1$ and $L_\ell \geq 1$ for all $1 \leq \ell \leq K$.

**Lemma 5.** *In a given frame, let $i$ and $j$ be the initial battery states, and $m_t$ and $m_r$ be the number of slots where energy is harvested, at the transmitter and receiver, respectively.*

1. *Consider a power control policy such that $\sum_{\ell=1}^K L_\ell \leq B_{\text{max}}^t$ and $KR \leq B_{\text{max}}^r$. Then, the number of feasible attempts, $\Psi_1$, computed using the approximations $E_{\text{avl}}^t \approx \min\{i + m_t, B_{\text{max}}^t\}$ and $E_{\text{avl}}^r \approx \min\{j + m_r, B_{\text{max}}^r\}$ are accurate.*

2. *Also, consider a policy such that $L_\ell \geq 1$ for all $1 \leq \ell \leq K$ and $R \geq 1$. Then, $E_{\text{avl}}^t = i + m_t$ and $E_{\text{avl}}^r = j + m_r$.*

*Proof.* See Appendix A.2. □

This completes the computation of the PDP in closed-form. In the scenarios mentioned in the above Lemma, the computed PDP is *exact*. However, when the hypotheses on the power control policy in the above Lemma do not hold, the above approximations are a lower bound on the available energy, $E_{\text{avl}}^t$ and $E_{\text{avl}}^r$, which results in an underestimation of the number of feasible attempts. Hence, in general, the PDP computed using these closed-form expressions serve as an *upper bound* on the actual PDP.

We next turn to the case of *fast fading* channels, and provide an expression for $p_{\text{D}}(i, j, m_t, m_r)$ in the next Lemma.

**Lemma 6.** *For fast fading channels, $p_{\text{D}}(i, j, m_t, m_r)$ simplifies as*

$$p_{\text{D}}(i, j, m_t, m_r) = \prod_{\ell=1}^{\Psi_1} p_{out,\ell}, \tag{2.15}$$

*where $\Psi_1$ is given by (2.12).*

*Proof.* In the fast fading case, since the channel is i.i.d. from slot to slot, $p_{\text{D}}(i, j, m_t, m_r)$ is the product of the outage probabilities of all the individual attempts. □

From Lemmas 3 and 6, it is evident that for a given policy, slow fading channels result in a higher $p_D(i, j, m_t, m_r)$ compared to fast fading channels. Hence, a given PDP can be achieved at a significantly lower harvesting rate when the channel is fast fading compared to the case when it is slow fading (see Figs. 5.5 and 2.6). In Sec. 2.4.4, for dual EH links operating in the energy unconstrained regime, we provide an expression for the performance gain of fast fading channels over slow fading channels.

## 2.3.2 Dual EH Links with HARQ-CC

To obtain closed-form expressions for the PDP of dual EH links with HARQ-CC, we use (4.8), which requires us to determine $p_D(i, j, m_t, m_r)$. With HARQ-CC, $p_D(i, j, m_t, m_r)$ is written as

$$p_D(i, j, m_t, m_r) = \Pr\left[\frac{\sum_{\ell=1}^{\Psi_1} P_\ell |h_\ell|^2}{\mathcal{N}_0} < \gamma_0\right], \tag{2.16}$$

where $\Psi_1$ is given by (2.12). For *slow fading* channels,

$$p_D(i, j, m_t, m_r) = \Pr\left[|h|^2 < \frac{\gamma_0 \mathcal{N}_0}{\sum_{\ell=1}^{\Psi_1} P_\ell}\right],$$
$$= 1 - e^{-\frac{\gamma_0 \mathcal{N}_0}{\sigma_c^2 \sum_{\ell=1}^{\Psi_1} P_\ell}}, \tag{2.17}$$

where (2.17) is written using (2.3). For *fast fading* channels

$$p_D(i, j, m_t, m_r) = \Pr\left[\sum_{\ell=1}^{\Psi_1} L_\ell |h_\ell|^2 < \frac{\gamma_0 \mathcal{N}_0 T_p}{E_s}\right]. \tag{2.18}$$

In the above equation, $\sum_{\ell=1}^{\Psi_1} L_\ell |h_\ell|^2$ is a sum of independent and non-identically distributed exponential random variables. The $p_D(i, j, m_t, m_r)$ can be written as [38]

$$p_D(i, j, m_t, m_r) = 1 - \sum_{s=1}^{M_{\Psi_1}} \sum_{t=1}^{\tau_s} \sum_{k=0}^{t-1} \frac{\chi_{s,t}(\mathbf{L}_{\Psi_1})}{k!} \left(\frac{X}{L_{\{s\}}}\right)^k e^{-\left(\frac{X}{L_{\{s\}}}\right)}, \tag{2.19}$$

where $X = \frac{\gamma_0 \mathcal{N}_0 T_p}{E_s}$, $\mathbf{L}_{\Psi_1} = \text{diag}(\frac{L_1}{\sigma_c^2}, \frac{L_2}{\sigma_c^2}, \ldots, \frac{L_{\Psi_1}}{\sigma_c^2})$, and $M_{\Psi_1}$, $1 \leq M_{\Psi_1} \leq \Psi_1$ is the number of distinct nonzero elements of $\mathbf{L}_{\Psi_1}$. $L_{\{1\}}, L_{\{2\}}, \cdots, L_{\{M_{\Psi_1}\}}$ denote the distinct nonzero elements of $\mathbf{L}_{\Psi_1}$, and $\tau_s$ denotes the multiplicity of $L_{\{s\}}$. Note that $\Psi_1$ is a function of $(i, j, m_t, m_r)$, given by (2.12). Here, $\chi_{s,t}(\mathbf{L}_{\Psi_1})$ denotes the $(s, t)^{\text{th}}$ characteristic coefficient

of $\mathbf{L}_{\Psi_1}$ such that

$$\det(\mathbf{I} + u\mathbf{L}_{\Psi_1})^{-1} = \frac{1}{(1 + uL_{\{1\}})^{\tau_1} \cdots (1 + uL_{\{M_{\Psi_1}\}})^{\tau_{M_{\Psi_1}}}},$$

$$= \sum_{s=1}^{M_{\Psi_1}} \sum_{t=1}^{\tau_s} \frac{\chi_{s,t}(\mathbf{L}_{\Psi_1})}{(1 + uL_{\{s\}})^t}, \tag{2.20}$$

where $u$ is a scalar satisfying $\det(\mathbf{I} + u\mathbf{L}_{\Psi_1}) \neq 0$. In the general case, $\chi_{s,t}(\mathbf{L}_{\Psi_1})$ is given by following

$$\chi_{s,t}(\mathbf{L}_{\Psi_1}) = \left(\frac{-1}{L_{\{s\}}}\right)^{\omega_{s,t}} \sum_{\substack{k_1 + \cdots + k_{M_{\Psi_1}} = \omega_{s,t} \\ k_s = 0 \\ k_n \in \{0, \omega_{s,t}\} \text{ for } n \neq s}} \left\{ \prod_{\substack{n=1 \\ n \neq s}}^{M_{\Psi_1}} \binom{\tau_n + k_n - 1}{k_n} \left( \frac{L_{\{n\}}^{k_n}}{\left(1 - \frac{L_{\{n\}}}{L_{\{s\}}}\right)^{\tau_n + k_n}} \right) \right\}, \tag{2.21}$$

where $\omega_{s,t} = \tau_s - t$. In the above, (2.19) simplifies in the special cases of *equal* power and *distinct* power policies. The simplified expressions, as well as details on the derivation of the above result, are presented in [38].

Thus, the outage probability, $p_D(i, j, m_t, m_r)$, of HARQ-CC depends on the number of realizable attempts, $\Psi_1$, which, in turn, depends on the EH profiles, the policy $\mathcal{P}$, and the energy required for decoding. We discuss the performance gain of HARQ-CC over ARQ and provide further insights in the next section.

Substituting the expressions for $p_D(i, j, m_t, m_r)$ derived above into the conditional PDP $P_D(K|i, j, \ell = 1)$ in (4.8), we can now compute the PDP using (2.6) and (2.7). This completes the PDP analysis of dual EH links for both ARQ and HARQ-CC, with both slow and fast fading channels.

In some applications, such as body area networks, an EHN may be a battery-less node [57], while in other applications the battery can be very large (practically infinite).

In the next section, we show how our framework can be used to obtain closed-form expressions for the PDP and discuss the insights obtained from the analysis of these special cases.

## 2.4 Special Cases: Zero and Infinite Battery

### 2.4.1 Dual EH Links with Battery-less EHNs

The PDP analysis of a node with *zero energy buffer* can be obtained as a special case of the above analysis by setting $B_n^t = B_n^r = 0$ for all $n$, and $E_s = PT_p$ and $R \leq 1$, as for a battery-less node it is optimal to use all the harvested energy immediately. Hence, the PDP for slow fading channels is given by

$$P_{\mathrm{D}}(K) = 1 - \left(1 - (1 - \rho_t\rho_r)^K\right) e^{-\frac{\gamma_0 \mathcal{N}_0 T_p}{E_s \sigma_c^2}},\tag{2.22}$$

where (2.22) is written using (2.2). The PDP of EH links with battery-less nodes in the other cases, i.e., ARQ with fast fading channel and with HARQ-CC, can be obtained similarly, and the corresponding expressions are provided in [58].

### 2.4.2 Dual EH Links with Infinite Batteries: the Energy Unconstrained Regime

The PDP of dual EH links with infinite capacity batteries at both the EHNs is determined by the statistics of the EH process, the wireless channel, and the transmit and receive power policies. Here, we characterize the conditions under which the randomness in the EH process does not affect the PDP of the system. We call it the *energy unconstrained regime* (EUR). In the EUR, we can obtain simplified expressions for the

PDP.

A dual EH link with infinite energy buffers at the nodes operates in the EUR if, at each node, the average energy harvested per frame is greater than the average energy consumed per frame. When this happens, the battery state executes a random walk with positive drift. As a consequence, over time, the available energy grows unboundedly, and the node is able to make all its transmission/reception attempts. Also, in this case, the coordinated sleep-wake protocol is not necessary.

Under our EH model, the expected energy harvested per frame at the transmitter and receiver are $K\rho_t E_s$ and $K\rho_r E_s$, respectively. Now, for *slow fading channels*, the average energy consumed at the transmitter and receiver are given by

$$E_{\text{av}_t}^c = \sum_{\ell=1}^{K} p_{\text{out},\ell-1} L_\ell E_s, \tag{2.23}$$

$$E_{\text{av}_r}^c = \sum_{\ell=1}^{K} \mathbb{1}_{\{L_\ell > 0\}} p_{\text{out},\ell-1} R E_s, \tag{2.24}$$

respectively, where $\mathbb{1}_{\{L_\ell > 0\}}$ is an indicator variable which is one when $L_\ell > 0$, and equals zero otherwise; and $p_{\text{out},\ell-1}$ is given by (2.2). Here, (2.23) is written using the fact that if the packet is transmitted at energy level $L_\ell$ is not successful, it is transmitted at power level $L_{\ell+1}$ in the next attempt, and so on. Hence, for slow fading channels, the EH link operates in the EUR if

$$\frac{1}{K} \sum_{\ell=1}^{K} p_{\text{out},\ell-1} L_\ell < \rho_t, \tag{2.25}$$

$$\frac{R}{K} \sum_{\ell=1}^{K} \mathbb{1}_{\{L_\ell > 0\}} p_{\text{out},\ell-1} < \rho_r. \tag{2.26}$$

For the other cases, conditions under which the system operates in the EUR can be
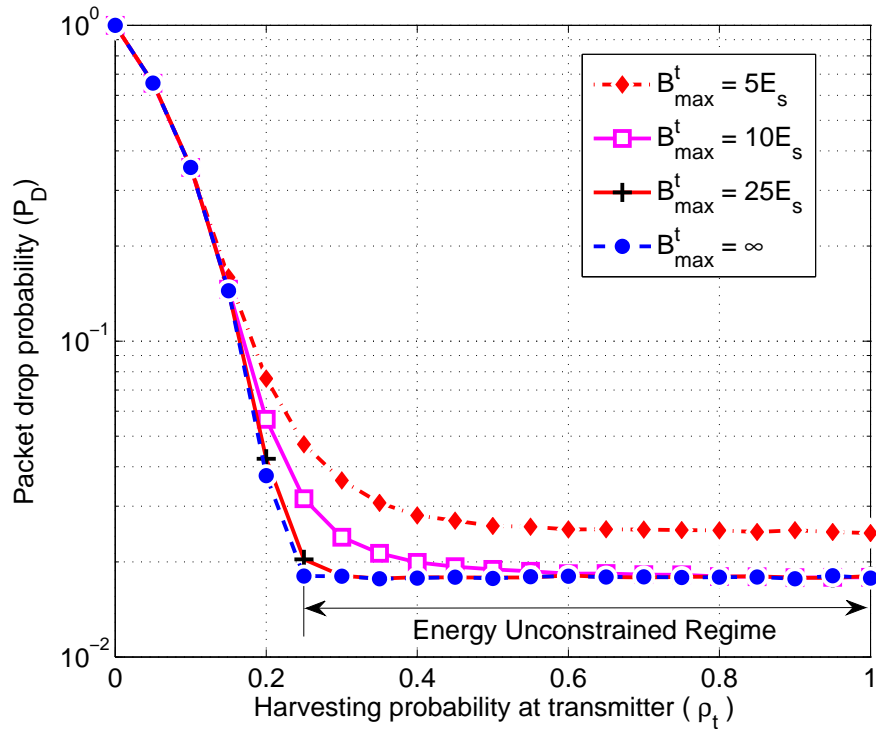
Figure 2.4: Illustration of the EUR in slow fading channels with ARQ. The average energy consumed per frame is $E_{av_t}^c \approx 0.83 E_s$. The transmission policy used is $[0.5 \ 1.5 \ 2.5 \ 3.5]$. The parameters chosen are $\gamma_0 = 10$ dB, $E_s = 15$ dB, and $K = 4$. The simulations are done for a slow fading channel and $\rho_r = 1$.

obtained similarly; but the expressions are omitted due to lack of space. Next, we derive the PDP of EH links with infinite buffers.

### 2.4.3 Packet Drop Probability in the Energy Unconstrained Regime

As mentioned earlier, in the EUR, the battery states at the transmitter and receiver have a net positive drift, and over time, accumulate infinite energy. Hence, all $K$ transmission attempts are possible. Thus, in the EUR, the PDP of dual EH links with infinite capacity batteries can be obtained by setting $\Psi_1 = K$ in Lemma 3, (2.15), (2.17), and (2.19). Note that, in this case, the PDP is equal to the conditional PDP.

Fig. 2.4 illustrates the EUR for ARQ-based links with a slow fading channel. As can be seen from the figure, in practice, an EH link with moderately sized energy buffers (e.g., $B_{\max}^t \approx 12E_{\mathrm{av}_t}^c$ or $10E_s$) can also operate in the EUR, at almost the same values of harvesting probability as for the infinite energy buffer case. Roughly, the probability that batteries at both nodes are in a state $(i, j)$ in which $K$ attempts can be made irrespective of the number of harvesting slots $m_t$ and $m_r$ is close to unity. A rigorous analysis of the achievability of the EUR for finite capacity batteries requires the use of tools from random walks and martingales, and will be presented in our follow up work. In the next subsection, we discuss the insights obtained from the closed-form PDP expression derived in Sec. 2.3, when the dual EH link is operating in the EUR.

### 2.4.4 Discussion on the PDP of Dual EH Links in the EUR

In this subsection, we consider ARQ-based dual EH links equipped with finite sized batteries, and we first compare the performance under slow fading with that under fast fading.

For the battery states $(i, j)$ where $\Psi_1 = K$ attempts are realizable, using Lemmas 3 and 6, it can be deduced that the $p_{\mathrm{D}}(i, j, m_t, m_r)$ takes the values $p_{\mathrm{out},K}$ and $\prod_{\ell=1}^K p_{\mathrm{out},\ell}$ for slow and fast fading channels, respectively. Hence, using (2.6), the PDP of the slow and fast fading channels can be approximated as $p_{\mathrm{out},K}$ and $\prod_{\ell=1}^K p_{\mathrm{out},\ell}$, respectively. Thus, for the dual EH links with the ARQ protocol, when the power policy $\mathcal{P}$ allows the link to operate in the EUR, the difference in the PDP of slow and fast fading channels is given by

$$\Delta P_{\mathrm{D}} = p_{\mathrm{out},K}\left(1 - \prod_{\ell=1}^{K-1} p_{\mathrm{out},\ell}\right).$$

For slow fading channels with ARQ, it is better to use a policy that makes a single attempt with high power, while for fast fading channels, using an equal power transmit policy will result in a lower PDP. Using similar arguments, one can deduce that for dual EH links with HARQ-CC and slow fading channels, the PDP of a policy $\mathcal{P}$ depends only on the accumulated energy $\sum_{\ell=1}^{K} L_\ell$, and not on the individual attempt energy levels. One can obtain similar insights for dual EH links with fast fading channels with HARQ-CC operating in the EUR.

In the next section, we show that the framework presented in Sec. 2.2 naturally extends to mono EH links, where one node is an EHN while the other node is connected to the mains, or is operating in the EUR. We also show that the PDP analysis for mono-T links presented in [2, 34] is a special case of our analysis.

## 2.5 PDP Analysis of Mono EH Links

In this section, for both slow and fast fading channels, we consider the PDP analysis of both mono-T and mono-R EH links, with both ARQ and HARQ-CC protocols.

First, we consider the mono-T case. Similar to the analysis of dual EH links, the evolution of the system within a frame can be modeled as a DTMC whose state is represented by the tuple $(B_n^t, U_n)$, where $B_n^t$ and $U_n \in \{-1, 1, \dots, K\}$ are as defined in Sec. 2.2. Hence, the PDP is given as

$$P_\mathrm{D}(K) = \sum_{i=0}^{B_\mathrm{max}^t} \pi(i) P_\mathrm{D}\left(K|i, \ell = 1\right), \tag{2.27}$$

where $\pi(i)$ denotes the stationary probability that the transmitting EHN has $iE_s$ energy in the battery at the beginning of the frame, and $P_\mathrm{D}\left(K|i, \ell = 1\right)$ denotes the conditional

PDP. In the above, the stationary probabilities can be obtained by using (2.7). Here, the $(i,j)^{\text{th}}$ entry of the TPM $\boldsymbol{G}'$ equals $\Pr(B_{(M+1)K} = j | B_{MK} = i)$, i.e., it contains the $K$-step transition probabilities of the battery state. These probabilities can be calculated using the one-step TPM $\boldsymbol{G}_m$, which can in turn be obtained from the TPM for dual EH links defined in (A.1), by setting $B^r_{\max} = \infty$ and $j_1 = j_2 = \infty$. The expression for $\boldsymbol{G}_m$ is provided in Appendix A.3.

The conditional PDP, $p_{\text{D}}(K|i, \ell = 1)$, is written as

$$P_{\text{D}}(K|i, \ell = 1) = \sum_{m_t=0}^{K} \binom{K}{m_t} \rho_t^{m_t} (1 - \rho_t)^{K-m_t} p_{\text{D}}(i, m_t). \tag{2.28}$$

The above equation is obtained using (4.8) with $m_r = K$ and $\rho_r = 1$. In (2.28), $p_{\text{D}}(i, m_t)$ denotes the PDP when the transmitter has $i$ units of energy at the beginning of the frame and harvests energy in exactly $m_t$ slots. For both slow and fast fading channels, the $p_{\text{D}}(i, m_t)$ can be obtained from $p_{\text{D}}(i, j, m_t, m_r)$ by setting $j = \infty$, i.e., $\Psi_1 = \kappa_t$ given by (2.13).

The analysis for mono-T links with HARQ-CC, as well as for mono-R links with ARQ and HARQ-CC can be obtained in a similar fashion. The results are summarized in Table 2.1. The conditions for operating in the EUR can be obtained using the results of dual EH links, by simply dropping the constraint corresponding to the non-EH node. Similarly, the expressions for the PDP of mono EH links with battery-less EH nodes can be obtained by setting $\rho_t = 1$ or $\rho_r = 1$, corresponding to the node that is connected to the mains.

The results presented thus far correspond to the case where the harvesting processes at the transmitter and receiver are spatially and temporally independent. In the next

Table 2.1: Conditional PDP of mono EH links

| **Expression for conditional PDP of mono-T links employing HARQ-CC** | |
|---|---|
| $P_{\mathrm{D}}(K\|i,\ell=1)$ | $\sum_{m_t=0}^{K}\binom{K}{m_t}\rho_t^{m_t}(1-\rho_t)^{K-m_t}p_{\mathrm{D}}(i,m_t)$ |
| $p_{\mathrm{D}}(i,m_t)$ | Obtained using (2.17) and (2.19) with $\Psi_1=\kappa_t$. |
| **Expression for conditional PDP of mono-R links employing ARQ** | |
| $P_{\mathrm{D}}(K\|j,\ell=1)$ | $\sum_{m_r=0}^{K}\binom{K}{m_r}\rho_r^{m_r}(1-\rho_r)^{K-m_r}p_{\mathrm{D}}(j,m_r)$ |
| $p_{\mathrm{D}}(i,m_r)$ | Obtained using Lemma 3 and (2.15) with $\Psi_1=\kappa_r$. |
| **Expression for conditional PDP of mono-R links employing HARQ-CC** | |
| $P_{\mathrm{D}}(K\|j,\ell=1)$ | $\sum_{m_r=0}^{K}\binom{K}{m_r}\rho_r^{m_r}(1-\rho_r)^{K-m_r}p_{\mathrm{D}}(j,m_r)$ |
| $p_{\mathrm{D}}(j,m_r)$ | Obtained using (2.17) and (2.19) with $\Psi_1=\kappa_r$. |

section, we briefly discuss the extension to the case where the EH processes are corre-
lated.

## 2.6 Extension to Spatially and Temporally Correlated EH Processes

In the subsection below, we show the extension of the PDP analysis to the case where
the EH process is temporally correlated, by modeling the process using a stationary
Markov model.

### 2.6.1 PDP Analysis with a Stationary Markov EH Process

In this subsection, we model the temporal correlation in the EH process using a first
order stationary Markov model, which is described by the set of harvesting energy
levels, $\mathcal{E} \triangleq \{e_1^t,\ldots,e_{\max}^t\}$, and the probabilities, $p_{a,b} = \Pr\left[E_{n+1}^t = e_b^t | E_n^t = e_a^t\right]$, that $e_b^t$
units of energy is harvested in the $(n+1)^{\mathrm{th}}$ slot, given that $e_a^t$ units of energy was
harvested in the $n^{\mathrm{th}}$ slot, where both $e_a^t$ and $e_b^t \in \mathcal{E}$. The EH process at the receiver is

modeled similarly.

When the EH processes follow a stationary Markov model, the system evolution over a frame depends not only on the initial battery states at the transmitter and receiver, but also on the initial state of the EH Markov chains. Hence, the evolution of the system can be modeled as a DTMC with state denoted by a tuple $(B_n^t, B_n^r, E_n^t, E_n^r, U_n)$. The PDP is given as

$$P_{\mathrm{D}}(K) = \sum_{(i,j,e_a^t,e_c^r)} \pi(i,j,e_a^t,e_c^r) P_{\mathrm{D}}(K|i,j,e_a^t,e_c^r,\ell = 1), \qquad (2.29)$$

where $\pi(i,j,e_a^t,e_c^r)$ denotes the stationary probability that, at the beginning of the frame, the state of the battery and EH process at the transmitter and receiver are $(i,j)$ and $(e_a^t, e_c^r)$, respectively, while $P_{\mathrm{D}}(K|i,j,e_a^t,e_c^r,\ell = 1)$ denotes the PDP conditioned on the state at the beginning of the frame. To obtain the stationary probabilities, using (2.7), one needs to determine the transition probabilities, $\Pr\left[(i_2, j_2, e_b^t, e_d^r) \,|\, (i_1, j_1, e_a^t, e_c^r)\right]$, which can be obtained as a straightforward extension of the transition probabilities given by (A.1) in Appendix A.1 for the Bernoulli harvesting model. The conditional PDP, $P_{\mathrm{D}}(K|i,j,e_a^t,e_c^r,\ell = 1)$, can be written as

$$P_{\mathrm{D}}(K|i,j,e_a^t,e_c^r,\ell = 1) = \sum_{E_t=0}^{Ke_{\max}^t} \sum_{E_r=0}^{Ke_{\max}^r} p(E_t, E_r|e_a^t,e_c^r) p_{\mathrm{D}}(i,j,E_t,E_r), \qquad (2.30)$$

where $p(E_t, E_r|e_a^t,e_c^r)$ denotes the probability that, during the frame, the transmitter and receiver harvest $E_t$ and $E_r$ units of energy, respectively, given the harvested energy at the beginning of the frame are $e_a^t$ and $e_c^r$, respectively, and $p_{\mathrm{D}}(i,j,E_t,E_r)$ denotes the PDP when the transmitter and receiver batteries have $i$ and $j$ units of energy, respectively, at the beginning of the frame. The $p(E_t, E_r|e_a^t,e_c^r)$ can be calculated using the transition probabilities, $p_{a,b}$, of the stationary Markov model. To compute

$p_{\mathrm{D}}(i, j, E_t, E_r)$, we use $E_{\mathrm{avl}}^t \approx \{i + E_t, B_{\max}^t\}$ and $E_{\mathrm{avl}}^r \approx \{j + E_r, B_{\max}^r\}$ and calculate $\Psi_1$ using Lemma 4. The obtained $\Psi_1$ can be used to compute $p_{\mathrm{D}}(i, j, E_t, E_r)$ using the expression for $p_{\mathrm{D}}(i, j, m_t, m_r)$ provided in Sec. IV.

Next, we extend our PDP analysis to the case of spatially correlated EH processes.

## 2.6.2 Extension to Spatially Correlated EH Processes

In case the independence between the EH process of the transmitter and receiver does not hold, the joint distribution of two correlated Bernoulli harvesting processes can be modeled as

$$p(e_t, e_r) = p_{00}(1 - e_t)(1 - e_r) + p_{01}(1 - e_t)e_r + p_{10}e_t(1 - e_r) + p_{11}e_te_r, \qquad (2.31)$$

where $e_t, e_r \in \{0, 1\}$ are random variables taking nonzero value if energy is harvested at the transmitter and receiver, respectively, and $p_{00}, p_{01}, p_{10},$ and $p_{11}$ are probability values that add up to 1. To obtain the exact conditional PDP and the 1-step TPM for spatially correlated EH processes, one needs to modify (2.9) and (A.1) in Appendix A.1 by replacing $\rho_t\rho_r$ by $p_{11}$, $\rho_t(1 - \rho_r)$ by $p_{10}$ and so on. Also, the above correlated harvesting model reduces to the independent harvesting case when $p_{00} = (1 - \rho_t)(1 - \rho_r)$, $p_{11} = \rho_t\rho_r$, $p_{10} = \rho_t(1 - \rho_r)$ and $p_{01} = (1 - \rho_t)\rho_r$.

Further, to obtain the closed-form expressions for the conditional PDP when the harvesting processes at the transmitter and receiver are spatially correlated, we modify (4.8) as

$$P_{\mathrm{D}}(K|i, j, \ell = 1) = \sum_{m_t=0}^{K} \sum_{m_r=0}^{K} p'(m_t, m_r)p_{\mathrm{D}}(i, j, m_t, m_r),$$

where

$$p'(m_t, m_r) = \sum_{z=\xi_1}^{\xi_2} \binom{K}{z} \frac{(K-z)!}{(m_r - z)!(K - m_t - m_r + z)!} \frac{1}{(m_t - z)!} p_{11}^z p_{10}^{(m_t - z)} p_{01}^{(m_r - z)} p_{00}^{(K - m_t - m_r + z)}$$

denotes the probability that the transmitter and receiver harvest energy in exactly $m_t$ and $m_r$ slots, respectively. Here, $\xi_1 = \max\{0, m_t + m_r - K\}$ and $\xi_2 = \min\{m_t, m_r\}$.

In the next section, we present simulation results to validate the accuracy of the analytical expressions, and illustrate the various cost-performance tradeoffs involved.

## 2.7 Numerical Results

### 2.7.1 Simulation Setup

We consider a system with slot duration $T_p = 100$ ms and carrier frequency $950$ MHz. The distance between transmitter and receiver is $d = 10d_0$, where $d_0 = 10$ m is the reference distance and the path loss exponent is $\eta = 4$. The additive noise corresponds to a bandwidth of $5$ MHz and $T = 300$ $K$. For this system, $E_s = 5$ dB corresponds to $100$ $\mu J$. To simulate meaningful PDP values ($10^{-2}$ to $10^{-4}$), for slow fading channels we choose $E_s = 12$ dB and $\gamma_0 = 10$ dB, while for fast fading channels we set $E_s = 5$ dB and $\gamma_0 = 12$ dB. The channel from the transmitter to the receiver is assumed to be i.i.d. Rayleigh block fading with block length equal to the packet duration and frame duration for the fast and slow fading cases, respectively. The PDP is computed by simulating the transmission of $10^7$ packets.
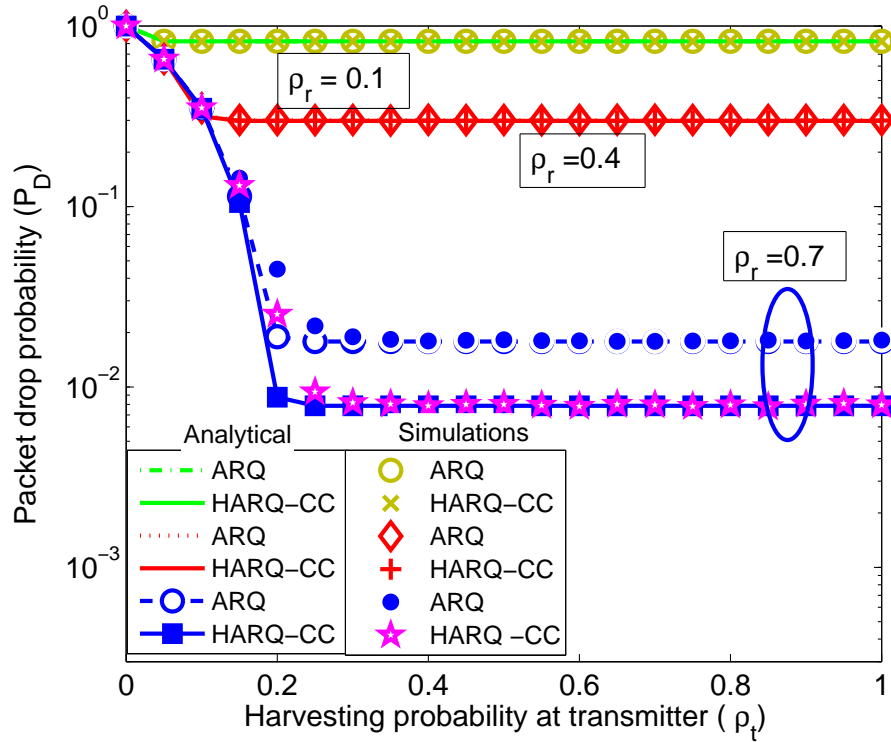
Figure 2.5: Dual EH links with slow fading channels: validation of analytical expressions against simulation results. The transmission policy used is $[0.5\ 1.5\ 2.5\ 3.5]$. The other parameters are $E_s = 12$ dB, $\gamma_0 = 10$ dB, $K = 4$, $R = 2$ and $B_{\max}^t = B_{\max}^r = 20E_s$.

## 2.7.2 Results

**Performance of Dual EH Links**

Figures 5.5 and 2.6 present the PDP as a function of $\rho_t$, in the slow and fast fading cases, respectively. In both the cases, it can be observed that the analytical expressions and simulation results match perfectly. The PDP is dominated by the node which supports the least number of attempts, which, in turn, is determined by the power control policy and EH profiles of the transmitter and receiver.

It can be observed that, for larger values of $\rho_r$, i.e., for $\rho_r = 0.7$ in Fig. 5.5 and $\rho_r = 1$ in Fig. 2.6, the PDP decreases initially and then it remains unchanged with the increase in $\rho_t$ (e.g., $\rho_t > 0.2$ in Fig. 5.5). This happens because at lower values of $\rho_t$, the packet

drops are dominated by the energy outage at the transmitter which gets mitigated as $\rho_t$ increases. For higher values of $\rho_t$ and $\rho_r$, since both nodes harvest enough energy to make all $K$ attempts, packets are dropped only due to the receiver noise or fading, and not due to lack of energy availability. Moreover, in both Figs. 5.5 and 2.6, we observe that for lower values of $\rho_r$ (e.g., $\rho_r = 0.4$) and for large enough $\rho_t$, the randomness of the EH process at the transmitter does not affect the PDP. These regions can be considered to be *partial EUR*, where only one node is able to operate in the EUR. However, the harvesting probability at which an EHN attains the EUR also depends on the power control policy and the EH profile of the other EHN. For example, as shown in both Figs. 5.5 and 2.6, the value of $\rho_t$ at which the transmitter achieves the partial EUR increases with the increase in $\rho_r$.

In Fig. 2.6, we can observe that, in contrast to the slow fading case, we obtain lower PDP values in the EUR, due to the time-diversity offered by the fast fading channels. Thus, the time-diversity offered by fast fading channels can compensate for lower harvested energy values.

For $\rho_r = 0.7$ and $\rho_r = 1$ in Figs. 5.5 and 2.6, respectively, the HARQ-CC outperforms ARQ by approximately a factor of $2$ and $10$ in the slow and fast fading cases, respectively, in the EUR. However, in both cases, for lower $\rho_r$, the HARQ-CC does not offer as significant a gain as for $\rho_r = 0.7$ in Fig. 5.5, and for $\rho_r = 1$ in Fig. 2.6. This is due to the fact that at lower values of $\rho_r$, the receiver does not have sufficient energy to exploit the benefits of chase combining. Note that, Figs. 5.5 and 2.6 correspond to the scenario when the hypothesis $(i)$ in Lemma 5 is satisfied.

In Fig. 2.7, we consider a small battery regime to compare the PDP computed using
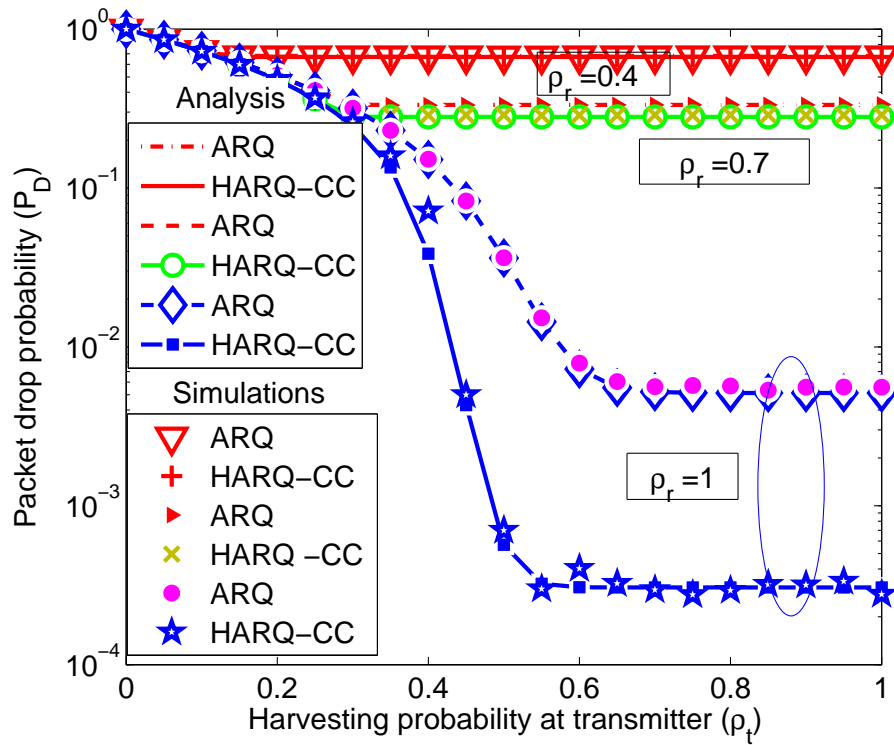
Figure 2.6: Dual EH links with fast fading channels: validation of analytical expressions against simulation results. The transmission policy used is [0.5 1.5 2.5 3.5]. The other parameters are $E_s = 5$ dB, $\gamma_0 = 12$ dB, $K = 4$, $R = 2$ and $B_{max}^t = B_{max}^r = 20E_s$.

the closed-form analytical expressions against the simulated PDP. We also plot the PDP

computed using *recursive* expression provided in Lemma 1. In this case, we consider

two policies: [1 1.25 1.5 2] and [0.5 0.75 1.5 2]. The policies represent two scenarios: in

the first case, the policy consumes more than $E_s$ energy in each slot, while, in the latter

case, the size of the battery at both transmitter and receiver is not sufficient to store

the total energy required by the policy to make all $K$ attempts during a frame. There-

fore, in the first case, the hypothesis $(ii)$ of Lemma 5 is satisfied, while in the latter case

*neither* of the two hypotheses in Lemma 5 is satisfied. In both these cases, we observe

that the simulated results closely match the closed-form analytical expression. For the

policy [0.5 0.75 1.5 2], the near-exact match between closed-form PDP and simulated
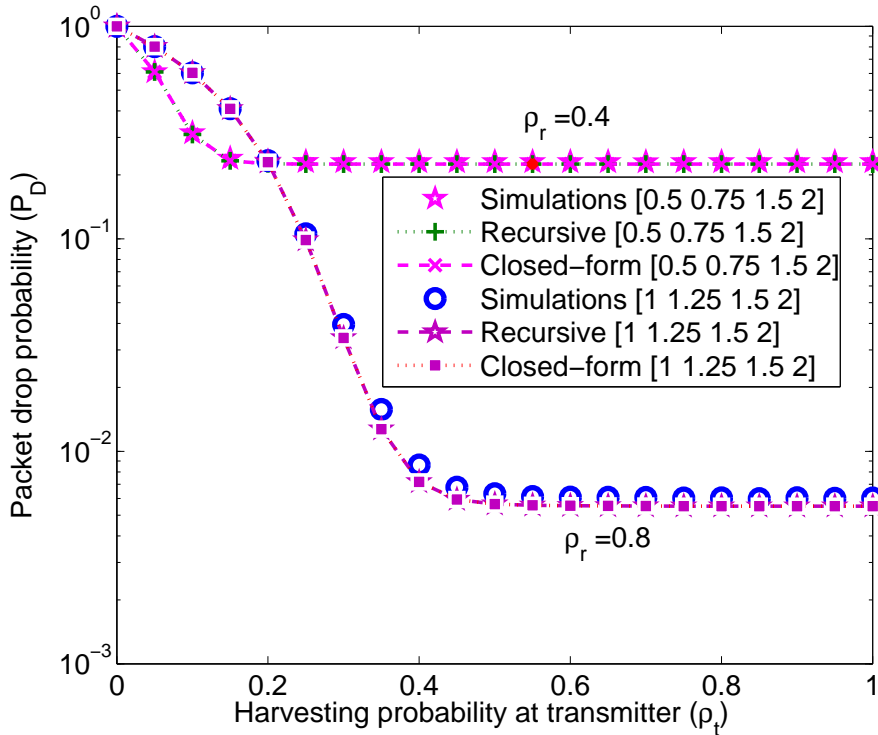
Figure 2.7: Accuracy of analytical expressions for small battery regime. The comparison is done for ARQ-based dual EH links over slow fading channels. The size of the batteries at the transmitter and receiver is $B_{\max}^t = B_{\max}^r = 3.5E_s$. Other parameters chosen are $K = 4$, $E_s = 12$ dB, $\gamma_0 = 1$ dB, and $R = 2$.

PDP is due to the small impact of the approximation error, as the number of feasible attempts are determined by the energy availability at the receiver in this case. Specifically, for $\rho_t = 1$, the actual number of feasible attempts for the transmitter and receiver are four and three, respectively, while using the approximation in Lemma 5, the estimated number of attempts are three for both the EHNs. However, since the number of feasible attempts under coordinated sleep-wake protocol are determined by the node which can support fewer attempts among the two EHNs, the approximation error does not impact the accuracy of the closed-form PDP.
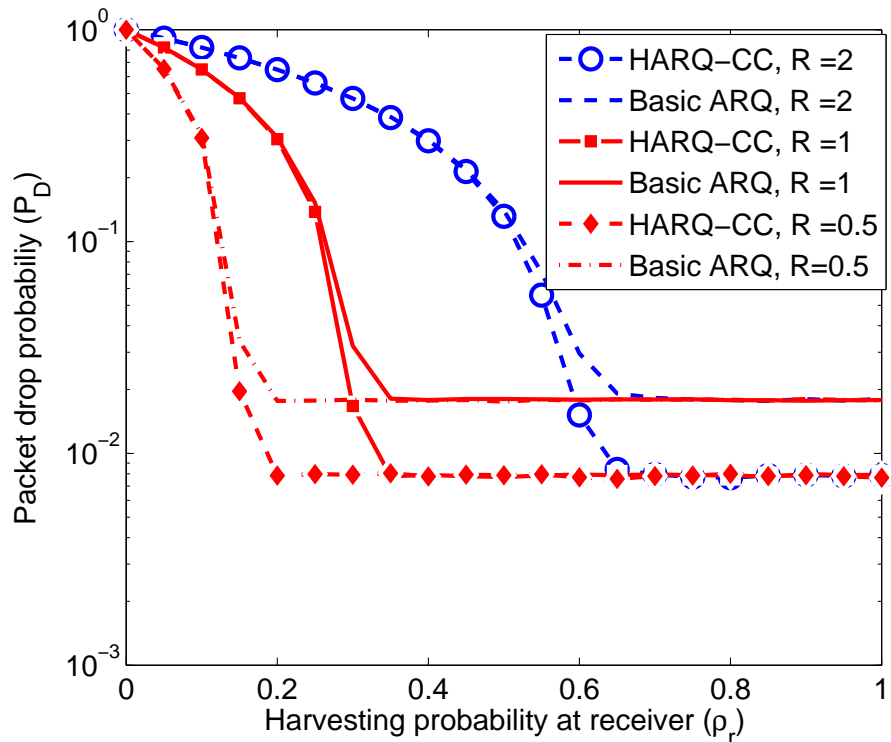
Figure 2.8: PDP of mono-R links with a slow fading channel. The transmission policy used is $[0.5\ 1.5\ 2.5\ 3.5]$. The other parameters are $E_s = 10$ dB, $\gamma_0 = 12$ dB, $K = 4$, and $B^r_{\max} = 20E_s$.

**Special Cases: Mono and Zero Energy Buffer EH Links**

The results in Fig. 2.8 demonstrate the PDP of mono-R links. As can be observed from Fig. 2.8, the value of $\rho_r$ at which the receiver attains EUR increases with $R$, because of the higher average energy consumption. Fig. 2.9 contains the results for dual EH links with zero energy buffers. Again, the analytical expressions and simulation results match perfectly. Also, the results in Figs. 2.8 and 2.9 again highlight the fact that the use of HARQ-CC results in better performance. For Dual EH links, even without an energy buffer, at higher values of $\rho_r$, the use of HARQ-CC results in performance improvement over ARQ approximately, by a factor of 2. However, for mono-R links, the gains occur
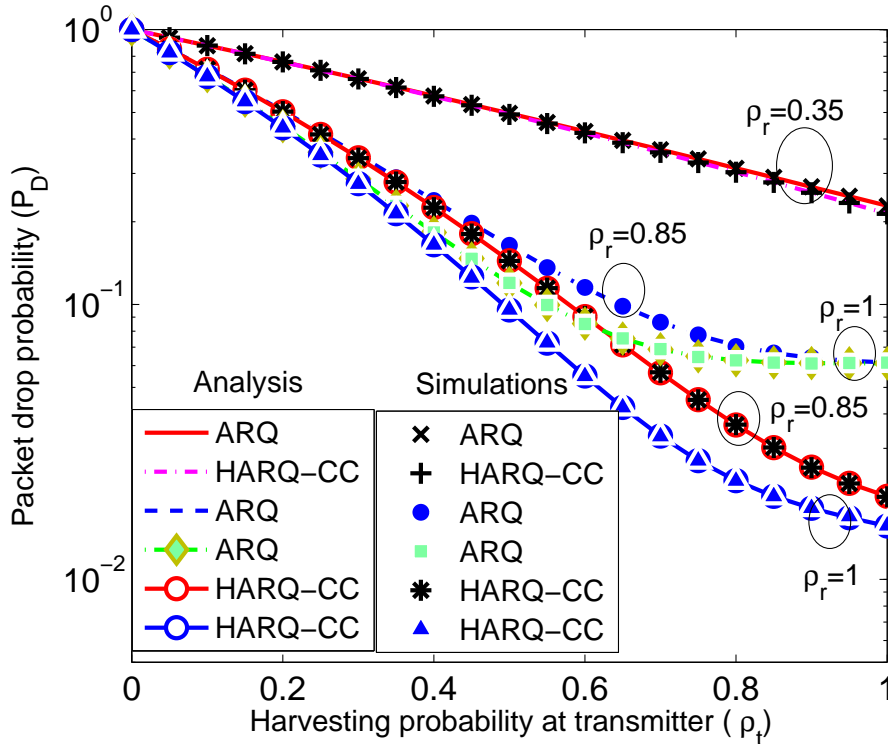
Figure 2.9: Dual EH links with zero energy buffer nodes: validation of analytical expressions against simulations. The other parameters are $E_s = 12$ dB, $\gamma_0 = 10$ dB, $K = 4$, and a slow fading channel.

only after the receiver harvests enough energy to enter the EUR.

## 2.8   Conclusions

In this chapter, we presented a general framework to analyze the PDP of dual EH links with retransmissions. We considered SoC-unaware policies, and slow and fast fading channels.We obtained closed form expressions for the PDP with both ARQ and HARQ-CC, by modeling the system evolution as a discrete-time Markov chain. We extended the analysis to handle correlated harvesting processes at the transmitter and receiver. The PDP expressions for mono EH links are obtained as a special case of the

analysis of dual EH links. Our analysis is useful in quantifying the impact of various system parameters such as the energy harvesting profiles, and energy buffer sizes of both transmitter and receiver, channel coherence time, transmit and receive power control policies etc., on the PDP. We also characterized the energy unconstrained regime of dual EH links and obtained simplified expressions for the PDP in the special cases of zero and infinite size energy buffers. In the next chapter, the closed form expressions derived in this chapter are used to find optimal RIPs for dual as well as mono EH links.

# Chapter 3

# Design of PDP-optimal SoC-unaware Policies for Dual EH Links with Retransmissions

In this chapter, we present a method to design the PDP-optimal SoC-unaware RIPs when the peak transmit power is constrained. To this end, first, we establish the near-optimality of policies that operate in the *energy unconstrained regime (EUR)*. Specifically, we analytically show that for such policies, the gap between the PDP of the dual EH systems with finite and infinite capacity batteries decreases exponentially with the size of the battery at the transmitter and receiver. Next, we show that the non-convex problem of designing optimal RIPs can be reformulated as a *geometric program* in the EUR, which leads to a provably convergent and computationally efficient solution. We design the RIPs for both slow and fast fading channels, and with two different retransmission protocols, namely, the automatic repeat request (ARQ) and hybrid ARQ with chase combining. Numerical results obtained through Monte Carlo simulations show that the proposed RIPs outperform state-of-the-art policies.

## 3.1 PDP Minimization

Our starting point is the closed-form PDP expressions obtained in Chapter 2. The objective function of the PDP optimization problem is given by (2.6). The problem of finding the optimal RIPs for dual EH links, subject to the *energy neutrality constraint* (ENC) and peak power constraint can be stated as follows:

$$\textbf{(P1)} \quad \min_{\mathcal{P}=\{P_1,\ldots,P_K\}} \sum_{(i,j)\in\mathcal{I}} \pi(i,j)P_{\mathrm{D}}(K|i,j,U_n=1), \tag{3.1}$$

subject to $0 \leq P_\ell \leq P_{\max}$, $1 \leq \ell \leq K$, where $P_{\max} \triangleq \frac{L_{\max}E_s}{T_p}$ and $\mathcal{I}$ represents the set of all possible tuples of battery states at the transmitter and receiver. Note that, in the above formulation, the ENC manifests through the stationary probabilities, $\pi(i,j)$, which are determined by the transition probabilities of the DTMC. Due to this, both $\pi(i,j)$ and $P_D(K|i,j,U_n=1)$ have a complicated dependence on the policy $\mathcal{P}$. Moreover, for moderate to large battery capacities, the large state space involved makes it computationally prohibitive to use dynamic programming based approaches.

To reformulate the problem in a computationally tractable form, we look to simplify both the objective and the constraints of (**P1**), without compromising the optimality of the solution. To this end, we first derive asymptotically tight lower and upper bounds on the PDP. The bounds are motivated by the observation that for all possible tuples $(i,j)$ of the battery state at the start of the frame such that the EHNs have sufficient energy to make all $K$ attempts irrespective of the amount of energy harvested during the frame ($m_t$ and $m_r$), the conditional PDP, $P_{\mathrm{D}}(K|i,j,U_n=1)$, is the same. This is because, for all such battery state tuples $(i,j)$, $p_{\mathrm{D}}(i,j,m_t,m_r)$ is equal to the probability

that the packet remains in outage after the $K$ attempts, for all $m_t$ and $m_r$. The bounds are obtained by recognizing that the PDP when all $K$ attempts cannot be guaranteed is at least equal to the PDP when all $K$ attempts can be made, and is at most equal to $1$. The next Lemma provides a lower and an upper bound on the PDP.

**Lemma 7.** *Consider a dual EH link operating with an RIP $\mathcal{P}$ such that $L_\ell \leq L_{\max}$ for all $1 \leq \ell \leq K$. Let $\mathcal{I}_1$ and $\mathcal{I}_2$ be a partition of the set $\mathcal{I}$ of tuples of battery states at the transmitter and receiver such that $\mathcal{I}_1 \triangleq \{(i,j)|0 \leq i < KL_{\max} < B_{\max}^t, \text{ and } 0 \leq j < KR < B_{\max}^r\}$, and $\mathcal{I}_2 \triangleq \mathcal{I}\backslash\mathcal{I}_1$. Then,*

$$P_{D_\infty}^* \leq \min_{\mathcal{P}} \sum_{(i,j)\in\mathcal{I}} \pi(i,j)P_D(K|i,j,U_n=1) \leq P_{D_\infty}^* + \sum_{(i_1,j_1)\in\mathcal{I}_1} \pi(i_1,j_1)\big|_{\mathcal{P}^*},$$

*where $P_{D_\infty}^* \triangleq \min\limits_{\mathcal{P}} P_D\left(K|i,j,U_n=1\right)$ and $\mathcal{P}^* \triangleq \arg\min\limits_{\mathcal{P}} P_D\left(K|i,j,U_n=1\right)$, both subject to $(i,j) \in \mathcal{I}_2$.*

*Proof.* See Appendix B.1. $\square$

Thus, the PDP of a dual EH link with finite sized batteries is lower bounded by $P_{D_\infty}^*$, the minimum conditional PDP that can be obtained when all $K$ attempts are feasible. The lower bound is also the optimum PDP with infinite size batteries. This is because the optimum policy with infinite size batteries is the one that minimizes the PDP among all policies for which the average energy consumed is less than or equal to the average energy harvested at both nodes [10], i.e., for the the links operating in the *energy uncon-strained regime* (EUR). Under EUR, the policy will induce a positive drift in the battery level of both EHNs, which ensures that the nodes will eventually always be able to make all $K$ attempts. On the other hand, the upper bound indicates that the optimal

policy will try to minimize the stationary probability of the set $\mathcal{I}_1$, i.e., the set of the battery states where all $K$ attempts are not guaranteed. Hence, the optimal policy will induce a drift away from the set $\mathcal{I}_1$, which, in turn, also implies a positive drift on the battery states. In the next section, we show that for the policies which induce a positive drift, the bounds proposed in Lemma 7 are tight, provided the battery sizes are sufficiently large. This allows us to approximate the objective function with the lower bound as well as to replace the ENC with a more amenable average power constraint.

## 3.2 Tightness of the Bounds in the EUR

In the following, we establish that, in the EUR, the bounds presented in Lemma 7 are asymptotically tight. It is shown that the difference between the bounds goes to zero as the sum of two terms, each of which decays exponentially with the battery size at the transmitter and receiver, respectively. We first present the following Lemma for the transmitter of a dual EH link.

**Lemma 8.** *Consider the transmitter of a dual EH link operating in the EUR with an RIP $\mathcal{P}$ such that $L_\ell \leq L_{\max}$ for all $1 \leq \ell \leq K$. The stationary probability of the battery at the transmitter being in a state $i \in \mathcal{I}_1^t \triangleq \{i : 0 \leq i < KL_{\max} < B_{\max}^t\}$, such that the transmitter cannot support all $K$ attempts, decays exponentially with $B_{\max}^t$, i.e., $\sum_{i \in \mathcal{I}_1^t} \pi_t(i) = \Theta(e^{r_*^t B_{\max}^t})$, where $\pi_t$ denotes the stationary distribution of the battery state at the transmitter and $r_*^t$ is the negative root of the asymptotic log moment generating function (MGF) of the drift process $X_n^t \triangleq \mathbb{1}_{\{E_n^t \neq 0\}} - \mathcal{L}(B_n^t, B_n^r, U_n)$. Here, $\mathbb{1}_{\{E_n^t \neq 0\}}$ is the indicator variable which equals one if the transmitter harvests the energy in the $n^{th}$ slot, and zero otherwise, while $\mathcal{L}(B_n^t, B_n^r, U_n)$ denotes the energy used by the RIP in the $n^{th}$ slot. The asymptotic log MGF is defined as*

$\Lambda(r) \triangleq \lim_{N \to \infty} \frac{1}{N} \log \mathbb{E}\left[\exp\left(r \sum_{n=1}^{N} X_n^t\right)\right]$, *where* $r \in \mathbb{R}$..

*Proof.* See Appendix B.2. □

Qualitatively, when the EHN operates in the EUR, the battery eventually becomes full and makes small excursions from the state $B_{\max}^t$ towards depleting the battery. Whenever the battery is not full, the drift becomes positive, and this drives the battery towards the full state. Hence, for an EHN with a large battery, the event of hitting the set $\mathcal{I}_1^t$ is a large deviation event, which occurs with the accumulation of a number of rare events (for example, when there is a long patch of slots where no energy is harvested). Intuitively, a similar argument holds for both nodes of a link operating in the EUR. Next, we use the above Lemma to substantiate this intuition via the following theorem.

**Theorem 1.** *For a dual EH link employing an RIP which satisfies the peak power constraint and operates in the EUR, $\sum_{(i,j) \in \mathcal{I}_1} \boldsymbol{\pi}(i,j) = \Theta(e^{r_*^t B_{\max}^t}) + \Theta(e^{r_*^r B_{\max}^r})$, where $r_*^t$ and $r_*^r$ are the negative root of the asymptotic log MGF of the drift process at the transmitter ($X_n^t \triangleq \mathbb{1}_{\{E_n^t \neq 0\}} - \mathcal{L}(B_n^t, B_n^r, U_n)$) and receiver ($X_n^r \triangleq \mathbb{1}_{\{E_n^r \neq 0\}} - \mathcal{R}(B_n^t, B_n^r, U_n)$), respectively. Here, $\mathbb{1}_{\{E_n^t \neq 0\}}$ or $\mathbb{1}_{\{E_n^r \neq 0\}}$ equal one if the energy is harvested at the transmitter or receiver in the $n^{th}$ slot, respectively, and zero otherwise. Also, $\mathcal{L}(B_n^t, B_n^r, U_n)$ and $\mathcal{R}(B_n^t, B_n^r, U_n)$ denote the amount of energy used in the $n^{th}$ slot at the transmitter and receiver, respectively.*

*Proof.* See Appendix B.4. □

The above result establishes that for dual EH links operating in the EUR, $\sum_{\mathcal{I}_1} \boldsymbol{\pi}(i,j)$ decreases exponentially with the size of the battery at the transmitter and receiver. In Fig. 3.1, we illustrate that for a dual EH link operating in the EUR and equipped with moderate sized energy buffers, the percentage difference between the lower and upper
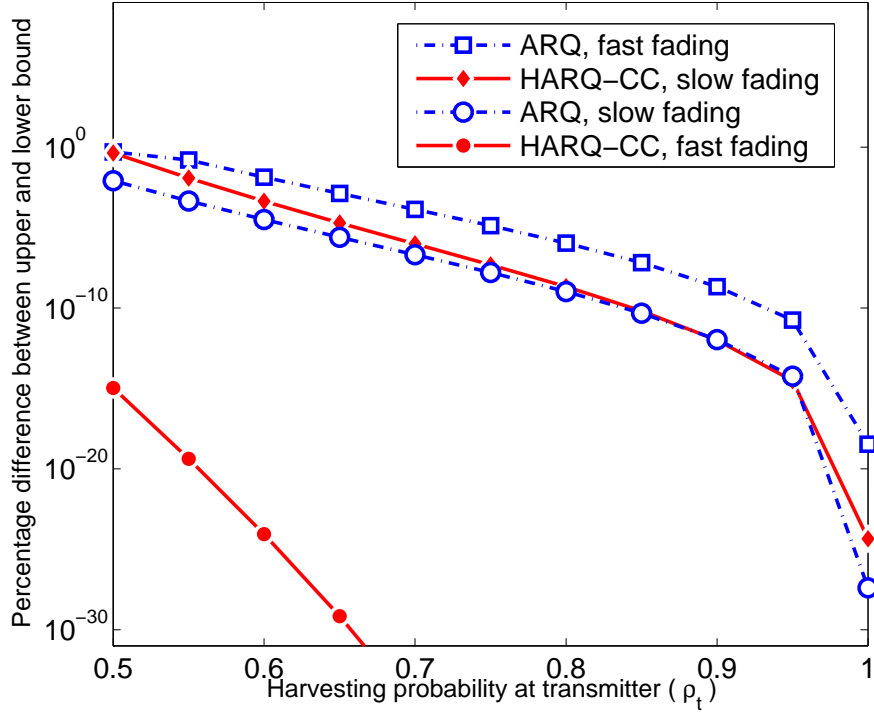
Figure 3.1: Difference between the lower bound and upper bounds on the objective function in (**P1**). The parameters chosen are $E_s = 5$ dB, $\gamma_0 = 10$ dB, $\rho_r = 0.9$, $R = 1$, $B_{\max}^t = B_{\max}^r = 25$ and $K = 4$. The policy used is $\left[ \frac{E_s}{T_p} \quad \frac{E_s}{T_p} \quad \frac{2E_s}{T_p} \quad \frac{2E_s}{T_p} \right]$. Note that, the nodes operate in the EUR under this policy.

bounds on the objective function is negligible. Thus, the lower bound in Lemma 7 is a close approximation to the objective function in (**P1**). Furthermore, the above result implies that the energy neutrality constraint in (**P1**) can be replaced by the simpler EUR constraint, without compromising on the optimality. We conclude this section with the following observation.

*Remark* 2. As shown in [33, Lemma 3], for a policy with a drift $\delta$ (the difference between the mean energy harvested and the mean energy consumed) the negative root of the asymptotic log MGF of the resulting drift process is equal to $-\frac{2\delta}{\sigma_e^2} + o(\delta)$, where $\sigma_e^2$ is

the asymptotic variance [33] of the harvesting process. Thus, for the processes $X_n^t$ and $X_n^r$, the negative roots $r_*^t$ and $r_*^r$ are of the order of the energy saved per frame at the transmitter and receiver, respectively. Thus, for a smaller drift, a larger battery would be needed to achieve the same performance (See Fig. 3.2). Furthermore, for a given drift $\delta$, the harvesting process with larger asymptotic variance, $\sigma_e^2$, would require a larger battery.

In the next section, we reformulate **(P1)** using the result obtained in Theorem 1.

## 3.3 Problem Reformulation

In this section, we design RIPs under the EUR constraints, and then choose the battery size according to Theorem 1.[1] Under Theorem 1, we can reformulate the problem **(P1)** by choosing the lower bound, i.e., $P_D\left(K|i,j,U_n=1\right)$ with $(i,j) \in \mathcal{I}_2$, as the objective function, and by replacing the ENC by the EUR constraints. Using (4.8), as a node operating in the EUR can make all $K$ attempts, $P_D\left(K|i,j,U_n=1\right) = p_D(i,j,m_t,m_r) = f(\mathcal{P})$ for all $(i,j) \in \mathcal{I}_2$, irrespective of the number of slots ($m_t$ and $m_r$), in which energy is harvested. Therefore, in general, for a dual EH link operating in the EUR, the PDP minimization problem is written as follows:

$$\min_{\bar{\mathbf{L}}=\{L_1,\ldots,L_K\}} p_D(i,j,m_t,m_r), \tag{3.2a}$$

$$\text{subject to} \quad \sum_{\ell=1}^{K} L_\ell p_{o,\ell-1} \leq K\rho_t, \text{ and } \quad \sum_{\ell=1}^{K} \chi^\ell p_{o,\ell-1} \leq \frac{K\rho_r}{R}, \tag{3.2b}$$

---

[1]The typical battery size for practical EHNs ranges between 200 mAh-2500 mAh [59]. A 200 mAh capacity battery can deliver 720 J of energy at a nominal voltage of 1 V. Also, using a small solar panel, at 66 % efficiency, NiMH batteries receive 0.13 mJ of energy per 10 ms slot. Thus, with two hours of sunlight, the typical battery size, normalized with respect to $E_s$, equals $5.33 \times 10^6$. Hence, the large battery size assumption is reasonable.

and $0 \leq L_i \leq L_{\max}$, $1 \leq i \leq K$, where $\chi^\ell \triangleq \mathbb{1}_{\{L_\ell \neq 0\}}$ is an indicator variable which is $= 1$ if $L_\ell \neq 0$ and $= 0$ otherwise, and $p_{o,\ell-1}$ denotes the probability that the first $\ell - 1$ transmission attempts have failed; $p_{o,0} = 1$. In the above, (3.2b) are the EUR constraints. For example, (3.2b) is written using the fact that the transmitter operates in the EUR if the average energy consumed by it, $\sum_{\ell=1}^{K} L_\ell E_s p_{o,\ell-1}$, is less than the average energy harvested, $K \rho_t E_s$. The average energy consumed is computed using the fact that $\ell^{\text{th}}$ attempt is made only if all the previous $\ell - 1$ attempts have failed, which happens with probability $p_{o,\ell-1}$, where $p_{o,\ell-1}$ can be written in terms of the outage probabilities defined in (2.2) and (2.3). The receiver operates in the EUR when a similar condition is satisfied. In (3.2b), $\chi^\ell$ denotes the fact that the receiver consumes $R$ units of energy only if the transmitter makes an attempt at a nonzero power level. The solution of (3.2) provides an RIP which achieves near-optimal PDP for the EHNs equipped with batteries of size as prescribed by Theorem 1.

Note that, due to the indicator variables $\chi^\ell$ in the formulation, the optimization problem (3.2) is of exponential complexity in $K$, the number of attempts allowed. In the next subsection, we discuss an interesting observation which reduces the computational complexity from being exponential to linear in the number of attempts.

### 3.3.1 Simplification of Integer Constraints

The problem (3.2) is essentially a set of $2^K - 1$ problems. Depending on the values taken by the variables $\chi^\ell$, the feasibility set of each problem changes. For a given value of the variables $\{\chi^\ell\}_{\ell=1}^{K}$, the objective and constraints in (3.2) are nonconvex functions, and hence, each individual subproblem is a nonconvex nonlinear program. Thus, (3.2)

is a nonconvex mixed integer nonlinear program (NMINLP). In general, finding the solution of an NMINLP is a strongly NP-hard problem [60]. Hence, in order to solve (3.2), we need to solve $2^K - 1$ subproblems, and choose the solution of the subproblem which gives minimum objective value among them as the solution to (3.2). However, we observe that the solution of (3.2) only depends on $\chi = \sum_{\ell=1}^{K} \chi_\ell$, i.e., if $\chi$ is same for two subproblems then both will have the same minimum. This observation leads to a simplification that, to find a solution to (3.2), we need to solve only $K$ nonconvex nonlinear subproblems corresponding to the different possible values of $\chi$, and pick the solution of the subproblem which results in the minimum objective value among them. Thus, the number of subproblems that need to be solved becomes linear rather than exponential in $K$. One approach to solving these $K$ subproblems is to use standard non-convex problem solvers such as interior point methods. However, such techniques may not be computationally feasible to implement as the problem dimension gets large. Hence, in this paper, we adopt a computationally efficient approach based on GP, to arrive at the optimal solution in a numerically stable manner.

In the next section, we present a method to find near-optimal RIPs for both ARQ and HARQ-CC based dual EH link with slow and fast fading channels.

## 3.4 Near-Optimal RIPs for Dual EH Links

### 3.4.1 Dual EH Links with ARQ and Fast Fading

In this subsection, we find near-optimal policies for a dual EH link with ARQ and fast fading channels. Using the expression for $p_{\mathrm{D}}(i, j, m_t, m_r)$ given in (2.15) and EUR

constraints in Sec. 2.4.2, the PDP optimization problem can be written as

$$\min_{\bar{\mathbf{L}}=\{L_1,...,L_K\}} \prod_{\ell=1}^{K}\left(1 - e^{-\frac{s}{L_\ell}}\right), \tag{3.3a}$$

$$\text{subject to } \sum_{\ell=1}^{K} L_\ell \prod_{i=1}^{\ell-1}\left(1 - e^{-\frac{s}{L_i}}\right) \leq K\rho_t, \tag{3.3b}$$

$$\sum_{\ell=1}^{K} \chi^\ell \prod_{i=1}^{\ell-1}\left(1 - e^{-\frac{s}{L_i}}\right) \leq \frac{K\rho_r}{R}, \tag{3.3c}$$

and $0 \leq L_\ell \leq L_{\max}$, $\chi^\ell \in \{0,1\}$, $1 \leq \ell \leq K$, where $s \triangleq \frac{\gamma_0 \mathcal{N}_0 T_p}{E_s \sigma_c^2}$. The constraints in (3.3b) and (3.3c) ensure that both the transmitter and receiver operate in the EUR. As discussed above, to solve (3.3), we need to solve $K$ subproblems, and pick the best among the resulting solutions. Hence, in the following, we focus on solving an individual subproblem, which is a nonconvex nonlinear program. We first convert the problem into a *complementary geometric* program (CGP) [61], as follows. Specifically, for $\chi = K'$, using the Taylor series expansion of $e^{-x}$, (3.3) can be rewritten as

$$\min_{\bar{\mathbf{Z}}=\{t,Z_1,...,Z_{K'}\}} t,$$

$$\text{subject to } \prod_{\ell=1}^{K'}(A_\ell - B_\ell) \leq t, \tag{3.4a}$$

$$\frac{Z_1^{-1} + Z_2^{-1}A_1 + Z_3^{-1}(A_1 A_2 + B_1 B_2) + \cdots}{\frac{K\rho_t}{s} + Z_2^{-1}B_1 + Z_3^{-1}(A_1 B_2 + A_2 B_1) + \cdots} \leq 1, \tag{3.4b}$$

$$\frac{1 + A_1 + A_1 A_2 + B_1 B_2 + \cdots}{\frac{K\rho_r}{R} + B_1 + (A_1 B_2 + A_2 B_1) + \cdots} \leq 1, \tag{3.4c}$$

and $0 \leq sZ_\ell^{-1} \leq L_{\max}$, $1 \leq \ell \leq K'$, where $A_\ell \triangleq \sum_{i=0}^{\infty} \frac{Z_\ell^{2i+1}}{(2i+1)!}$, $B_\ell \triangleq \sum_{i=1}^{\infty} \frac{Z_\ell^{2i}}{(2i)!}$, and $Z_\ell \triangleq \frac{s}{L_\ell}$. In the above problem, $A_\ell$ and $B_\ell$ are infinite summations. First, we construct a finite (say, 5th) order approximation of the infinite summations involved. It is worth mentioning that the loss in optimality in making this approximation has a negligible

effect on the performance, when one considers 5 or 7 terms in the expansion. The resulting finite order approximation of the constraints in (3.4a), (3.4b) and (3.4c) are ratios of posynomials, which are nonconvex, and hence (3.4) is a CGP which is an intractable NP-hard problem [61]. Since directly solving (3.4) is hard, we solve it by solving a series of approximations, each of which can be easily solved optimally. Specifically, using a result in [61, Lemma 1], we approximate the denominators of (3.4a), (3.4b) and (3.4c) with monomials. This results in a *geometric* program (GP) approximation of (3.4), which can be solved efficiently and optimally.

The monomial approximation for a posynomial is constructed as follows. Let $g(\mathbf{x}) = \sum_i v_i(\mathbf{x})$ be a posynomial, with $v_i(\mathbf{x})$ being monomials (which are nonnegative by definition), then

$$g(\mathbf{x}) \geq \tilde{g}(\mathbf{x}) \triangleq \prod_i \left( \frac{v_i(\mathbf{x})}{\beta_i} \right)^{\beta_i}, \tag{3.5}$$

where $\beta_i \triangleq \frac{v_i(\mathbf{x}_0)}{g(\mathbf{x}_0)}, \forall i$, (and note that $0 \leq \beta_i \leq 1$), for any fixed $\mathbf{x}_0 > 0$. Then $\tilde{g}(\mathbf{x}_0) = g(\mathbf{x}_0)$, and $\tilde{g}(\mathbf{x})$ is the best local monomial approximation to $g(\mathbf{x})$ near $\mathbf{x}_0$ in the sense of the first order Taylor approximation [61].

We solve (3.4) iteratively. In the $p^{\text{th}}$ iteration, we use the GP approximation in (3.5), with the coefficients $\beta_i$ computed by evaluating the denominator posynomials in (3.4a), (3.4b) and (3.4c) at $\mathbf{Z}^{(p)}$, the solution of the $(p-1)^{\text{th}}$ iteration. The procedure is summarized in Algorithm 2.

It can be shown that Algorithm 2 converges to a point which satisfies the Karush-Kuhn-Tucker (KKT) conditions of the original problem [61]. In the sequel, we show, through simulations, that it actually converges to a point at which the objective function is very close to the global optimum. This substantiates our use of GP techniques,

---

**Algorithm 2** : Solution to the Complementary GP

    **Initialize**: $\mathbf{Z}^{(1)} = \{Z_1, Z_2, \ldots, Z_{K'}, 0, \ldots, 0\}$, where $\mathbf{Z}^{(1)}$ is any feasible vector for (3.4). $p \leftarrow 1$.

    **do**

        1. Evaluate the denominator posynomials $G_a(\mathbf{Z})$, $G_b(\mathbf{Z})$ and $G_c(\mathbf{Z})$ in (3.4a), (3.4b) and (3.4c), respectively, with the given $\mathbf{Z}^{(p)}$.

        2. For each term $V_\ell^q$ in the denominator posynomials $G_q(\mathbf{Z})$, where $q = a, b$ and $c$, compute $\beta_\ell^q = \frac{V_\ell^q(\mathbf{Z}^{(p)})}{G_q(\mathbf{Z}^{(p)})}$.

        3. Replace the denominator posynomial of (3.4a), (3.4b) and (3.4c) with a monomial using (3.5), with the weights $\beta_\ell^q$.

        4. Solve the GP (e.g., using GGPLAB [62]) to obtain $\mathbf{Z}^{(p+1)}$; set $p \leftarrow p + 1$.

        5. Go to step 1, and use $\mathbf{Z}^{(p)}$ obtained in step 4.

    **while** $\|\mathbf{Z}^{(p+1)} - \mathbf{Z}^{(p)}\|_2 \leq \epsilon$.

    **Output:** The near-optimal RIP and PDP are given by $\mathbf{Z}^{(p+1)}$ and $t$, respectively.

---

specifically Algorithm 2, to solve the problem (3.4) in a provably convergent manner.

## 3.4.2   Design of Optimal Policies for Other Cases

The problems of finding optimal policies for dual EH links for slow fading channels with ARQ and HARQ-CC as well as for fast fading channels with HARQ-CC are solved similarly, and the details are presented in Appendices B.5 and B.6, respectively.

*Remark* 3. The results presented in this section can also be used to design the RIPs for mono EH links, by dropping the constraint corresponding to the non-EH node.

  In the following section, we extend the presented design to a scenario when the EH processes at both nodes are spatially and temporally correlated.

## 3.5 Spatio-Temporally Correlated EH Processes

### 3.5.1 Temporal Correlation

In this section, to account for the temporal correlation, we assume that the EH processes at both nodes can be modeled as a first-order stationary Markov chain [51, 63]. The harvesting process at the transmitter is described by the set of harvesting energy levels, $\mathcal{E} = \{e_1^t, \ldots, e_{\max}^t\}$, and the probabilities, $p_{a,b} = \Pr[E_{n+1}^t = e_a^t | E_n^t = e_b^t]$, that in the $(n+1)^{\text{th}}$ slot the transmitter harvests $e_a^t$ units of energy, given that it harvested $e_b^t$ units of energy in $n^{\text{th}}$ slot, where both $e_a^t$ and $e_b^t \in \mathcal{E}$. The harvesting process at the receiver is modeled similarly. The PDP of dual EH links with stationary Markov EH process at the transmitter and receiver is given as (see Sec. 2.6.1):

$$P_{\text{D}}(K) = \sum_{(i,j,e_a^t,e_c^r)} \pi(i, j, e_a^t, e_c^r) P_{\text{D}}(K|i, j, e_a^t, e_c^r, U_n = 1), \qquad (3.6)$$

where $\pi(i, j, e_a^t, e_c^r)$ denotes the stationary probability that at the beginning of the frame, the state of the battery and the EH process at the transmitter and receiver are $(i, j)$ and $(e_a^t, e_c^r)$, respectively. Also, $P_{\text{D}}(K|i, j, e_a^t, e_c^r, U_n = 1)$ denotes the PDP conditioned on the state at the beginning of the frame, and is computed as follows

$$P_{\text{D}}(K|i, j, e_a^t, e_c^r, U_n = 1) = \sum_{E_t=0}^{Ke_{\max}^t} \sum_{E_r=0}^{Ke_{\max}^r} p(E_t, E_r|e_a^t, e_c^r) p_{\text{D}}(i, j, E_t, E_r). \qquad (3.7)$$

In the above, $p(E_t, E_r|e_a^t, e_c^r)$ denotes the probability that the transmitter and receiver harvest $E_t$ and $E_r$ units of energy during the frame, given that they started with $e_a^t$ and $e_c^r$ units of energy, respectively, at the start of the frame. In (3.7), $p_{\text{D}}(i, j, E_t, E_r)$ denotes the packet drop probability when the batteries are in state $(i, j)$ at the start of the frame

and the nodes harvest $(E_t, E_r)$ units of energy during the frame. Next, the PDP in (3.6) can be rewritten as

$$
\begin{aligned}
P_{\mathrm{D}}(K) &= \sum_{(i,j)} \pi(i,j) \sum_{(e_a^t, e_c^r)} \pi(e_a^t, e_c^r | i, j) P_{\mathrm{D}}(K | i, j, e_a^t, e_c^r, U_n = 1), \\
&= \sum_{(i,j)} \pi(i,j) P_{\mathrm{D}}(K | i, j, U_n = 1),
\end{aligned}
\tag{3.8}
$$

where $P_{\mathrm{D}}(K | i, j, U_n = 1) \triangleq \displaystyle\sum_{(e_a^t, e_c^r)} \pi(e_a^t, e_c^r | i, j) P_{\mathrm{D}}(K | i, j, e_a^t, e_c^r, U_n = 1).$

The goal of the RIP design problem is to minimize the PDP in (3.8) subject to energy neutrality and peak power constraints. Although the objective function in this problem has same expression as in problem (P1), the stationary probabilities, $\pi(i,j)$, are different. Nonetheless, as shown in Appendix B.7, Theorem 1 is applicable in this scenario also. For dual EH links operating in the EUR, this allows us to replace the objective function by the lower bound $P_{\mathrm{D}}(K | (i,j) \in \mathcal{I}_2, U_n = 1)$ and the energy neutrality constraints by the EUR constraints. Using the definition of the set $\mathcal{I}_2$, (3.7), and the definition of $P_{\mathrm{D}}(K | i, j, U_n = 1)$ given above, we get $P_{\mathrm{D}}(K | (i,j) \in \mathcal{I}_2, U_n = 1) = p_{\mathrm{D}}(i, j, E_t, E_r)$, where, for ARQ-based slow fading links operating with a strictly increasing policy, $p_{\mathrm{D}}(i, j, E_t, E_r) = p_{\mathrm{out},K}$. Hence, in all cases, $p_{\mathrm{D}}(i, j, E_t, E_r)$ is the probability that the packet remains in outage after making all $K$ attempts.

Thus, the optimization problem of finding an optimal RIP in the EUR is obtained from problem (3.3), (B.15), (B.16) and (B.17) by replacing the $K\rho_t E_s$ and $K\rho_r E_s$ with $K\bar{E}_t$ and $K\bar{E}_r$, respectively. Here, $\bar{E}_t$ and $\bar{E}_r$ denote the mean harvesting rates at the transmitter and receiver. Note that, even with modified EUR constraints, the expressions for

the objective and the constraints remain the same, and hence, Algorithm 1 yields a near-optimal RIP. This completes the discussion on RIPs for temporally correlated EH processes.

## 3.5.2 Spatial Correlation

In case the Bernoulli EH process of the transmitter and receiver are correlated, the joint distribution of the harvesting processes can be modeled as [1]

$$p(e_t, e_r) = p_{00}(1 - e_t)(1 - e_r) + p_{01}(1 - e_t)e_r + p_{10}e_t(1 - e_r) + p_{11}e_t e_r,$$

where $e_t, e_r \in \{0, 1\}$ are random variables taking nonzero value if energy is harvested at the transmitter and receiver, respectively, and $p_{00}, p_{01}, p_{10},$ and $p_{11}$ are probability values that add up to $1$. In this case, the PDP is given by (2.6). Further, the conditional PDP for the spatially correlated case is written as (see Sec. 2.6.2)

$$P_{\mathrm{D}}(K|i, j, \ell = 1) = \sum_{m_t=0}^{K} \sum_{m_r=0}^{K} p'(m_t, m_r) p_{\mathrm{D}}(i, j, m_t, m_r), \tag{3.9}$$

where $p'(m_t, m_r)$ denotes the probability that the transmitter and receiver harvest energy in exactly $m_t$ and $m_r$ slots, respectively.

Note that, since the result in Theorem 1 is directly applicable in this scenario, the problem to find optimal RIPs can be formulated by using conditional PDP in (3.9) as the objective when $(i, j) \in \mathcal{I}_2$. The EUR constraints are written by replacing the $\rho_t E_s$ and $\rho_r E_s$ in (3.3a) and (3.3b), respectively, by $(p_{10} + p_{11})E_s$ and $(p_{01} + p_{11})E_s$. The resulting optimization problem is solved using Algorithm 2.

In the next section, we evaluate the performance of the designed RIPs and benchmark them against the state-of-the-art policies. We also validate the results obtained in Sec. 3.2.

## 3.6 Numerical Results

### 3.6.1 Simulation Setup

We consider a ZigBee system with carrier frequency $950$ MHz and four slots per frame, with a slot duration of $T_p = 100$ ms [64]. The transmitter and receiver are $d = 10d_0$ distance apart, where $d_0 = 10$ m is the reference distance. The path loss exponent is $\eta = 4$. The additive noise corresponds to a bandwidth of $2$ MHz and temperature $T = 300 \ K$. For this system, $E_s = 5$ dB corresponds to $100 \ \mu J$. This is a typical amount harvested from indoor illumination, with a harvester of size $10 \ \text{cm}^2$ [63]. Note that, due to the time-diversity offered by fast fading channels, the same value of the PDP can be achieved at significantly lower harvesting levels when the channel is fast fading compared to when it is slow fading. Hence, we use $E_s = 12$ dB and $\gamma_0 = 10$ dB for slow fading channels, and $E_s = 5$ dB and $\gamma_0 = 12$ dB for fast fading channels, to obtain the PDP values in a meaningful range ($10^{-2}$ to $10^{-4}$) [40]. This also allows us to show performance under the two channel models in the same plot.

Note that, for short distance communications, the energy consumed by the transmitter and receiver are of the same order [23]. Hence, in each experiment, we set $1 \leq R \leq 1.5$. The size of the battery at the transmitter and receiver is determined using Theorem 1. The channel from the transmitter to the receiver is assumed to be i.i.d. Rayleigh block fading which remains constant for a slot (frame) for the fast (slow) fading channel. In

all the experiments, the PDP is computed by averaging over $10^7$ frames.

## 3.6.2 Results

**Battery size required to achieve the lower bound on the PDP**

In Fig. 3.2, we illustrate the size of the battery required to meet the PDP achieved under infinite-capacity batteries. The policies used in this experiment are designed using Algorithm 2. In all the cases, we observe that the PDP obtained with finite capacity batteries is very close to the lower bound (PDP obtained with a battery size of $10^6$), e.g., for ARQ over slow fading channels, the lower bound is achieved when the buffer size exceeds $40$ at both the EHNs. In contrast, for ARQ-based fast fading links, the size of the battery required is $10^4$. This is because, as noted in Remark 2, the exponents in Theorem 1, $r_*^t$ and $r_*^r$, are of the order of the drift induced by the RIP. When the drift is low, the system takes a long time to come out of a bad battery state, and therefore, a larger battery size is required to ensure that the probability of hitting a bad state is sufficiently low. For instance, as shown in the figure, in case of ARQ over fast fading channels, the required battery size to achieve near-optimal performance reduces from $10^4$ to $10^2$ when the drift induced by the RIP increases from $7.1276 \times 10^{-5}$ to $0.0159$. Similar behavior can be observed for HARQ-CC, in slow fading scenarios. Due to this, for ARQ with slow fading channels, a smaller sized energy buffer is required to meet the lower bound compared to ARQ with fast fading channels. This validates the result obtained in Theorem 1 for the required battery capacity.
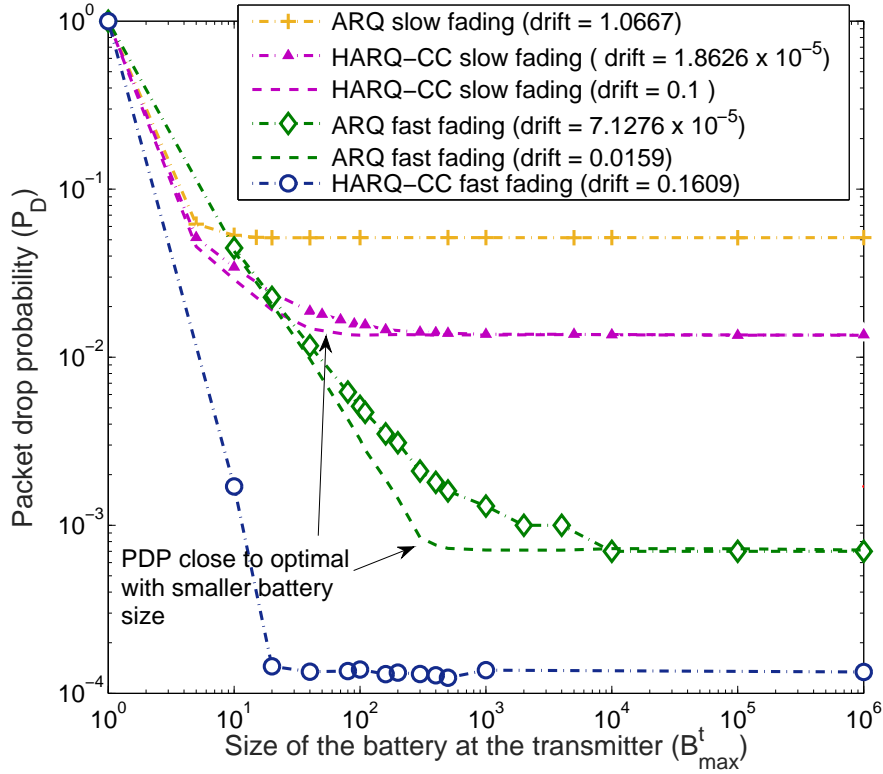
Figure 3.2: The PDP of dual EH links with finite size batteries asymptotically goes to the PDP of dual EH link with infinite size batteries. The rate of convergence is determined by the drift induced by the policy, i.e., the larger the drift, the faster the convergence. The parameter values are $R = 1$, $\rho_t = 0.75$, $\rho_r = 0.8$ and $L_{\max} = 3$. For HARQ-CC with fast fading channels, $L_{\max} = 2$. The size of the battery at the receiver is the same as the size of the battery at transmitter. The drift induced by a policy is equal to the average of the difference between the energy consumed and the energy harvested in a frame.

**Performance of proposed RIPs**

The results in Fig. 3.3 show the performance of the proposed policies for ARQ and HARQ-CC with slow fading channels. The performance of the policies matches with that obtained by solving $K$ subproblems using an interior point method (IPM). In addition, compared to the equal power scheme [34], for ARQ-based links, there is an
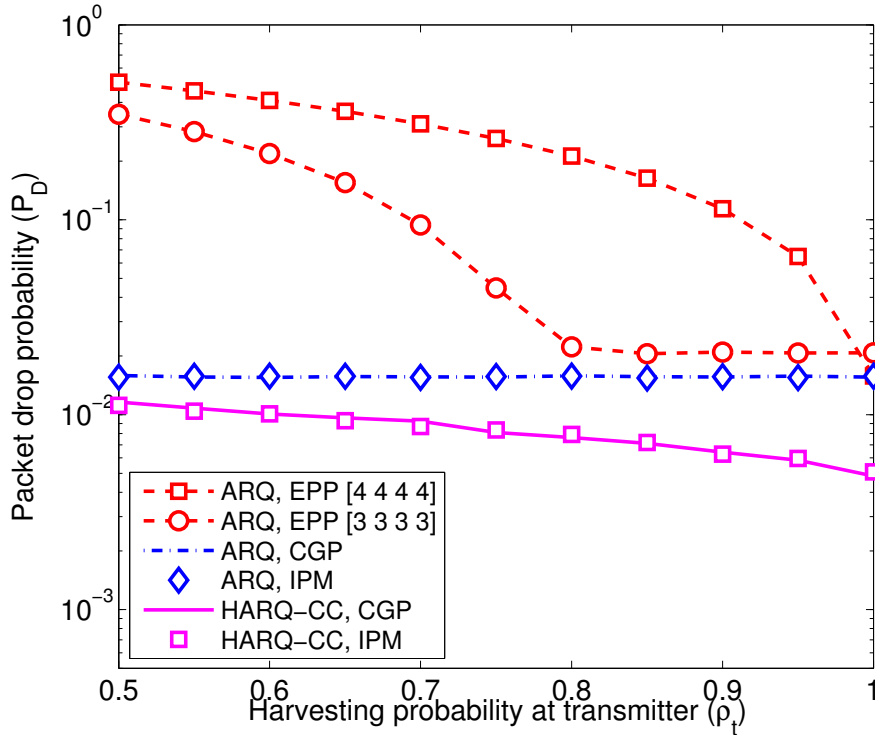
Figure 3.3: Slow fading channels

approximately tenfold reduction in the PDP. Similar performance improvement is observed in the proposed policy over the equal power scheme for the HARQ-CC based links also; we omit the plot to avoid repetition.

The results in Fig. 3.4 compare the performance of the proposed policies over fast fading channels. In the case of ARQ, to solve the CGP, we approximate the infinite summations by their first three terms only, which leads to a computationally inexpensive optimization procedure, which, nonetheless, matches with the performance obtained using the IPM. For HARQ-CC, the RIPs are obtained by solving a GP, which can be solved efficiently by directly converting it into a convex program. In this case, solving the GP directly using IPM is inefficient. Hence, for HARQ-CC, we omit the comparison with IPM. We observe that, compared to ARQ, HARQ-CC offers an approximately
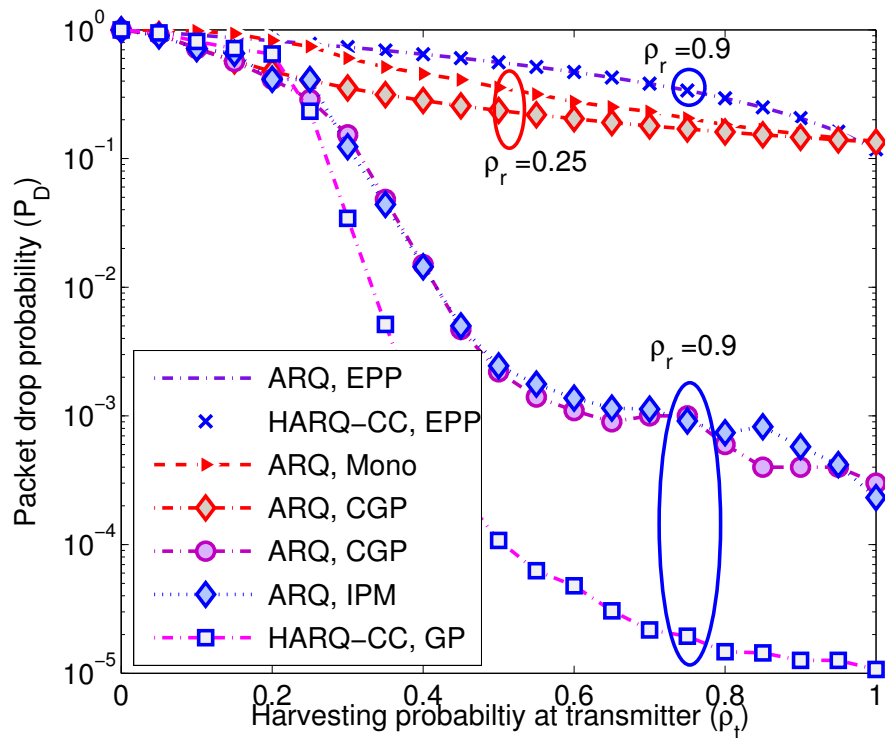
Figure 3.4: Fast fading channels

tenfold improvement in the PDP. Also, the equal power policy with transmit power

level $4E_s$ performs poorly compared to the designed RIPs. In addition, we compare the

performance of the proposed RIP against a policy obtained by solving an optimization

problem formulated ignoring the harvesting constraint at the receiver. Note that, for

this case, we consider $\rho_r = 0.25$ which corresponds to a scenario when the receiver is

energy constrained. The results for this scenario show that it is suboptimal to ignore

the harvesting constraint at the receiver.

In Fig. 3.5, we compare the performance of the proposed RIP designed for ARQ with

fast fading channels, against the joint threshold based policy (JTBP), which is essentially

an equal power policy with its transmit power level optimized using a global search al-

gorithm [1]. It can be seen that the RIP outperforms both the JTBP and linear policy.
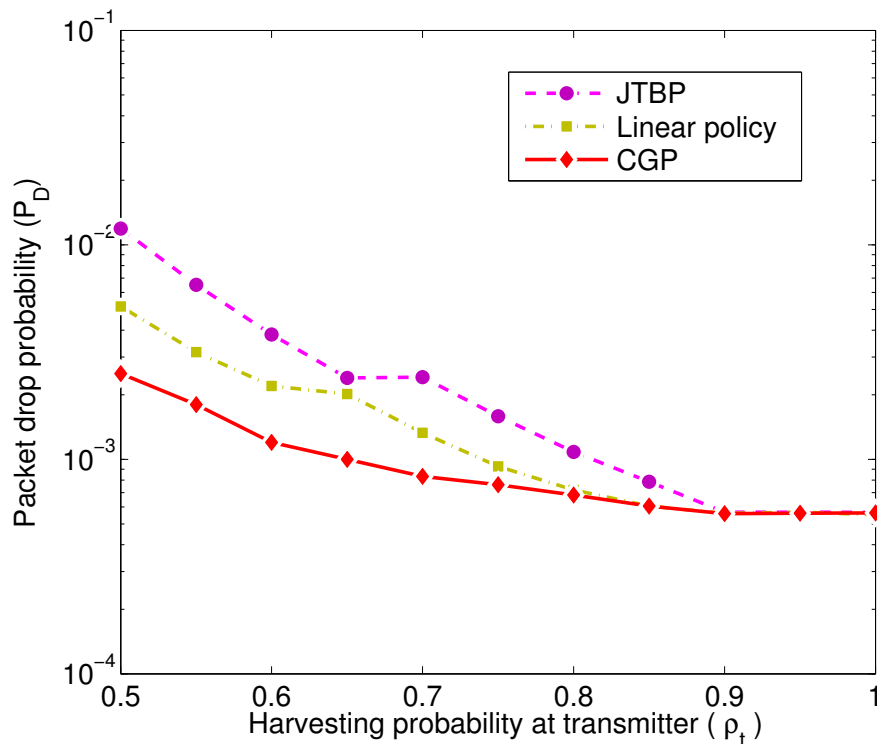
Figure 3.5: Performance comparison against the joint threshold based policy (JTBP) and linear policy [1]. The parameters are $R = 1.25$, $\rho_r = 0.7$, $B^t_{\max} = 4000$ and $B^r_{\max} = 500$.

This is because the JTBP and linear policy, although simple to implement, are suboptimal. Moreover, the computational complexity of the global search method used to optimize the transmit power levels increases with the buffer size, which is prohibitively large even for moderate sized energy buffers. For example, with $B^t_{\max} = B^r_{\max} = 35E_s$, the size of the search space is approximately $10^8$.

**Impact of decoding energy $R$**

In Fig. 3.6, we study the impact of energy required for decoding, $RE_s$. For this experiment, we consider an energy constrained receiver, i.e., the energy required for decoding a packet is close to the average energy harvested by the receiver, in a frame. Also, the

receiver has a small battery. We consider two scenarios when the receiver consumes 15 and 20 $\mu J$ for maximal ratio combining the packet. Thus, the total energy required for decoding a packet in these scenarios are $1.15E_s$ and $1.2E_s$, respectively. Note that, in these scenarios, the receiver can only support two or one attempts in a frame, on average, respectively, and it is unable to fully exploit the benefits of chase combining. Due to this, in contrast to conventional communication system where HARQ-CC results in improved performance, the ARQ outperforms the HARQ-CC. Also observe that, for $\rho_t > 0.4$, the PDP improves with decrease in $R$. This is because, for $R = 1.15$, the receiver can support two attempts, while for $R = 1.2$, it can support only one attempt on average. Also, it is easy to observe that we can trade off $R$ for $\rho_r$. However, once the receiver has sufficient energy to support all $K$ attempts, the decrease in $R$ (or increase in $\rho_r$) does not further improve the PDP.

**Performance of RIPs for Mono-T links**

As noted in Remark 3, the proposed scheme can also be used to design near-optimal RIPs for mono-T EH links by simply dropping the EUR constraint at the receiver. The results in Fig. 3.7 compare the performance of the RIPs designed for an ARQ-based mono-T EH link with the SoC-dependent policies designed using the Markov decision process (MDP) based framework. The performance is compared for both slow and fast fading channels with different number of quantization levels for the channel gain. In theory, SoC-dependent policies designed using the MDP framework perform at least as well as, and possibly better, than the proposed SoC independent RIPs. However, in practice, the MDP is formulated by quantizing the battery and channel states, and increasing the number of quantization levels increases the computational complexity
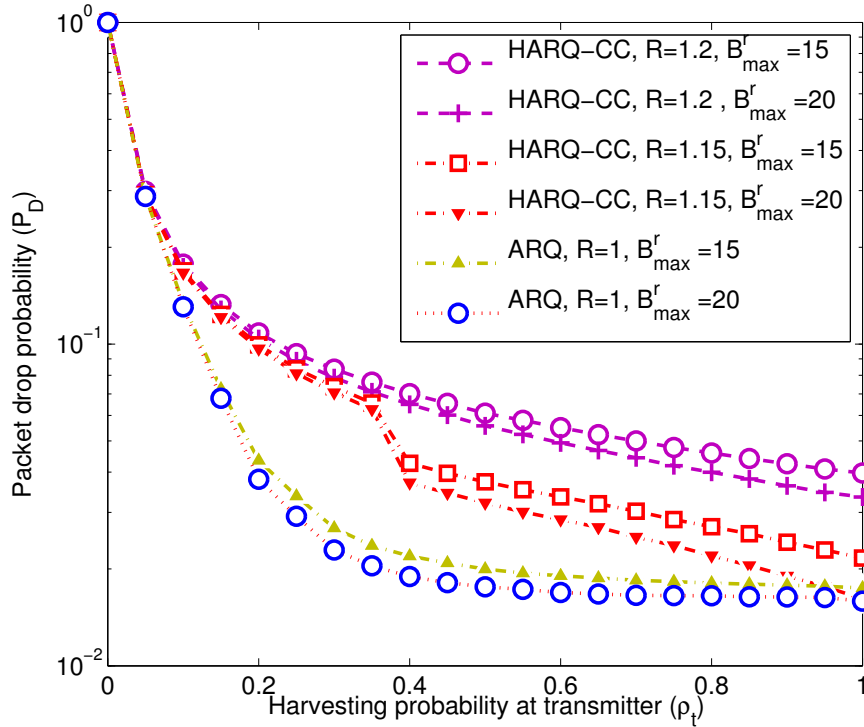
Figure 3.6: Impact of decoding energy: ARQ outperforms HARQ-CC when the receiver is energy constrained and the energy cost of combining packets is nonzero. The parameters used are $B_{\max}^t = 20$, $\rho_r = 0.3$ and $L_{\max} = 4$.

of MDP. Thus, due to the effect of quantization of the battery and channel states, in practice we find that the designed RIPs can even outperform the policies obtained using MDPs.

The results in this section illustrate that the RIPs obtained using the proposed GP based design procedure improves the PDP of the system compared to the state-of-the-art schemes. Moreover, the values of the system parameters used for the experiments correspond to practical scenarios. For example, in Fig. 3.5, for an ARQ-based fast fading link, the size of the battery used at the transmitter is 4000 units, which is much less than the size of the battery used in practical EHNs (see footnote 2). The results thus reaffirm
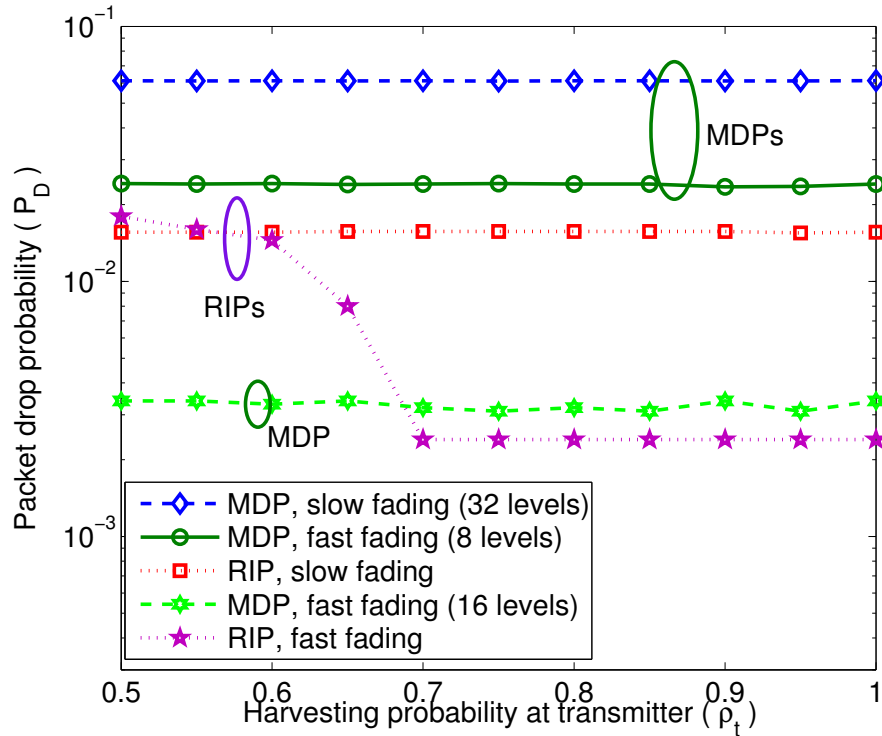
Figure 3.7: Performance comparison of RIPs for ARQ based mono-T links with policies designed using an MDP approach assuming access to perfect SoC information [2]. For slow fading channels, the proposed RIP uniformly outperforms the MDP, while in the fast fading case, for $\rho_t \geq 0.7$, the RIPs outperform the corresponding MDP based policies. The parameters used are $B^t_{\max} = 40$ and $L_{\max} = 4$ and $2$ for slow and fast fading channels, respectively.

that the proposed scheme is suitable for implementation in present-day EHNs.

## 3.7 Conclusions

In this chapter, we designed near-optimal, SoC-unaware, retransmission index based

power control policies for *dual* EH links with both slow and fast fading channels. We

showed that, in the energy unconstrained regime, the performance of the proposed

SoC independent policies converge asymptotically to that of the optimal policy under

infinite batteries, as the size of the battery size gets large. These results characterized the battery size required to achieve a PDP sufficiently close to that of a system with infinite capacity batteries. By reformulating the problem as a geometric program, we obtained near-optimal RIPs in a computationally efficient manner. Using Monte Carlo simulations, we showed that the designed RIPs outperform state-of-the-art policies in terms of their PDP.

# Chapter 4

# Packet Drop Probability Analysis of Multi-hop Energy Harvesting Links with ARQ

This chapter investigates the design of ARQ based Multi-hop energy harvesting links. As highlighted in Chapter 1, due to the coupling among the policies of different nodes, polices that are optimal for point-to-point EH links could be suboptimal for multi-hop EH links. As a first step towards finding optimal policies for multi-hop EH links with ARQ, we extend the analysis presented in Chapter 2, and derive closed-form PDP expressions. However, different from Chapter 2, we consider an *exponential outage model*, where the probability of outage decays exponentially with the received SNR. We start with a short survey of literature on multi-hop EH links.

The design and analysis of power management policies for multi-hop EH links has been studied with various objectives such as the long-term rate [65], energy efficiency [66], transmission reliability [67], distortion [68], fairness [69], utility [70,71], throughput [72], and sensing rate [73]. However, these studies do not consider the design of *ARQ based*

multi-hop EH links, which is the focus of this chapter.

In the next section, we present our system model.

## 4.1 System Model

We consider an $N$-hop link formed by $N + 1$ EHNs as shown in Fig. 1.1. The first EHN (source) takes a measurement at the beginning of every *frame* of duration $T_f$. The measurement packet needs to be delivered to the last node (destination), before the end of the frame. If a packet does not reach the destination by the end of the frame, it is *dropped*. Each packet is relayed to the destination using $N - 1$ half-duplex relays which operate in a decode and forward manner.

### 4.1.1 Transmission Protocol on Each Hop

The transmission of a packet between two successive EHNs follows the ARQ protocol where each packet attempt by the transmitter is followed by an acknowledgment (ACK) or negative ACK (NACK) signal from the receiver, indicating the success or failure of the attempt, respectively. The ACK/NACK messages are assumed to be received without any error and delay [1, 2, 34, 45]. This is a reasonable assumption because compared to a measurement packet ACK/NACK messages are smaller in the size and can be transmitted with significant protection to keep the error rate negligibly small. If the transmitter receives an ACK, then it does not retransmit the packet and goes to sleep and harvests the energy until it is time to receive the next packet. On the other hand, reception of a NACK results in retransmission of the packet, provided both the transmitter and receiver have sufficient energy to make the next attempt.

We consider a time-slotted system, and let $T_s$ denote the duration of a slot, which is the total time required to make an attempt and receive the ACK/NACK from the receiver. Hence, a frame contains $K = \left\lfloor \frac{T_f}{T_s} \right\rfloor$ slots. Out of these $K$ slots, the $n^{\text{th}}$ node is allocated $K_n$ slots, such that $\sum_{n=1}^{N} K_n = K$. Thus, the $n^{\text{th}}$ node remains awake for at most $K_{n-1} + K_n$ slots in a frame, and receives in a slot $s$ if $s \in \left\{ \sum_{p=1}^{n-2} K_p + 1, \ldots, \sum_{p=1}^{n-1} K_p \right\}$ and transmits if $s \in \left\{ \sum_{p=1}^{n-1} K_p + 1, \ldots, \sum_{p=1}^{n} K_p \right\}$. The duration $\left\{ \sum_{p=1}^{n-1} K_p + 1, \ldots, \sum_{p=1}^{n} K_p \right\}$ is called the $n^{\text{th}}$ *sub-frame*, and is of duration $K_n$ slots. A packet received in $(n-1)^{\text{th}}$ sub-frame needs to be delivered to the $(n + 1)^{\text{th}}$ node within the $n^{\text{th}}$ sub-frame, otherwise it is dropped. This type of fixed slot allocation can be pre-programmed during the network deployment phase and is more energy efficient compared to dynamic slot allocation which requires a node to remain awake in anticipation of a transmission by the previous node.

## 4.1.2 Energy Harvesting Model

The energy harvesting process at the nodes is modeled as a temporally i.i.d. Bernoulli process, independent across nodes [1, 2, 17, 34, 63]. That is, in a slot, node $n$ harvests energy $E_s$ with probability $\rho_n$, and does not harvest energy with probability $1 - \rho_n$, for $1 \leq n \leq N + 1$. Without loss of generality, we normalize $E_s = 1$, throughout the paper. The Bernoulli model is motivated by switch-based and vibration based harvesting mechanisms [34, 74]. The simplicity of Bernoulli model facilitates the exposition of the key ideas presented in the paper, while still capturing the sporadic and random nature of the energy availability at the EHNs. However, the Markov chain based framework presented in the sequel directly extends to more general models, e.g., the stationary

Markov model [63] and generalized Markov model [51] as well as to account for spatial correlation in the harvesting process.

### 4.1.3 Power Management Policy

The transmit power policy of node $n$ is an RIP denoted by $\mathcal{P}^n \triangleq \{P_1^n = \frac{E_1^n}{T_s}, P_2^n = \frac{E_2^n}{T_s}, \cdots, P_{K_n}^n = \frac{E_{K_n}^n}{T_s}\}$, for $1 \leq n \leq N$. The RIP $\mathcal{P}^n$ is an *attempt* based prescription, i.e., the $n^{\text{th}}$ node uses $E_\ell^n$ amount of energy to make its $\ell^{\text{th}}$ attempt[1], $1 \leq \ell \leq K_n$. In addition, due to the restriction imposed by RF-front end, $E_\ell^n \leq E_{\max}$, where $E_{\max}$ is the maximum allowed transmission energy per slot. At the receiver, since the size as well as the modulation and coding scheme remain fixed for each packet, we assume that a node consumes $R$ units of energy to receive and decode a packet, including the energy required to transmit the ACK/NACK message [1, 26]. The Markovian evolution of the battery at each node ensures that the operation of the node satisfies the *energy neutrality constraint* (ENC), and is given as follows

$$B_{s+1}^n = \min\left(\left(B_s^n + \mathbb{1}_{\{\mathcal{H}_s^n\}} - E_\ell^n \mathbb{1}_{\{\mathcal{E}_{t,s}^n\}} - R\mathbb{1}_{\{\mathcal{E}_{r,s}^n\}}\right)^+, B_n^{\max}\right), \tag{4.1}$$

for $1 \leq n \leq N + 1$. In the above, $B_n^{\max} < \infty$ denotes the size of the battery at the $n^{\text{th}}$ node and $(x)^+ \triangleq \max(0, x)$. Also, $\mathbb{1}_{\{\mathcal{E}\}}$ denotes an indicator function which equals one when the event $\mathcal{E}$ occurs, and equals zero otherwise. $\mathcal{E}_{t,s}^n$ and $\mathcal{E}_{r,s}^n$ denote the events that node $n$ is acting as a transmitter and receiver, respectively, in the $s^{\text{th}}$ slot. The event that node $n$ harvests energy in the $s^{\text{th}}$ slot is denoted by $\mathcal{H}_s^n$. We let $U_s^n$ denote the *local*

---

[1] The subscript is used for either time or node index, depending on the context. However, when both time index and node index appear together, they are indicated in the subscript and superscript, respectively.

*transmission index* of the $n^{\text{th}}$ node in the $s^{\text{th}}$ slot, $s \geq \sum_{p=1}^{n-1} K_p + 1$. It is defined as

$$U_s^n \triangleq \begin{cases} -1 & \text{ACK received,} \\ \ell & \ell - 1 \text{ NACKs received, } \ell \in \{1, \ldots, K_n\}. \end{cases} \tag{4.2}$$

For $s \leq \sum_{p=1}^{n-1} K_p$, $U_s^n = 0$, i.e., the $U_s^n$ is zero until the start of $n^{\text{th}}$ sub-frame, and at the start of $n^{\text{th}}$ sub-frame the local transmission index is set to one. It is incremented by one each time a NACK is received, and set to $-1$ if an ACK is received. Thus, the $n^{\text{th}}$ node makes the $\ell^{\text{th}}$ attempt in the $s^{\text{th}}$ slot if and only if all the following conditions are satisfied:

1. The $n^{\text{th}}$ node has received the packet successfully, i.e., the local transmission index of all the previous $n - 1$ nodes is equal to $-1$.

2. The $s^{\text{th}}$ slot is a slot in the $n^{\text{th}}$ sub-frame.

3. $U_s^n = \ell$, i.e., previous $\ell - 1$ attempts made by the $n^{\text{th}}$ node has failed.

4. Both the $n^{\text{th}}$ and $(n + 1)^{\text{th}}$ nodes have sufficient energy in the battery to transmit and receive the packet, respectively. That is, $E_\ell^n \leq B_s^n$ and $R \leq B_s^{n+1}$.

Based on the above, we can define $\mathcal{E}_{t,s}^n$ and $\mathcal{E}_{r,s}^n$ in (4.1) as $\mathcal{E}_{t,s}^n \triangleq \{B_s^n \geq E_\ell^n, B_s^{n+1} \geq R, (U_s^i = -1)_{i=1}^{n-1}, U_s^n = \ell, K_n + 1 \leq s \leq K_{n+1}\}$, and $\mathcal{E}_{r,s}^n \triangleq \{B_s^{n-1} \geq E_\ell^{n-1}, B_s^n \geq R, (U_s^i = -1)_{i=1}^{n-2}, U_s^{n-1} = \ell, K_{n-1} + 1 \leq s \leq K_n\}$ for some $\ell$ such that $1 \leq \ell \leq s$. Note that, $\mathcal{E}_{t,s}^n$ and $\mathcal{E}_{r,s}^{n+1}$ are the same events. The system dynamics of our system is shown in Fig. 4.1.

Note that, to ensure that an attempt is made only if $E_\ell^n \leq B_s^n$ and $R \leq B_s^{n+1}$, the transmitter and receiver need to have one bit information about the SoC of the other node. This can be obtained using a coordinated sleep-wake protocol between the transmitter
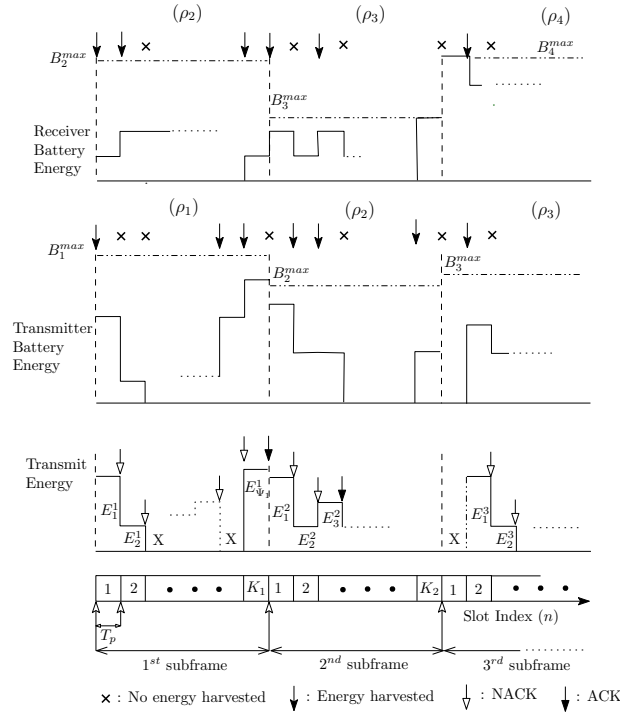
Figure 4.1: Evolution of the batteries at the transmitter and receiver during the transmission of a packet. In the first sub-frame, the source node is the transmitter and the $2^{\text{nd}}$ node is the receiver. More generally, in the $n^{\text{th}}$ sub-frame, the $n^{\text{th}}$ node transmits to the $(n+1)^{\text{th}}$ node. In the illustrated scenario, the first node delivers the packet in the $K_1^{\text{th}}$ slot, while the second node receives an ACK in the $3^{\text{rd}}$ slot. Note that, after receiving the ACK signal, the $2^{\text{nd}}$ node does not make further attempts and harvests energy for the rest of the frame. Also, after receiving the packet successfully, the $3^{\text{rd}}$ node starts its transmission only at the start of $3^{\text{rd}}$ sub-frame. A packet is dropped if any node in the multi-hop link fails to deliver the packet to next node.

and receiver proposed in [27] and described in the previous chapter.

## 4.1.4 Channel Model

The wireless channel between two consecutive nodes is modeled as a *block* fading channel [1, 34] with two different scenarios for the block duration. In the first scenario, named as *slow fading*, the channel remains constant for the duration of a sub-frame and changes in an i.i.d. fashion at the start of next sub-frame. In the second scenario, called as *fast fading*, the channel stays constant for a slot duration and changes in an i.i.d.

fashion at the beginning of a new slot. The transmitting node does not have access to channel state information, but it can possibly infer about the channel using the received ACK/NACK messages. In both slow and fast fading cases, the channel is assumed to be Rayleigh distributed, with the complex baseband channel distributed as $\mathcal{CN}(0, \sigma_c^2)$. The probability that the $\ell^{\text{th}}$ attempt of the $n^{\text{th}}$ node is in *outage* is given as [75–77]

$$P_e(E_\ell^n, \gamma) = \exp\left(-\frac{E_\ell^n \gamma}{N_0}\right),\tag{4.3}$$

where $\gamma$ and $N_0$ denote the instantaneous channel gain and power spectral density of the AWGN at the receiver, respectively. Thus, in a given slot, the packet can be in outage either due to unavailability of energy at the transmitting or receiving EHN, due to a bad channel state, or noise at the receiver.

The goal in this chapter is to design the set of RIPs $\{\mathcal{P}^n\}_{n=1}^N$ such that the PDP is minimized. To do so, we need to characterize the dependence of the PDP on the system parameters and transmit power levels of the RIPs. In the next section, we derive the approximate closed-form expressions for the PDP which are accurate over a wide range of system parameters. Using the closed-form expressions, we will formulate our main optimization problem in next chapter.

## 4.2 Packet Drop Probability

The system described in the previous section can be modeled as a discrete time Markov chain (DTMC). The state of the DTMC in slot $s$ is represented by the tuple $(\boldsymbol{B}_s, \boldsymbol{U}_s, s)$, where $\boldsymbol{B}_s \triangleq \left(B_s^1, B_s^2, \ldots, B_s^{N+1}\right)$ and $\boldsymbol{U}_s \triangleq (U_s^1, U_s^2, \ldots, U_s^N)$ are the vectors denoting the battery state and local transmission index of all the nodes. For a *slow* fading channel,

the state transition probability matrix (TPM) is denoted by $\boldsymbol{G}(\gamma)$ and its $(a, b)^{\text{th}}$ entry denotes the probability of transitioning from state $\boldsymbol{a} \triangleq (\boldsymbol{B}_a, \boldsymbol{U}_a, s)$ to $\boldsymbol{b} \triangleq (\boldsymbol{B}_b, \boldsymbol{U}_b, s+1)$, i.e.,

$$G_{a,b}(\gamma) \triangleq \Pr\Big[(\boldsymbol{B}_{s+1} = \boldsymbol{B}_b, \boldsymbol{U}_{s+1} = \boldsymbol{U}_b, s+1) \,|\, (\boldsymbol{B}_s = \boldsymbol{B}_a, \boldsymbol{U}_s = \boldsymbol{U}_a, s), \gamma\Big], \qquad (4.4)$$

The transition probabilities are determined by the RIPs, $\{\mathcal{P}^n\}_{n=1}^N$, and the channel and EH statistics. For a *fast* fading channel, entries of the TPM, $\boldsymbol{G}$, are written similarly. The expressions for the transition probabilities are provided in Appendix C.1.

Using the above DTMC, for a given set of RIPs $\mathcal{P} \triangleq \{\mathcal{P}^n\}_{n=1}^N$, the PDP can be written as

$$P_{\text{D}} = \sum_{\boldsymbol{B}} \pi(\boldsymbol{B}) \mathbb{E}_{\boldsymbol{\gamma}} \left\{ P_D \left( K | \boldsymbol{B}, \boldsymbol{U} = \boldsymbol{1}, \boldsymbol{\gamma}, s = 0 \right) \right\}, \qquad (4.5)$$

where $\pi(\boldsymbol{B})$ denotes the stationary probability that, at the start of the frame, the battery states of the nodes in the system is $\boldsymbol{B}$, and $P_D(K|\boldsymbol{B}, \boldsymbol{U} = \boldsymbol{1}, \boldsymbol{\gamma}, s = 0)$, termed as the *conditional PDP*, denotes the probability that the packet is dropped after $K$ slots, given that at the start of the frame the battery state is $\boldsymbol{B}$ and the channel encountered by the packet is $\boldsymbol{\gamma}$. For a slow fading channel $\boldsymbol{\gamma} \triangleq (\gamma_1, \gamma_2, \ldots, \gamma_N)$, where $\gamma_n$ denotes the channel in the $n^{\text{th}}$ subframe, while for a fast fading channel $\boldsymbol{\gamma} \triangleq (\gamma_1, \gamma_2, \ldots, \gamma_K)$, where $\gamma_s$ denotes the channel in $s^{\text{th}}$ slot. Conditioning on $\boldsymbol{U} = \boldsymbol{1}$ signifies that the local transmission index at all the nodes is reset to one at the start of the frame. Thus, to compute the PDP using (4.5), we need to find the stationary distribution of the DTMC, $\boldsymbol{\pi}$, and the average conditional PDP, $\mathbb{E}_{\boldsymbol{\gamma}} \{P_D(K|\boldsymbol{B}, \boldsymbol{U} = \boldsymbol{1}, \boldsymbol{\gamma}, s = 0)\}$, where $\mathbb{E}_{\gamma}(\cdot)$ denotes the expectation over the channel state $\gamma$.

Now, since the number of states of the DTMC is finite, the DTMC is positive recurrent.

This ensures the existence of the stationary distribution $\boldsymbol{\pi}$. The stationary distribution over the battery states at the start of the frame is given as [56, Lemma 1]

$$\boldsymbol{\pi} = \left(\mathbb{E}\left[\boldsymbol{G}'(\boldsymbol{\gamma})\right] - \boldsymbol{I} + \boldsymbol{A}\right)^{-1} \mathbf{1}, \tag{4.6}$$

where $\mathbf{1}$ is a $\prod_{n=1}^{N+1}(B_n^{\max} + 1)$ dimensional all ones vector, $\boldsymbol{A}$ an all ones matrix, and $\boldsymbol{I}$ is the identity matrix. $\boldsymbol{G}'(\boldsymbol{\gamma})$ is the $K$-step TPM with entries $\Pr\left[\boldsymbol{B}_{(M+1)K} = \boldsymbol{B}_2 | \boldsymbol{B}_{MK} = \boldsymbol{B}_1, \boldsymbol{\gamma}\right]$, where $M$ is the frame index. The entries of $\boldsymbol{G}'(\boldsymbol{\gamma})$ are computed using $\boldsymbol{G}^K(\boldsymbol{\gamma})$, by marginalizing out the local transmission index vector $\mathbf{U}$, as follows

$$\sum_{\mathbf{u}} \Pr\left[\left(\boldsymbol{B}_{(M+1)K} = \boldsymbol{B}_2, \boldsymbol{U}_{(M+1)K} = \mathbf{u}, s = K\right) \Big| \left(\boldsymbol{B}_{MK} = \boldsymbol{B}_1, \boldsymbol{U}_{MK} = \mathbf{1}, \boldsymbol{\gamma}, s = 0\right)\right].$$

$$\tag{4.7}$$

*Remark:* Computing the stationary distribution for a fast fading multi-hop link is simpler than the slow fading case. This is because, as noted in the Appendix C.1, the TPM $\boldsymbol{G}$ directly contains the channel averaged entries. Thus, in the fast fading case, the expression to compute $\boldsymbol{\pi}$ is similar to (4.6), and can be written by directly replacing $\mathbb{E}\left[\boldsymbol{G}'\right]$ with $\boldsymbol{G}'$. Next, we derive an expression for the average conditional PDP.

## 4.2.1 Average Conditional PDP

For a given channel state, $\boldsymbol{\gamma}$, the conditional PDP is determined by the number of transmit and receive attempts supported by each node. Since this probability is conditioned on the battery state at the start of the frame, it is important to account for the number of slots in which energy is harvested by a node from the start of the frame till the subframe in which it remains active. Let $M_n \triangleq (m_{r,n}, m_{t,n})$, where $0 \leq m_{r,n} \leq \sum_{i=1}^{n-1} K_i$ and

$0 \le m_{t,n} \le K_n$ denote the total number of slots in which energy is harvested by the $n^{\text{th}}$ node in the first $n-1$ sub-frames and during the $n^{\text{th}}$ sub-frame, respectively. Note that, $m_{r,1} = 0$ and $m_{t,1} \le K_1$. Similarly, $m_{r,N+1} \le K$ and $m_{t,N+1} = 0$. The following Lemma expresses the average conditional PDP in terms of the probability that the packet is dropped when the initial battery state vector and harvesting pattern vector are $\boldsymbol{B}$ and $\boldsymbol{M} = (M_1, \ldots, M_{N+1})$, respectively, when the channel encountered by the packet is $\boldsymbol{\gamma}$, denoted by $p_{\text{D}}(\boldsymbol{B}, \boldsymbol{M}, \boldsymbol{\gamma})$. The result directly follows from the spatial independence of the harvesting processes across the nodes, and hence is omitted.

**Lemma 9.** *The average conditional PDP can be written as*

$$\mathbb{E}_{\boldsymbol{\gamma}} \left\{ P_D(K|\boldsymbol{B}, \boldsymbol{U} = \boldsymbol{1}, \boldsymbol{\gamma}) \right\} = \sum_{\boldsymbol{M}=(M_1,\ldots,M_{N+1})} q(\boldsymbol{M}) \mathbb{E}_{\boldsymbol{\gamma}} \{ p_D(\boldsymbol{B}, \boldsymbol{M}, \boldsymbol{\gamma}) \}, \tag{4.8}$$

*where $q(\boldsymbol{M})$ denotes the probability of a harvesting pattern $\boldsymbol{M}$, and is given by*

$$q(\boldsymbol{M}) = \prod_{n=1}^{N+1} \binom{\sum_{i=1}^{n-1} K_i}{m_{r,n}} \binom{K_n}{m_{t,n}} \rho_n^{m_{r,n}+m_{t,n}} (1 - \rho_n)^{\sum_{i=1}^{K_n} K_i - m_{r,n} - m_{t,n}}. \tag{4.9}$$

Next, to compute the conditional PDP using Lemma 9, we need to find $p_{\text{D}}(\boldsymbol{B}, \boldsymbol{M}, \boldsymbol{\gamma})$, which can be expressed in terms of the outage probability of the individual hops as follows.

**Lemma 10.** *Let the battery state at the start of the frame and the harvesting pattern be $\boldsymbol{B}$ and $\boldsymbol{M}$, respectively. When the channel encountered by the packet is $\boldsymbol{\gamma}$, the probability that the*

*packet is dropped, $p_D(\boldsymbol{B}, \boldsymbol{M}, \boldsymbol{\gamma})$ can be expressed as*

$$p_D(\boldsymbol{B}, \boldsymbol{M}, \boldsymbol{\gamma}) = \sum_{n=1}^{N} p_{D,n} \prod_{i=1}^{n-1} (1 - p_{D,i}), \tag{4.10}$$

*where $p_{D,n}$ denotes the probability that the packet is dropped at the $n^{th}$ hop.*

*Proof.* The proof follows from the fact that the packet drop event can be written as the union of $N$ mutually exclusive events, where the $n^{th}$ event is that the packet is dropped at the $n^{th}$ hop, for all $1 \leq n \leq N$. The probability that the packet is dropped in the $n^{th}$ hop is written using the independence of channel states across the sub-frames. $\square$

Next, we characterize the $p_{D,n}$ using the following observations. First, $p_{D,n}$ is a function of $B^n$, $B^{n+1}$, $M_n$, $m_{r,n+1}$, and the channel between the $n^{th}$ and $(n+1)^{th}$ node. Here, $B^n$ and $B^{n+1}$ denote the $n^{th}$ and $(n+1)^{th}$ components of $\boldsymbol{B}$. Second, $p_{D,n}$ depends only on the channel state and the number of feasible attempts, $\Psi_n$, supported in the $n^{th}$ subframe. It does not depend on the exact slot indices in which the attempts are made. Based on this, $p_{D,n}$ can be written as

$$p_{D,n} = \prod_{\ell=1}^{\Psi_n} P_e \left( \frac{E_\ell^n \gamma_n}{N_0} \right). \tag{4.11}$$

To compute $p_{D,n}$ using (4.11), we need to determine the number of feasible attempts, $\Psi_n$, in the $n^{th}$ subframe. A method to compute $\Psi_n$ is provided in Appendix C.2.

Thus, using Lemmas 9, 10 and the procedure to compute the number of feasible attempts in Appendix C.2, $\mathbb{E}_{\boldsymbol{\gamma}} \{p_D(\boldsymbol{B}, \boldsymbol{M}, \boldsymbol{\gamma})\}$ in (4.8) can be written as

$$\mathbb{E}_{\boldsymbol{\gamma}} \{p_D(\boldsymbol{B}, \boldsymbol{M}, \boldsymbol{\gamma})\} = \sum_{n=1}^{N} \mathbb{E}_{\boldsymbol{\gamma}}\{p_{D,n}\} \prod_{i=1}^{n-1} (1 - \mathbb{E}_{\boldsymbol{\gamma}}\{p_{D,i}\}), \tag{4.12}$$

In the above equation, computing $\mathbb{E}_\gamma\{p_{D,n}\}$ depends on whether the channel is slow or fast fading. In the slow fading case, from (4.3) and (4.11), and since the channel state $\gamma$ is exponentially distributed and constant through the subframe, we get

$$\mathbb{E}_\gamma\{p_{D,n}\} = \frac{1}{1 + \sum_{\ell=1}^{\Psi_n} \frac{E_\ell^n}{N_0}}. \tag{4.13}$$

Similarly, in the fast fading case, we have

$$\mathbb{E}_\gamma\{p_{D,n}\} = \frac{1}{\prod_{\ell=1}^{\Psi_n} \left(1 + \frac{E_\ell^n}{N_0}\right)}. \tag{4.14}$$

This completes the derivation of the PDP expressions in both the cases.

## 4.3 Extension to General EH Processes

In this section, we extend the PDP analysis to capture the spatio-temporal correlation of the EH processes at the EHNs. In the following, we first consider the case where the EH process at each node is temporally correlated. The temporal correlation in the EH process is modeled as a stationary first order Markov process.

### 4.3.1 PDP Expressions for Temporally Correlated EH Processes

To model the temporal correlation in the EH process at the $n^{\text{th}}$ node, we use a stationary first order Markov chain [63], which is described by the set of harvesting energy levels, $\mathcal{E}^n \triangleq \{e_1^n, \ldots, e_{\max}^n\}$, and the probabilities, $p_{a,b}^n = \Pr\left[E_{m+1}^n = e_b^n | E_m^n = e_a^n\right]$, that $e_b^n$ units of energy is harvested in the $(m+1)^{\text{th}}$ slot, given that $e_a^n$ units of energy was harvested in the $m^{\text{th}}$ slot, where both $e_a^n$ and $e_b^n \in \mathcal{E}^n$.

When the EH process at each node is modeled as a stationary Markov chain, the conditional PDP depends not only on the channel and the battery states of the nodes at the start of the frame, but also on the states of the EH processes at the start of the frame. Hence, state of the DTMC describing the evolution of the system must now include the states of the EH processes. That is, the state of the DTMC is described by a tuple $(\boldsymbol{B}_s, \boldsymbol{U}_s, \boldsymbol{\mathcal{E}_s}, s)$. To obtain the transition probabilities of this modified DTMC, one needs to account for the transition probabilities of the harvesting processes. Thus, the entries of the TPM of the DTMC can be derived as a straightforward extension of the entries given in Appendix C.1. Then, the packet drop probability is written as

$$P_{\mathrm{D}} = \sum_{(\boldsymbol{B}, \boldsymbol{E})} \pi(\boldsymbol{B}, \boldsymbol{E}) \mathbb{E}_{\boldsymbol{\gamma}} \left\{ P_D \left( K | \boldsymbol{B}, \boldsymbol{U} = \boldsymbol{1}, \boldsymbol{E}, \boldsymbol{\gamma}, s = 0 \right) \right\}, \qquad (4.15)$$

where $\boldsymbol{E} \triangleq (E^1, \ldots, E^{N+1})$ denotes the state of the harvesting process at the start of the frame and $\pi(\boldsymbol{B}, \boldsymbol{E})$ denotes the stationary probability that at the start of the frame the DTMC is in a state such that the battery and energy state are $\boldsymbol{B}$ and $\boldsymbol{E}$, respectively. The stationary probabilities can be obtained using (4.6). Also, in (4.15), $P_D \left( K | \boldsymbol{B}, \boldsymbol{U} = \boldsymbol{1}, \boldsymbol{E}, \boldsymbol{\gamma}, s = 0 \right)$ denotes the conditional PDP, i.e., the probability that the packet is dropped given that at the start of the frame the battery energy state are $\boldsymbol{B}$ and $\boldsymbol{E}$, respectively, and channel states of the links is $\boldsymbol{\gamma}$. The conditional PDP can be written as

$$P_D \left( K | \boldsymbol{B}, \boldsymbol{U} = \boldsymbol{1}, \boldsymbol{E}, \boldsymbol{\gamma}, s = 0 \right) = \sum_{(\boldsymbol{H})} p \left( \boldsymbol{H} | \boldsymbol{E} \right) p_D \left( \boldsymbol{B}, \boldsymbol{H} \right), \qquad (4.16)$$

where $p \left( \boldsymbol{H} | \boldsymbol{E} \right)$ denotes the probability that nodes harvest the energy according to the pattern described by $\boldsymbol{H}$, given that the harvesting process is in state $\boldsymbol{E}$ at the start of the frame. The probability $p \left( \boldsymbol{H} | \boldsymbol{E} \right)$ can be computed using the transition probabilities,

$p_{a,b}$, of the stationary Markov chain. In (4.16), $p_D(\boldsymbol{B}, \boldsymbol{H})$ denotes the probability that the packet is dropped, given that the battery state of the nodes is $\boldsymbol{B}$ at the start of the frame, and they harvest energy according to the pattern $\boldsymbol{H} \triangleq \{(H_{r,n}, H_{t,n})\}_{n=1}^{N+1}$, where $H_{r,n}$ and $H_{t,n}$ denote the amount of energy harvested by the $n^{\text{th}}$ node in the first $n-1$ subframes, and in the $n^{\text{th}}$ subframe, respectively. To compute $p_D(\boldsymbol{B}, \boldsymbol{H})$, we need to characterize the number of feasible transmit and receive attempts for each node. This is accomplished using the method to compute $\Psi_n$, provided in Appendix C.2, with $E_{\text{avl},r}^n \triangleq \min\{B^n + H_{r,n}, B_{\max}^n\}$ and $E_{\text{avl},t}^n \triangleq \min\{B^n + H_{r,n} + H_{t,n} - \Psi_{n-1}R, B_{\max}^n\}$. Using the computed $\Psi_n$, one can compute $p_D(\boldsymbol{B}, \boldsymbol{H})$ using the expressions provided in Sec. 4.2.

In the following, we extend the PDP expressions to the scenario where the harvesting process at the EHNs are spatially correlated.

## 4.3.2 Spatially Correlated EH Processes

The joint distribution of the spatially correlated Bernoulli harvesting processes is denoted by $f(\boldsymbol{I})$, the probability that the nodes harvest the energy according to pattern $\boldsymbol{I} \in \{0,1\}^{N+1}$. In this scenario, the 1-step TPM can be obtained by replacing $p(\boldsymbol{I}_s)$ in the expression for the transition probabilities, given in Appendix C.1, by $f(\boldsymbol{I}_s)$. Also, the conditional PDP can be written as

$$P_D(K|\boldsymbol{B}, \boldsymbol{U} = 1) = \sum_{\boldsymbol{M}} q(\boldsymbol{M}) p_D(\boldsymbol{B}, \boldsymbol{M}), \tag{4.17}$$

where $q(\boldsymbol{M})$ denotes the probability that the harvesting pattern is $\boldsymbol{M}$. The probability $q(\boldsymbol{M})$ can be computed using the distribution $f$. In the above, $p_D(\boldsymbol{B}, \boldsymbol{M})$ denote the probability that the packet is dropped if the battery state of the node at the start of the

frame is $B$, and the nodes harvest energy according to pattern $M$. This completes the analysis for general case.

## 4.4   Simulations and Discussion

We consider a two-hop EH link, with a frame and slot duration of $800$ ms and $100$ ms, respectively. Thus, throughout the simulations, unless stated otherwise, the frame has a total of $8$ slots, which are distributed equally between the first and second subframe, i.e., $K_1 = K_2 = 4$. The distance between the transmitter and receiver at both the hops is $500$ m, with a reference distance $d_0 = 10$ m and path-loss exponent $\eta = 4$. We consider a typical ZigBee system with the carrier frequency $950$ MHz and the system bandwidth $2$ MHz [35]. The noise at the receiver is corresponds to $300$ K. In this system, $E_s = 0$ dB is equivalent to $25$ $\mu J$. The channel is assumed to be i.i.d. Rayleigh faded for both slow and fast fading cases, with the channel remaining constant for the frame and slot duration, respectively. The PDP is measured by averaging the performance over $10^7$ packets.

**Accuracy of the closed-form PDP expressions**

Figure 4.2 illustrates the accuracy of our closed-form expressions for the PDP of a multi-hop link in both slow and fast fading cases derived in Sec. 4.2. The analytical expressions match closely with the simulation results. We observe that the PDP initially decreases with the harvesting probability at the source node, $\rho_1$, and later saturates. The latter regime is the EUR, because, under the RIP $[1, 1]$, the average energy consumed is lower than the average energy harvested for $\rho_1$ greater than about $0.4$. Also, the PDP
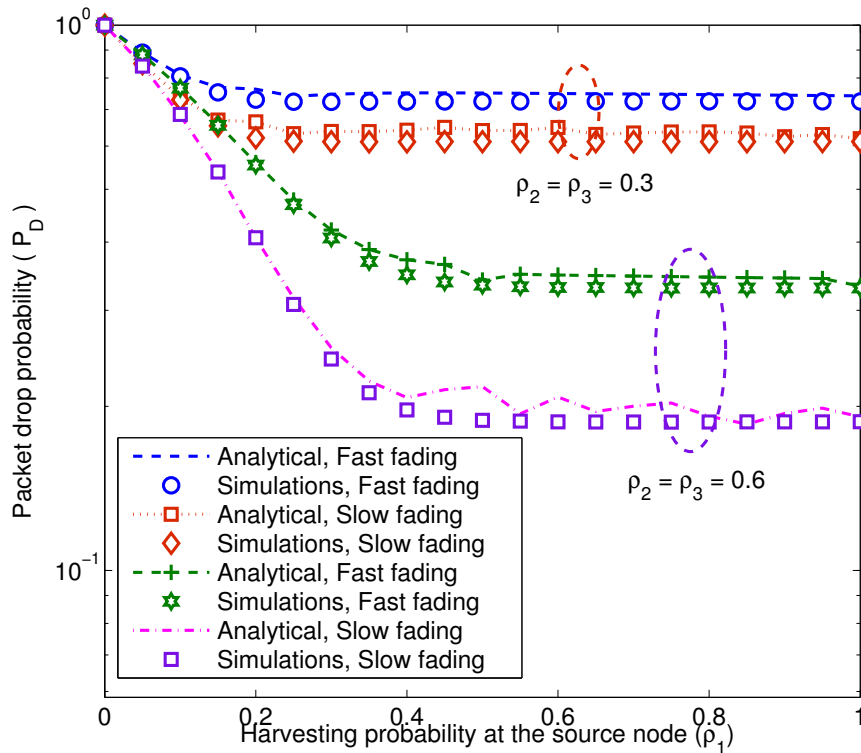
Figure 4.2: Accuracy of the closed-form PDP expressions. Parameters used: $K_1 = K_2 = 2$, $R = 1$, and $B^{\max} = 3$ for all the nodes. The RIP is $[1\ 1]$ at both source and relay nodes. The harvested energy for slow and fast fading cases are $E_s = 8$ dB and $3$ dB, respectively.

obtained for $\rho_2 = \rho_3 = 0.6$ is lower than the PDP for $\rho_2 = \rho_3 = 0.3$. This is because, in the latter case, the energy availability at the relay and destination is lower, and therefore fewer attempts are supported at each hop.

**Effect of slot allocation**

Fig. 4.3 demonstrate the impact of different slot allocations on the PDP. Here, total 6 slots are distributed among two hops and PDP performance corresponding to each slot allocation is plotted against the harvesting probability at the source node. For both
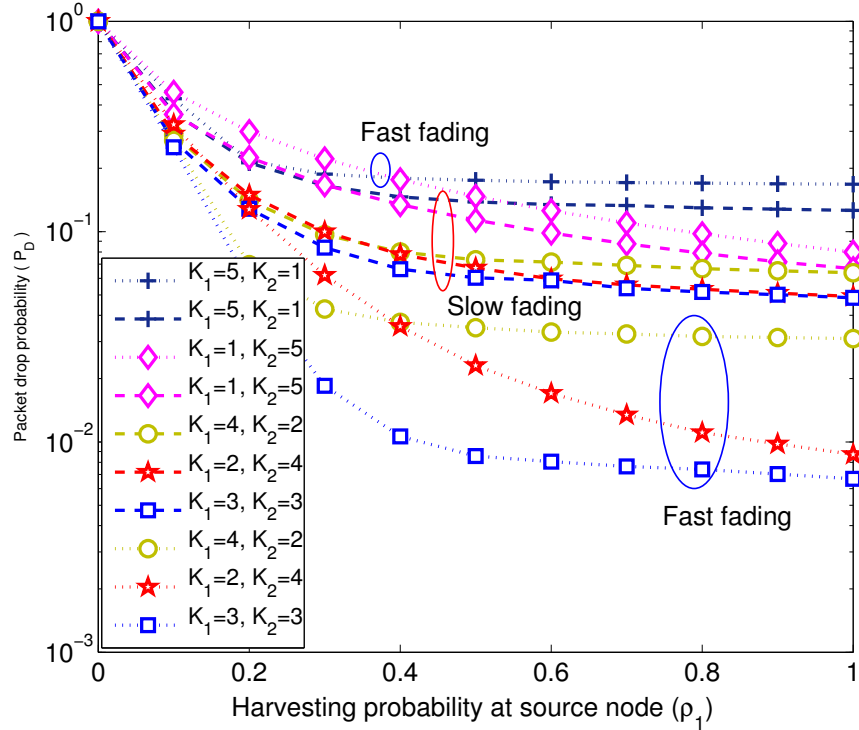
Figure 4.3: Impact of slot allocation on the PDP: equal slot allocation performs the best. The harvested energy for slow and fast fading case is $E_s = 5$ dB and $E_s = 3$ dB, respectively, while the size of the battery at each node is $50E_s$ and $200E_s$, respectively. In both the cases: the energy required for decoding at each node is $1E_s$ and the maximum transmit power allowed is $P_{\max} = \frac{10E_s}{T_s}$. $B^n_{\max} = 50$ for all nodes.

slow and fast fading channels, the PDP is lowest when both the first and second node have equal number of slots to forward the packet to next node, i.e., $K_1 = K_2 = 3$. Also, the performs degrades with more asymmetric distribution. For example, $K_1 = 4$ and $K_2 = 2$ is worse than $K_1 = 3$ and $K_2 = 3$. Moreover, for asymmetric distribution of slots, it is interesting to note that for lower harvesting rates at the source node it is better to allocate more slots to it. In contrast, at higher harvesting rates it is better to allocate more slot to the second node. For instance, for the lower harvesting rates the PDP for the allocation $K_1 = 5$ and $K_2 = 1$ is better than $K_1 = 1$ and $K_2 = 5$, while at

higher harvesting rates $K_1 = 1$ and $K_2 = 5$ results in better PDP. Same holds true in other cases also. This is because of the trade-off between the time-diversity offered by the channel and the harvesting rate. This is confirmed by the marginal gains obtained for slow fading channels. Note that, for $K_1 = 1$ and $K_2 = 5$, and $K_1 = 5$ and $K_2 = 1$ the PDP of slow fading multi-hop link is better than the fast fading link. This is due to the lower value of harvested energy, i.e., $E_s = 3$ dB for fast fading link, compared to slow fading link. However, once we allocate more than one slot to each node the PDP of fast fading case is better than the slow fading scenario as the fast fading links are benefited by the time-diversity.

## 4.5   Conclusions

In this chapter, we derived closed-form PDP expressions for ARQ-based multi-hop EH links. We also derived expressions for the PDP when the EH processes of the nodes are spatio-temporally correlated. We illustrated the accuracy of the closed-form expressions using computer simulations. In the next chapter, we use these closed-form expressions to find optimal power management policies for the multi-hop EH network considered in this thesis.

# Chapter 5

# Design of PDP-Optimal SoC-unaware Energy Management Policies for ARQ-based Multi-hop Links

In this chapter, a RIP optimization problem is formulated which is solved in two scenarios. In the first scenario, we find closed-form expressions for the transmit power levels of the optimal policies, when the energy cost to receive a packet is negligible compared to energy required for transmission. In the second scenario, namely, when the energy cost to receive and decode a packet is non-negligible, we propose an iterative procedure to obtain near-optimal energy management policies.

## 5.1   Packet Drop Probability Minimization

In this section, we formulate an optimization problem for obtaining the RIPs that minimize the PDP. Using (4.5), we can express the optimization problem as:

$$\min_{\{\mathcal{P}^n\}_{n=1}^N} \quad \sum_{\boldsymbol{B}} \pi(\boldsymbol{B})\mathbb{E}_{\boldsymbol{\gamma}}\left\{P_D\left(K|\boldsymbol{B},\boldsymbol{U}=\mathbf{1},\boldsymbol{\gamma}\right)\right\}, \qquad (5.1a)$$

$$\text{subject to } 0 \leq E_\ell^n \leq E_{\max} \quad \text{ for all } 1 \leq \ell \leq K_n \text{ and } 1 \leq n \leq N. \tag{5.1b}$$

In (5.1), $\boldsymbol{\pi}$ is obtained using (4.6), which, in turn, is determined by the energy neutrality constraint (ENC). This implicit dependence on the ENC makes the above problem hard to solve. Furthermore, due to the large state space of the problem, it is challenging to find a numerical solution using the dynamic programming techniques. Hence, in the following, we reformulate the above optimization problem by finding tight bounds on the objective function. The following Lemma provides an upper bound and a lower bound on the PDP. The proof is similar to the proof of Lemma 7, and hence is omitted.

**Lemma 11.** *Let $\mathcal{P} \triangleq \{\mathcal{P}^n\}_{n=1}^N$ be a set of RIPs satisfying $E_\ell^n \leq E_{\max}$ for all $1 \leq \ell \leq K_n$ and $1 \leq n \leq N$. Let $\mathcal{I}_A \triangleq \{\boldsymbol{B} \,|\, 0 \leq B^n \leq B_n^{\max}, \; B^n - K_n E_{\max} - K_{n-1} R \geq 0, \text{ for all } 1 \leq n \leq N+1\}$ and $\mathcal{I}_A^c \triangleq \mathcal{I} \setminus \mathcal{I}_A$, where $\mathcal{I} \triangleq \{\boldsymbol{B} \,|\, 0 \leq B^n \leq B_n^{\max} \text{ for all } 1 \leq n \leq N+1\}$ is the set of all battery state tuples. Then, for a multi-hop EH link operating using RIP $\mathcal{P}$,*

$$P_{D_\infty}^* \leq \min_{\{\mathcal{P}^n\}_{n=1}^N} \sum_{\boldsymbol{B}} \pi(\boldsymbol{B}) \mathbb{E}_{\boldsymbol{\gamma}} \left\{ P_D\left(K | \boldsymbol{B}, \boldsymbol{U} = \boldsymbol{1}, \boldsymbol{\gamma}\right) \right\} \leq P_{D_\infty}^* + \sum_{\boldsymbol{B} \in \mathcal{I}_A^c} \pi(\boldsymbol{B}) \Big|_{\mathcal{P}^*}, \tag{5.2}$$

*where $P_{D_\infty}^* \triangleq \min_{\{\mathcal{P}^n\}_{n=1}^N} \mathbb{E}_{\boldsymbol{\gamma}} \left\{ P_D\left(K | \boldsymbol{B}, \boldsymbol{U} = \boldsymbol{1}, \boldsymbol{\gamma}\right) \right\}$ and $\mathcal{P}^* \triangleq \arg \min_{\{\mathcal{P}^n\}_{n=1}^N} \mathbb{E}_{\boldsymbol{\gamma}} \left\{ P_D\left(K | \boldsymbol{B}, \boldsymbol{U} = \boldsymbol{1}, \boldsymbol{\gamma}\right) \right\}$ for any $\boldsymbol{B}$ such that $\boldsymbol{B} \in \mathcal{I}_A$.*

In the above, $P_{D_\infty}^*$ is the minimum PDP obtainable, when, at the start of the frame, each node has sufficient energy in its battery to support all the possible transmit and receive attempts, regardless of its harvesting pattern. This set of "good" inital battery state tuples is denoted by $\mathcal{I}_A$.

Note that, the lower bound $P_{D_\infty}^*$ can also be interpreted as the minimum PDP achievable for a multi-hop link whose nodes are equipped with infinite sized batteries. This

is because, as noted in [69], with infinite battery, it is necessary and sufficient to operate under an average power constraint[1] to satisfy the ENC.

On the other hand, the difference between the two bounds, $\sum_{\boldsymbol{B} \in \mathcal{I}_A^c} \pi(\boldsymbol{B})\Big|_{\mathcal{P}^*}$, is the sum of the stationary probabilities of the battery state vectors that do not necessarily support all transmission and reception attempts. Its value depends on the policy $\mathcal{P}^*$ as well as the size of the batteries at the nodes. Intuitively, the policy minimizing the lower bound has an additional side-benefit: it induces a (small) positive drift on the battery states at the nodes, causing the states to drift away from the set $\mathcal{I}_A^c$, and thereby reducing the gap between the upper and lower bounds. Hence, policies designed under the average power constraint are likely to be near-optimal. In the following subsection, we make this intuition mathematically precise. Specifically, we prove that for a multi-hop EH link with each node satisfying the average power constraint, the difference between the upper and lower bound decays exponentially with the size of the battery at the nodes. This, in turn, allows us to replace the objective function in (5.1) by the lower bound and the ENC by the average power constraint, to obtain near-optimal policies.

## 5.1.1 Tightness of the Bounds

In this subsection, we show that the difference between the upper and lower bound in (5.2) can be expressed as the sum of $N + 1$ terms, and each term decays exponentially with the size of the battery at a node, provided the multi-hop EH link is operating in the energy unconstrained regime (EUR), i.e., when all nodes operate under an average power constraint.

---

[1]When operating under an average power constraint, a node consumes $\epsilon$ less power than it harvests, on average, where $\epsilon > 0$ can be arbitrarily small. Due to this, the battery states drift to infinity over time, and energy outages do not occur.

**Theorem 2.** *If each node of a multi-hop EH link operates using a policy $\mathcal{P}$ with finite power levels and satisfying the EUR constraint, then $\sum_{\boldsymbol{B} \in \mathcal{I}_A^c} \pi(\boldsymbol{B}) = \sum_{n=1}^{N+1} \Theta(e^{r_n^* B_n^{\max}})$ where $r_n^*$ is a negative root of the asymptotic log moment generating function (MGF) of the battery drift process $\left( Y_s^n \triangleq B_s^n + \mathbb{1}_{\{\mathcal{H}_s^n\}} - L(B_s^n, B_s^{n+1}, \{U_s^i\}_{i=1}^n) - R(B_s^{n-1}, B_s^n, \{U_s^i\}_{i=1}^{n-1}) \right)$ of the $n^{th}$ node. Here, $L(.)$ and $R(.)$ denote the energy consumed for transmission and reception, respectively. The asymptotic log MGF is defined as $\Lambda(r_n) = \lim_{T \to \infty} \frac{1}{T} \log \mathbb{E}\left[ \exp\left( r_n \sum_{s=1}^T Y_s^n \right) \right]$.*

*Proof.* The proof follows using arguments similar to the proof in Theorem 1. □

In the above, $r_n^* = -\frac{2\delta_n}{\sigma_e^2} + o(\delta_n)$ [33], where $\delta_n$ is the battery drift (difference between the average energy harvested and average energy consumed) at node $n$ and $\sigma_e^2$ is the asymptotic variance of the harvesting process. For further details, see [33, Lemma 3].

Theorem 2 implies that, for a multi-hop EH link operating in EUR, the probability that the battery state of a node at the start of the frame cannot support all the receive and transmit attempts that could occur during the frame can be made arbitrarily small by choosing a sufficiently large battery at each node. Thus, for a multi-hop EH link with large enough battery at each node, the difference between the upper and lower bounds in (5.2) is negligible, when operating in the EUR. Hence, in the large battery regime, we can replace the objective in (5.1) by the lower bound obtained in Lemma 11. Moreover, the stringent energy neutrality requirement can be replaced by the relaxed EUR constraint. This leads to the following *reformulated optimization problem:*

$$\min_{\{\mathcal{P}^n\}_{n=1}^N} \mathbb{E}_{\boldsymbol{\gamma}} \{p_{\mathrm{D}}(\boldsymbol{B}, \boldsymbol{M}, \boldsymbol{\gamma})\}, \tag{5.3a}$$

$$\text{subject to } T_n + R_n \le K\rho_n, \text{ for all } 1 \le n \le N+1, \tag{5.3b}$$

$$0 \le E_\ell^n \le E_{\max} \text{ for all } 1 \le \ell \le K_n \text{ and } 1 \le n \le N, \tag{5.3c}$$

$$\text{where } T_n \triangleq \Pr[n] \left( \sum_{\ell=1}^{K_n} E_\ell^n \, \mathbb{E}_\gamma \left\{ \prod_{i=1}^{\ell-1} P_e(E_i^n, \gamma) \right\} \right), \tag{5.4}$$

$$\text{and } R_n \triangleq \Pr[n-1] \left( \sum_{\ell=1}^{K_{n-1}} R \mathbb{1}_{\{E_\ell^{(n-1)} \neq 0\}} \mathbb{E}_\gamma \left\{ \prod_{i=1}^{\ell-1} P_e(E_i^{(n-1)}, \gamma) \right\} \right) \tag{5.5}$$

denote the average energy consumed by the $n^{\text{th}}$ node for transmission and reception, respectively. The average energy consumed for transmitting the packet, $T_n$, is written by accounting for the following events:

1. The packet reaches the $n^{\text{th}}$ node, the probability which is denoted by $\Pr[n]$.

2. The $\ell^{\text{th}}$ attempt is made only if all the previous $\ell - 1$ attempts have failed. This happens with probability $\mathbb{E}_\gamma \left\{ \prod_{i=1}^{\ell-1} P_e(E_i^n, \gamma) \right\}$.

The average energy consumed by $n^{\text{th}}$ node in receiving a packet, $R_n$, is written similarly. Note that, in the expression for $R_n$, $\mathbb{1}_{\{E_\ell^{(n-1)} \neq 0\}}$ is an indicator function and captures the fact that the receiving node spends $R$ units of energy only if the transmitter attempts the packet at nonzero power. Also, the average energy consumed for reception and transmission at the source and destination node, i.e., $R_1$ and $T_{N+1}$, respectively, are defined to be equal to zero.

In the above,

$$\Pr[n] \triangleq \prod_{m=1}^{n-1} \mathbb{E}_\gamma \left( 1 - \prod_{i=1}^{K_m} P_e(P_i^m, \gamma) \right) \tag{5.6}$$

denotes the probability that a given packet reaches the $n^{\text{th}}$ node, and is written as the product of the probabilities of $n - 1$ independent events that the packet is delivered

successfully at the previous $n - 1$ hops. Further, at $m^{\text{th}}$ hop, the probability of successful delivery is written using the fact that a packet is dropped if all $K_m$ transmission attempts fail.

The constraint (5.3b) requires that the average energy consumed by each node in both transmission and reception, i.e., $T_n + R_n$, must be less than the average energy harvested by it, $K\rho_n$. Note that, the average power consumed by the $n^{\text{th}}$ node in receiving a packet, $R_n$, depends on $\mathcal{P}^{n-1}$, the transmit policy of $(n - 1)^{\text{th}}$ node. In turn, $R_n$ determines the average amount of energy, $T_n$, remaining for the $n^{\text{th}}$ node to transmit the packet. Hence, $\mathcal{P}^n$ depends on $\mathcal{P}^{n-1}$, and so on. This coupling between the policies of all the nodes necessitates the joint design of policies and renders the design problem in (5.3) challenging. However, for multi-hop links where the distance between consecutive nodes is large, the transmit energy dominates the power consumption of a node. In such a scenario, one can neglect the energy consumed in the reception, and the $R_n$ term in constraint (5.3b) can be dropped. This breaks the coupling between the policies of the nodes and admits a closed-form optimal solution. Therefore, before presenting the solution for the general problem in (5.3) with non-negligible $R_n$, in the following section, we present the solution for the special case when the energy cost of receiving a packet is negligible.

## 5.2 Special Case: Negligible Reception Cost

When the energy cost for receiving a packet is negligible, by dropping the $R_n$ term in constraint (5.3b), the optimization problem in (5.3) can be written as

$$\max_{\{\mathcal{P}^n\}_{n=1}^N} \Pr[N+1], \tag{5.7a}$$

$$\text{subject to} \quad \Pr[n] \left( \sum_{\ell=1}^{K_n} E_\ell^n \mathbb{E}_\gamma \left\{ \prod_{i=1}^{\ell-1} P_e(E_i^n, \gamma) \right\} \right) \leq K\rho_n, \text{ for all } 1 \leq n \leq N+1, \tag{5.7b}$$

$$0 \leq E_\ell^n \leq E_{\max} \text{ for all } 1 \leq \ell \leq K_n \text{ and } 1 \leq n \leq N. \tag{5.7c}$$

In (5.7), the objective is written in terms of the probability of reaching the destination node, $\Pr[N+1]$, which is given by (5.6), which is a product of $N$ terms with disjoint optimization variables. Hence, the problem can be solved by minimizing the packet outage probability of each individual hop. Thus, the problem splits as $N$ independent subproblems, and admits a closed-form solution for both fast and slow fading cases. We discuss the slow fading case next, and relegate the fast fading case to Sec. 5.3.

Consider the optimization problem for the $n^{\text{th}}$ hop and with a slow fading channel:

$$\min_{\mathbf{E}^n = \{E_1^n, \dots, E_{K_n}^n\}} \mathbb{E}_\gamma \left\{ \prod_{\ell=1}^{K_n} P_e(E_\ell^n, \gamma) \right\}, \tag{5.8a}$$

$$\text{subject to} \quad \Pr[n] \left( \sum_{\ell=1}^{K_n} E_\ell^n \mathbb{E}_\gamma \left\{ \prod_{i=1}^{\ell-1} P_e(E_i^n, \gamma) \right\} \right) \leq K\rho_n, \tag{5.8b}$$

$$0 \leq E_\ell^n \leq E_{\max} \text{ for all } 1 \leq \ell \leq K_n. \tag{5.8c}$$

Note that, in the above $\Pr[n]$ is function of power control policies of the previous $n-1$ nodes. Hence, it does not depend on the optimization variables of the problem (5.8) and can be treated as a constant for solving the problem (5.8). In the following, we first

solve (5.8) without the peak power constraint and then we adapt the solution to satisfy (5.8c).

## 5.2.1 Optimal Policy without the Peak Power Constraint

Using (4.3), for slow fading channels, the optimization problem (5.8) with only the EUR constraint can be written as

$$\min_{\mathbf{E}^n=\{E_1^n,\ldots,E_{K_n}^n\}} \left(1+\sum_{\ell=1}^{K_n}\frac{E_\ell^n}{N_0}\right)^{-1}, \tag{5.9a}$$

$$\text{subject to:} \quad \sum_{\ell=1}^{K_n}E_\ell^n\left(1+\sum_{i=1}^{\ell-1}\frac{E_i^n}{N_0}\right)^{-1} \leq \frac{K\rho_n}{\Pr[n]}, \tag{5.9b}$$

and $E_\ell^n \geq 0$ for $1 \leq \ell \leq K_n$. Due to the monotonic relationship between the transmit power level and the objective, for optimal policy the constraint in (5.9b) satisfies with equality. Hence, in the following we consider (5.9) only with equality constraint. Also, the objective function can be simplified to be maximize: $E_{\text{sum}} = \sum_{\ell=1}^{K_n} E_\ell^n$. Note that the above optimization problem is nonconvex, as the constraint set defined by (5.9b) is nonconvex. The following result provides a closed-form expression for the optimal policy. It has been proved in [78] in the context of point-to-point links and for slow fading channels; the same proof is applicable here also.

**Theorem 3.** *The unique optimal solution to* (5.9) *is given by*

$$E_k^{n^*} = \frac{\rho_n K}{K_n Pr[n]}\left(1+\frac{\rho_n K}{K_n N_0 Pr[n]}\right)^{k-1}, \ k=1,2,\ldots,K_n. \tag{5.10}$$

The above result shows that the transmit power levels in the optimal policy increases

monotonically and geometrically with the transmission index. Note that, the optimal policy ensures that the average power consumed in an attempt equals the average harvested energy that is available per active slot, $\frac{\rho_n K}{K_n \Pr[n]}$. Next, we adapt the solution obtained in Theorem 3 to the case where the peak transmit power is constrained.

## 5.2.2 Optimal Power Control Policy with Peak Power Constraint

In the rest of this section, we drop the superscript $n$ (the node index) to simplify the notation. Let $\mathbf{E}^* \triangleq \{E_1^*, \ldots, E_{K_n}^*\}$ be the RIP obtained from Theorem 3, and let $E_i^p$ denote the $i^{\text{th}}$ component of a feasible power vector of the original problem (5.8) under the peak power constraint. Consider forcing the solution $\mathbf{E}^*$ to satisfy the peak power constraint by setting $E_i^p = E_{\max}$ for all $i \in \mathcal{I}_p \triangleq \{i : E_i^* > E_{\max}, 1 \leq i \leq K_n\}$, and $E_j^p$ for all $j \notin \mathcal{I}_p$ obtained by solving a reduced dimensional optimization problem with the energy levels for indices $j \notin \mathcal{I}_p$ determined using Theorem 3. We recursively apply this procedure until a vector feasible to the original problem is obtained. We have the following Lemma, which is an immediate consequence of Lemma 2 in [79].

**Lemma 12.** *Let* $\mathcal{I}_p \triangleq \{i : E_i^* > E_{\max}, 1 \leq i \leq K_n\}$, *and let* $E_i^{p*}$ *denote the optimal solution to* (5.8). *If* $\mathcal{I}_p = \phi$ *then* $E_i^{p*} = E_i^*$ *for all* $1 \leq i \leq K_n$, *else* $E_i^{p*} = E_{\max}$ *for all* $i \in \mathcal{I}_p$.

The above Lemma shows that limiting the components of the closed-form solution (5.10) to take a value at most $E_{\max}$ yields the corresponding components of the optimal solution to (5.8). Now, the solution in (5.10) is nondecreasing in the attempt index. Hence, we can set the transmit power for the last $K'$ attempts to $E_{\max}$, where $K'$ is cardinality of $\mathcal{I}_p$. This results in the average energy consumption being strictly less than the energy harvested, leaving room for further optimizing the first $K_n - K'$ power levels.

Let $t \triangleq \sum_{\ell=1}^{K_n - K'} E_\ell$ denote the sum of the first $K_n - K'$ power levels. Considering $t$ to be an auxiliary optimization variable, and ignoring the constant terms in the objective, we obtain the following reduced dimensional version of (5.8):

$$\max_{\{E_1, \ldots, E_{K_n - K'}, t\}} t \tag{5.11a}$$

$$\text{subject to: } \sum_{\ell=1}^{K_n - K'} E_\ell \frac{1}{1 + \sum_{i=1}^{\ell-1} \frac{E_i}{N_0}} \leq \frac{K \rho_n}{\Pr[n]} - \sum_{i=1}^{K'} \frac{E_{\max}}{1 + \frac{t}{N_0} + \frac{(i-1)E_{\max}}{N_0}}, \tag{5.11b}$$

with $t = \sum_{\ell=1}^{K_n - K'} E_\ell$. From Theorem 3, the optimal solution to the problem (5.11) is given as

$$E_k^* = \frac{K_n}{K_n - K'} \left( \frac{\rho_n}{\Pr[n]} - \frac{F(t^*)}{K_n} \right) \left( 1 + \frac{K_n}{(K_n - K')N_0} \left( \frac{\rho_n}{\Pr[n]} - \frac{F(t^*)}{K_n} \right) \right)^{k-1}, \tag{5.12}$$

for $1 \leq k \leq K_n - K'$. In the above, $F(t)$ is given by

$$F(t) \triangleq \sum_{i=1}^{K'} \frac{E_{\max}}{1 + \frac{t}{N_0} + \frac{(i-1)E_{\max}}{N_0}}. \tag{5.13}$$

Since $\sum_{\ell=1}^{K_n - K'} E_\ell = t^*$, we compute $t^*$ as the solution to the fixed point equation

$$N_0 \left[ 1 + \frac{K_n}{(K_n - K')N_0} \left( \frac{\rho_n}{\Pr[n]} - \frac{F(t^*)}{K_n} \right) \right]^{K_n - K'} - 1 = t^*. \tag{5.14}$$

The following Lemma shows that a fixed point exists for the above equation.

**Lemma 13.** $f_2(t^*) \triangleq \left[ 1 + \frac{K_n}{(K_n - K')N_0} \left( \frac{\rho_n E}{\Pr[n]} - \frac{F(t^*)}{K_n} \right) \right]^{K_n - K'} - 1$ *has a fixed point when* $N_0 \leq 1$.

*Proof.* See Appendix D.1. $\qquad \square$

In case there are multiple fixed points, we pick the largest one among them, since the

goal is to maximize the objective function. Thus, we obtain the optimal solution to (5.8) in closed form.

Using the optimal power vectors of the individual hops, we can now obtain the optimal solution in the multi-hop EH case. We set $\Pr[1] = 1$. For $n = 1, 2, \ldots, N$, we compute $\mathbf{E}^n$, the power vector of the $n^{\text{th}}$ hop, using the procedure described above. From $\mathbf{E}^n$, compute $\Pr[n + 1]$ using (5.6). The output is the set of optimal RIPs $[\mathbf{E}^1, \ldots, \mathbf{E}^N]$. This completes the description of the solution to the optimization problem with negligible reception cost in the slow fading case. We next turn to the case where the channel is fast fading.

## 5.3 Negligible Reception Cost: Fast Fading Channel

In this section, we first present the optimal RIP with only the EUR constraint and then adapt it to find the optimal RIP under both EUR and peak power constraints. For a point-to-point link with fast fading channel, the optimization problem with only the EUR constraint can be written from (5.8) and using (4.14) as

$$\min_{\mathbf{E} = \left\{ E_1^n, \ldots, E_{K_n}^n \right\}} \frac{1}{\prod_{\ell=1}^{K_n} (1 + E_i^n)}, \tag{5.15a}$$

$$\text{subject to} \quad \sum_{\ell=1}^{K_n} E_\ell^n \frac{1}{\prod_{i=1}^{\ell-1} (1 + E_i^n)} \leq \frac{K \rho_n}{\Pr[n]}. \tag{5.15b}$$

The following Theorem provides a recursive relationship between the power levels for successive attempts in the optimal solution $\mathbf{E}^* = \{ E_1^{n^*} \ldots, E_{K_n}^{n^*} \}$ to (5.15).

**Theorem 4.** *For all $1 \leq \ell \leq K_n$, the optimal solution to (5.15) satisfies*

$$E_{\ell+1}^{n^*} = \frac{E_\ell^{n^*} (E_\ell^{n^*} + 2)}{2}. \tag{5.16}$$

*Proof.* See Appendix D.2. □

Based on the above Theorem, all the power levels can be expressed in terms of $E_1^n$, and the objective function in (5.15a) is a monotonically decreasing function of $E_1^n$. Hence, the optimal $E_1^n$ is simply the largest value that satisfies the constraint (5.15b). The following expression provides a close approximation to $E_1^{n^*}$

$$E_1 \approx L \left( 1 + \sqrt{1 + \frac{f(K_n)}{L^2(2^{K_n} - 1)}} \right), \tag{5.17}$$

where $L = \frac{(1 + K_n \rho_n E)2^{K_n - 1}}{2(2^{K_n} - 1)}$ and $f(K_n) \triangleq \frac{2 * (K_n - 2)}{(C - K_n + 5)}$, further $C = \frac{K_n \rho_n E}{\Pr[n]} + 1$.

It is observed through simulations, $E_1^{n^*}$ computed (5.17) provides a lower bound on the optimal $E_1^{n^*}$. Also, for moderate to large values of average harvested energy per slot, $\rho E_s$, the error incurred by using the approximation in (5.17) is small. Thus, it can be used as an initializer to solve the polynomial numerically. Alternatively, it can be found using the bisection method, as the left hand side of (5.15b) is monotonically increasing in $E_1^n$.

Also, we see that the optimal RIP in the fast fading case increases exponentially in the attempt index. This is in contrast to the slow fading case in Theorem 3, where the power levels increased geometrically in the attempt index.

Finally, it is straightforward to extend the solution in Theorem 4 to handle peak power constraints, using the procedure described in Sec. 5.2.2, since Theorem 12 is valid for both slow and fast fading channels. The only difference from the slow fading case is that, at each iteration, we need to solve a fixed-point equation obtained by expressing
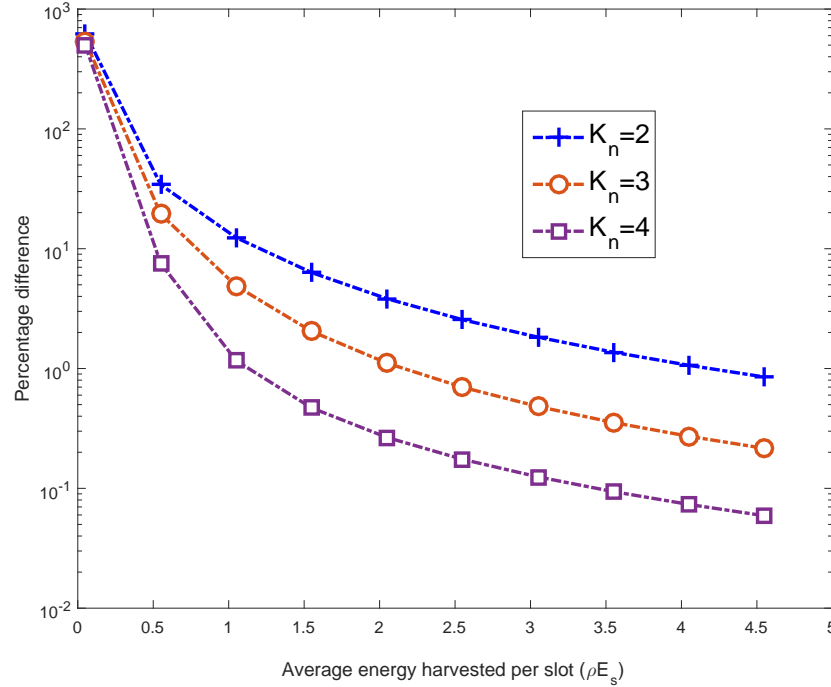
Figure 5.1: Accuracy of the approximation in (5.17). For moderate to large values of average harvested energy per slot, the error incurred by using the approximation in (5.17) incurs small error. In general, the $E_1^{n^*}$ computed using (5.17) lower bounds the exact value.

all other power levels in terms of $E_1^n$ to find its optimal value. Since the details are identical, we skip them.

This completes our discussion of the optimal RIPs when the reception cost is negligible. In the next section, we present the solution for the general problem in (5.3).

## 5.4 General Case: Nonzero Reception Cost

In this section, we present the solution in the scenario when the energy cost of packet reception is non-negligible. The nonzero reception cost leads to a coupling of the policies across the nodes and makes the problem challenging. In the following, we transform

the optimization problem in (5.3) to a complementary geometric program (CGP), and then solve it iteratively through a series of geometric program (GP) approximations. In the next subsection, we present the solution for the slow fading case. The solution in the fast fading case is similar, and can be found in D.3.

## 5.4.1   Multi-hop Links with Slow Fading Channel

In the slow fading case, the optimization problem in (5.3) can be rewritten as

$$\min_{\{\mathcal{P}^n\}_{n=1}^N} 1 - \Pr[N+1], \tag{5.18a}$$

$$\text{s. t.: } \Pr[n-1] \left( \sum_{\ell=1}^{K_{n-1}} \frac{\mathbb{1}_{\{E_\ell^{n-1}>0\}} R}{1 + \sum_{i=1}^{\ell-1} E_i^{n-1}} \right) + \Pr[n] \left( \sum_{\ell=1}^{K_n} \frac{E_\ell^n}{1 + \sum_{i=1}^{\ell-1} E_i^n} \right) \leq K\rho_n \text{ for all } n \tag{5.18b}$$

$$0 \leq E_\ell^n \leq E_{\max} \text{ for all } 1 \leq \ell \leq K_n \text{ and } 1 \leq n \leq N,$$

where $\Pr[m] = \prod_{n=1}^{m-1} \left( 1 - \frac{1}{1+\sum_{\ell=1}^{K_n} E_\ell^n} \right)$. The objective in the above problem is written using the fact that the PDP can also be expressed in terms of the probability that the packet reaches the destination, $\Pr[N+1]$. The constraint in (5.18b) captures the fact that, in each frame, the average energy consumed by $n^{\text{th}}$ node, for both transmission and reception, must be less than or equal to the average energy harvested by it. Both the objective and constraint in (5.18) are non-convex functions. In addition, due to the indicator function involved in the constraint (5.18b), the feasibility set of the above optimization problem depends on whether or not a particular element of the power control policy is zero. Hence, the optimization problem (5.18) is a nonconvex mixed integer nonlinear program (NMINLP), which is strongly NP hard to solve in general [60].

Depending on whether the indicator variable in constraint (5.18b) take the value zero

or one, the problem described in (5.18) is essentially a set of $2^K$ subproblems. However, as noted in the case of dual EH links, in Chapter 3, the solution of the above optimization problem depends only on the number of nonzero power attempts by each node, i.e., it does not depend on the precise indices of the nonzero attempts at each node. Hence, the computational complexity of the above problem can be reduced from $2^K$ to $\prod_{n=1}^{N} K_n$. Thus, the optimal solution to (5.18) can be obtained by solving $\prod_{n=1}^{N} K_n$ subproblems, with each subproblem corresponding to a combination of number of nonzero attempts across the hops. In the following, we focus on solving one subproblem, for a given pattern of nonzero transmit power levels. We solve it by transforming it into a CGP [61].

Without loss of generality, we present the solution for the case when all attempts are made at nonzero power levels. Using the substitution $L_\ell^n = 1 + \sum_{i=1}^{\ell} E_\ell^n$, the above problem can be reformulated as a CGP, as follows

$$\max_{\{\mathcal{P}^n\}_{n=1}^{N}} V, \tag{5.19a}$$

$$\text{subject to:} \quad V \leq \prod_{n=1}^{N} \left(1 - \frac{1}{L_{K_n}^n}\right) \tag{5.19b}$$

$$\prod_{m=1}^{n-2} \left(1 - \frac{1}{L_{K_m}^m}\right) \left(\sum_{\ell=1}^{K_{n-1}} \frac{R}{L_{\ell-1}^{n-1}}\right) + \prod_{m=1}^{n-1} \left(1 - \frac{1}{L_{K_m}^m}\right) \left(\sum_{\ell=1}^{K_n} \frac{L_\ell^n - L_{\ell-1}^n}{L_{\ell-1}^n}\right) \leq K\rho_n \text{ for all } n \tag{5.19c}$$

$$L_{\ell-1}^n (L_\ell^n)^{-1} \leq 1, \quad \frac{L_\ell^n}{L_\ell^{n-1} + E_{\max}} \leq 1 \text{ for all } 1 \leq \ell \leq K_n \text{ and } 1 \leq n \leq N+1. \tag{5.19d}$$

Note that (5.19b) and (5.19c) can be expressed as a ratio of posynomials. Hence, (5.19)

is a CGP. Therefore, as discussed for dual EH links, we construct a monomial approximation for the denominator posynomial of the constraints. This results in a GP approximation of (5.19), which can be solved optimally, since a GP is a convex problem. Thus, we solve the original problem iteratively, by solving a GP approximation to the problem at each iteration. The recipe to solve the CGP in (5.19) is similar to Algorithm 2.

In fast fading case, the problem of finding optimal RIPs is solved similarly, the details are provided in Appendix D.3 This completes our solution to the problem in the case where the energy cost of packet reception is non-negligible. Next, we present simulation results to illustrate the performance of the proposed solution.

In the next subsection, we present the design of optimal policies for the general EH processes.

## 5.5 Design of Optimal Policy for General EH Processes

First, we present the design of near-optimal policies for the temporally correlated EH processes.

**Design of Optimal Policies for Stationary Markov Harvesting Process**

The packet drop probability in (4.15) can be rewritten as

$$P_D = \sum_{(B)} \pi(B) \sum_E \pi(E|B) \mathbb{E}_\gamma \{P_D(K|B, U = 1, E, \gamma, s = 0)\}, \quad (5.20)$$

$$= \sum_{(B)} \pi(B) \mathbb{E}_\gamma \{P_D(K|B, U = 1, \gamma, s = 0)\}, \quad (5.21)$$

where $\mathbb{E}_\gamma \{P_D(K|B, U = 1, \gamma, s = 0)\} \triangleq \sum_E \pi(E|B) \mathbb{E}_\gamma \{P_D(K|B, U = 1, E, \gamma, s = 0)\}$.

Since the Theorem 2 is applicable in this scenario also (For further details on this

we refer the reader to Chapter 2), the objective of the PDP optimization problem can be replaced by $\mathbb{E}_{\gamma} \{p_{\mathrm{D}}(\boldsymbol{B}, \boldsymbol{M}, \boldsymbol{\gamma})\}$. Furthermore the ENC can be replaced by average power constraint. The average power constraint in this case is written by replacing the $\rho E_s$ by the average energy harvested per slot, for the Markov process. The optimization problem obtained this way can be solved using the CGP based procedure, provided in Sec. 5.4.1.

As in Chapter 2, similar arguments can be used to account for the spatial correlation of the EH processes across the nodes, and obtain the optimal policies. We skip the details.

## 5.6 Simulations and Discussion

The simulation set up here is same as in Chapter 4.

**Performance under negligible reception cost**

In Figs. 5.2 and 5.3, we illustrate the performance of the closed-form RIP derived in Secs. 5.2.2 and 5.3 for slow and fast fading links, respectively. The performance of the proposed policy for multi-hop links with finite sized battery nodes is close to the lower bound presented in Lemma 11. The proposed RIP offers a ten-fold improvement in the PDP compared to the equal power policy (EPP) which uses $P_{\mathrm{max}} = 10E_s/T_s$ as the transmit power in every attempt. It is interesting to observe that the PDP of the EPP with ($E_s = 2$ dB, $\rho_2 = 0.6$) is lower than the PDP of the EPP with ($E_s = 5$ dB, $\rho_2 = 0.3$), even though the average energy harvested in the two scenarios is the same. On the other hand, for the proposed policy, the PDP with ($E_s = 2$ dB, $\rho_2 = 0.6$) is higher than the PDP with ($E_s = 5$ dB, $\rho_2 = 0.3$). This can be explained as follows. The EPP for
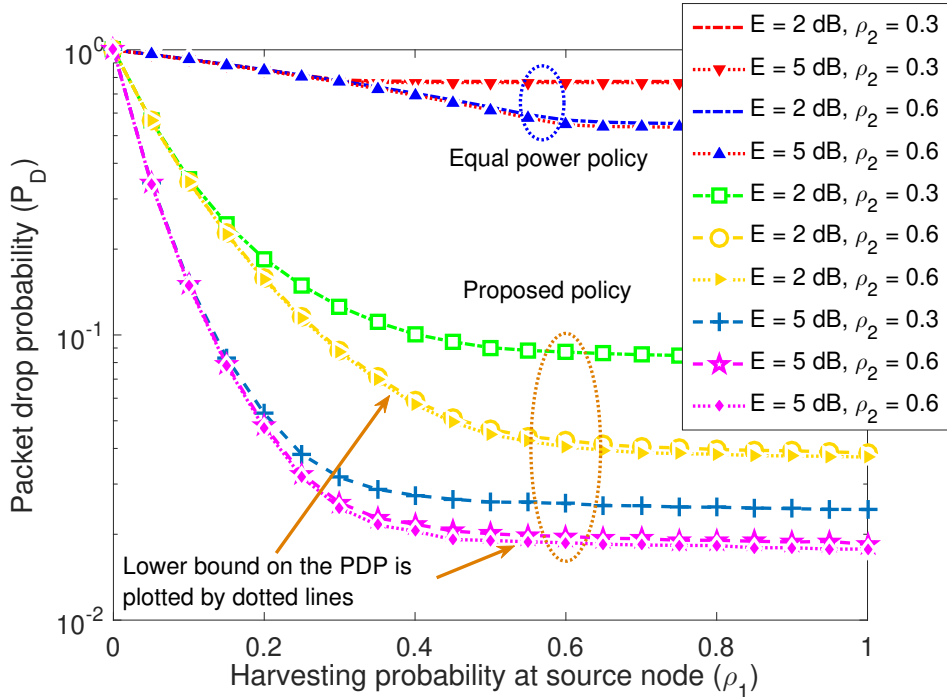
Figure 5.2: Performance of the policy designed under negligible reception cost assumption for a slow fading channel: our closed-form policy outperforms the equal power policy which attempts the packet with transmit power level $P_{\max}$. The setup considers a multi-hop link with packet reception cost $R = 1$. Parameters: $P_{\max} = \frac{10E_s}{T_s}$ and $E_s = 5$ dB. For all nodes, $B_n^{\max} = 50$.

$E_s = 2$ dB uses lower power in each attempt than the EPP for $E_s = 5$ dB. Due to this, the second node runs out of energy less frequently when $E_s = 2$ dB, ensuring better packet delivery at the destination. For the proposed policy, the range of power values available to the transmitter for designing the RIP is higher when $E_s = 5$ dB than that with $E_s = 2$ dB, since $P_{\max} = 10E_s/T_s$ is set as the maximum *allowed* transmit power. Therefore, the performance of the optimal policy in the former case is better than the latter.

In Fig. 5.4, the performance of the closed-form optimal RIP designed by ignoring the packet reception cost using the approach in Secs. 5.2 and 5.3 is compared against the performance of the near-optimal policy for the general case, when $R = 1$. We note that,
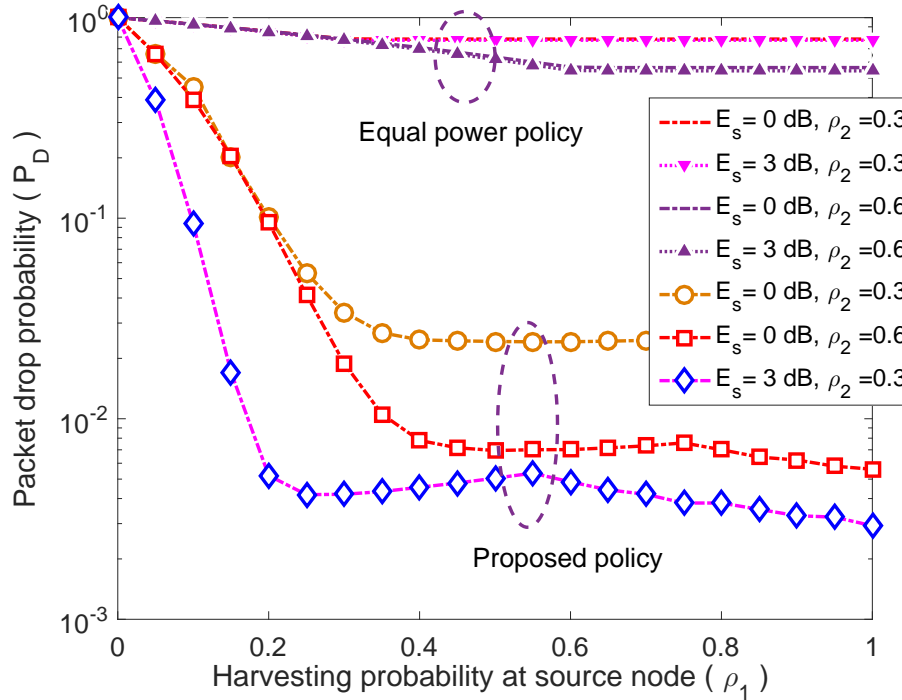
Figure 5.3: Performance of the policy in special case, for a fast fading channel. In this scenario the proposed policy outperforms the equal power policy $[P_{\max} \; P_{\max} \; P_{\max} \; P_{\max}]$. The parameters chosen are $P_{\max} = \frac{10E_s}{T_s}$. $B_{\max}^n = 200$ for all nodes.

the PDP of closed-form policy is inferior to the PDP of near-optimal policy for general case. Under the settings considered, when the channel is slow fading, the peak power constraint saturates the transmit power levels of the CGP-optimal solution saturates to $P_{\max}$ for all attempts. Because of this, the performance of the CGP-based and the closed-form solution is similar. In the fast fading case, there is a much larger performance improvement over the closed-form solution. This highlights the value of solving the coupled optimization problem when the packet reception cost is nonzero.

Figure 5.5 illustrates the performance of the proposed iterative GP approximation based solution presented in Sec. 5.4.1, for slow fading channels. In this case also, the PDP of the proposed policy is close to the lower bound presented in the Lemma 11.
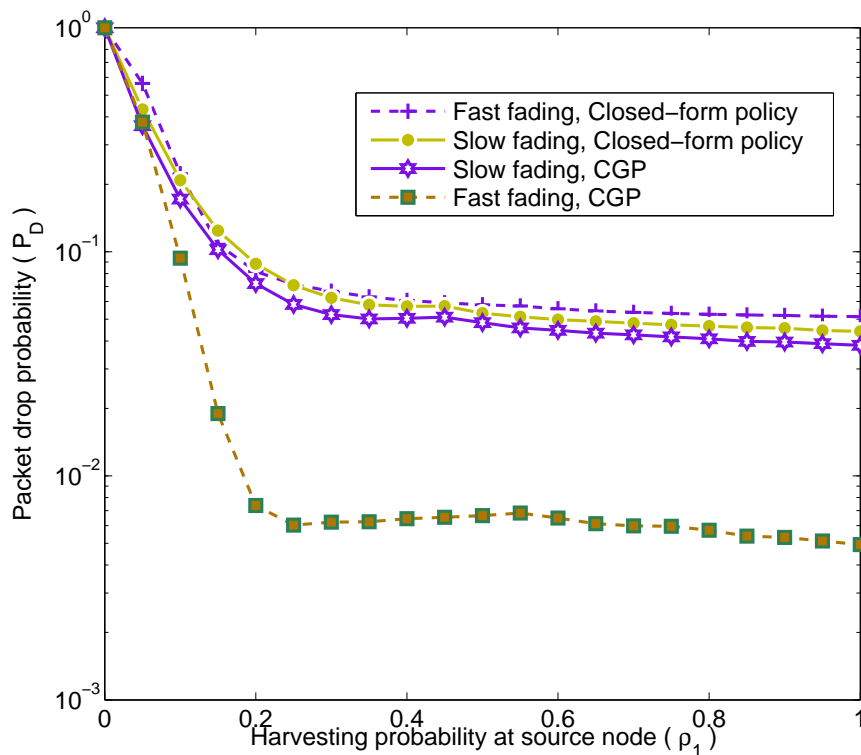
Figure 5.4: Comparison of CGP policy with closed-form policy: Performance of optimal policy designed by ignoring the energy cost of packet reception, compared to the near-optimal policy for the general case. The setup considers a multi-hop link with packet reception cost $R = 1$. As before, $P_{\max} = \frac{10E_s}{T_s}$. The harvested energy in the slow fading case is $E_s = 5$ dB, while for the fast fading case, $E_s = 3$ dB. For all nodes, $B_n^{\max} = 50$ and $200$ for the slow and fast fading channels, respectively.
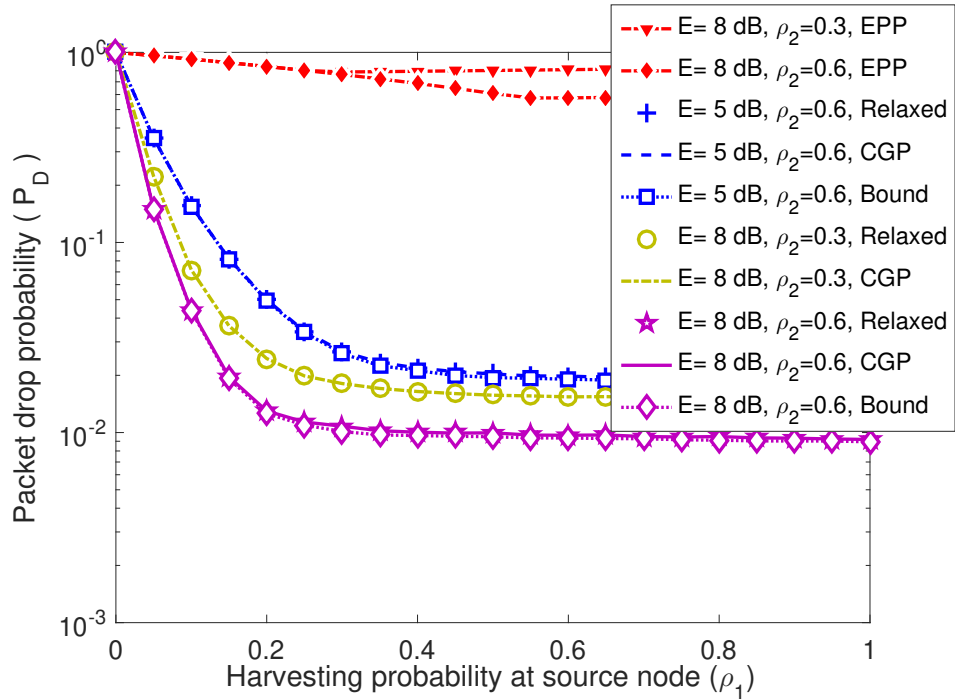
Figure 5.5: Performance of the proposed CGP based algorithm for finding near-optimal RIPs, for a slow fading channel. Parameters: $R = 1$ and $P_{\max} = 10E_s/T_s$. For both the hops, the EPP is $[P_{\max}\ P_{\max}\ P_{\max}\ P_{\max}]$. $B_{\max}^n = 50$ for all the nodes. (a) The CGP based policy outperforms both the EPP as well as the closed-form policy obtained by ignoring the energy cost of packet reception.

The curves corresponding to the lower bound are labeled as `Bound`. The PDP of our solution is also compared against the EPP that uses power $P_{\max}$ for all attempts. The PDP of the proposed policy is approximately ten-fold better than the PDP obtained by the EPP. Also, we plot the performance of the policy designed by setting the indicator function in (5.5) to be always one, i.e., by assuming that all the transmit attempts are made at a nonzero power level. We label the corresponding curves as `Relaxed`. By setting the indicator functions to unity, we only need to solve a single sub-problem instead of $\prod_{n=1}^{N} K_n$ sub-problems. We see that the performance gap between the two policies is almost negligible. Thus, in a wide range of scenarios, nearly optimal policies can be
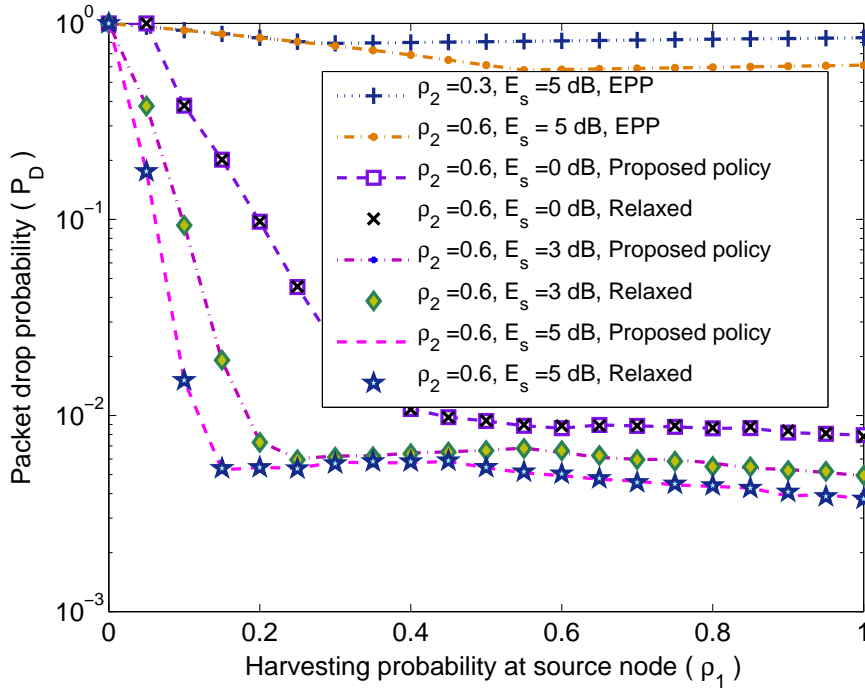
Figure 5.6: Fast fading channel: Performance of the proposed algorithm for finding near-optimal power management policies. The parameters chosen are $R_2 = R_3 = 1$ and $P_{\max} = \frac{10E_s}{T_s}$. For both the hops, the equal power policy is $[P_{\max} \ P_{\max} \ P_{\max} \ P_{\max}]$. $B_{\max}^n = 200$ for all nodes.

obtained by solving the relaxed problem. Similar behavior is seen in Fig. 5.6 for the fast fading case: in fact, our policy offers over 100 times improvement in PDP compared to the EPP.

In Fig. 5.7, we illustrate that the PDP at the second hop decreases with increase in the harvesting probability at the source node. This is because, at higher harvesting rate, the source node can attempt the packet transmission at higher transmit power levels. This reduces the average power consumed for packet reception at the $2^{\text{nd}}$ node, which, in turn, allows it to transmit at higher power levels to the destination, while still meeting its own average power constraint. Also, the relatively smaller improvement in the PDP
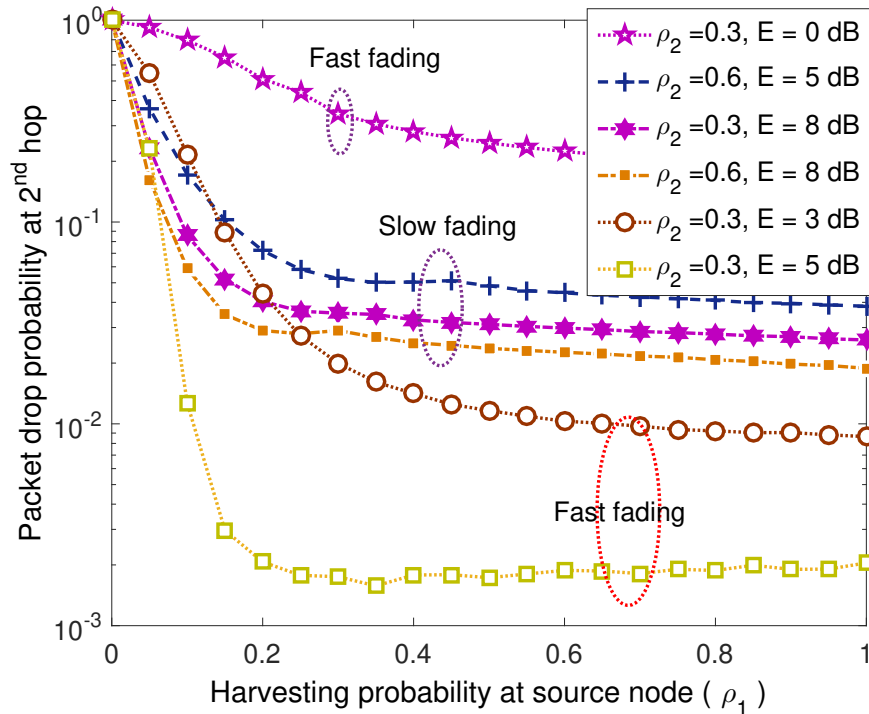
Figure 5.7: the PDP at the second hop improves with increase in the harvesting rate at the source node. The parameters used are same in Fig. 5.5

at higher harvesting rates is because of the peak transmit power constraint, which limits the benefit obtainable by higher harvesting rates.

## 5.7 Conclusions

In this chapter, we setup a RIP optimization problem, which was solved in two different scenarios. First, we considered a scenario when the energy cost for reception is negligible, and derived closed-form expressions for the optimal RIPs. Next, we presented an iterative geometric programming based solution to the RIP optimization problem under non-negligible energy reception cost. Through simulations, we illustrated that our proposed policies significantly outperform equal power policies. In addition, our

results provided interesting insights into the trade-offs in the system parameters and highlighted the coupled nature of the problem. Future extensions of this work can consider the design of RIPs for multi-hop links with time-correlated channels, under different quality of service requirements, and solve the optimization problem with dynamic slot allocation across the nodes.

# Chapter 6

# Distributed Power Control for Uncoordinated Dual Energy Harvesting Links: Performance Bounds and Near-Optimal Policies

In the previous chapters, we assumed that the transmitter and receiver employ the coordinated sleep-wake protocol, i.e., that they are aware about the energy availability of the other node. This, in turn, facilitates coordinated transmission between the nodes and completely avoids the wastage of energy that could occur when either only the transmitter or only the receiver make an attempt. In order to achieve coordination, 1-bit SoC information needs to be exchanged between the nodes. For retransmission protocols, this 1-bit SoC information can be exchanged easily, by simply deferring the ACK/NACK message (or the transmission of the next packet) when the node runs out of energy. However, in absence of any feedback from the receiver (e.g., in the form of ACK/NACK messages), sending 1-bit SoC information is an additional overhead on the protocol. This overhead may be significant in low power and energy starved EH

applications, making it relevant to investigate the performance of EH communication systems in the absence of sleep-wake coordination and design the energy management policies that achieve optimal performance, which is the focus of this chapter.

We consider a point-to-point link between an EH transmitter and receiver, where neither node has the information about the battery state or energy availability at the other node. We consider a model where data is successfully delivered only in slots where both nodes are *active*. Energy loss occurs whenever one node turns on while the other node is in sleep mode. In each slot, based on their own energy availability, the transmitter and receiver need to independently decide whether or not to turn on, with the aim of maximizing the long-term time-average throughput.

The goal of this chapter is to design a distributed and online power control policy to maximize the long-term time-averaged throughput with minimal feedback (ideally, no feedback) about the battery state at the other node. First, we derive an upper bound on the maximum achievable throughput without coordination, by analyzing a system that has non-causal knowledge of energy arrivals. Next, we present an online, distributed power control policy whose throughput is within one bit of the upper bound, and requires an occasional one bit feedback. In order to further reduce the amount of feedback to achieve the upper bound, we propose a time-dilated policy which achieves the upper bound and requires no feedback as the time dilation gets large. We also propose a near-optimal, deterministic, fully uncoordinated policy which requires no feedback about the battery state, and analytically characterize its gap from the occasional one bit feedback based coordinated policy. Our simulation results confirm the theoretical findings and illustrate the impact of the policy on the performance achieved.

## 6.1 System Model

We consider a point-to-point link where an energy harvesting node (EHN) needs to transmit data to another EHN over an AWGN channel. The harvesting process at the transmitter and receiver are assumed to be independent stationary and ergodic random processes with their mean harvesting rates denoted by $\mu_t$ and $\mu_r$, respectively. The energy harvested at the transmitter and receiver in the $n^{\text{th}}$ slot is denoted by $\mathcal{E}_t(n)$ and $\mathcal{E}_r(n)$, respectively. At both the nodes, the harvested energy is stored in a perfectly efficient, finite capacity battery. Since the amount of energy harvested is random, both the transmitter and receiver do not know the exact battery state at their counterpart. Hence, in any slot, the transmitter does not know if the receiver will be 'on' to receive the data or not, and vice-versa. A data packet is successfully delivered if and only if the transmitter and receiver are simultaneously *on* in a slot.

The power control policy at the transmitter and receiver over an $N$ slot horizon is denoted by $\mathcal{P}_t = \{p_t(n)\}_{n=1}^{N}$ and $\mathcal{P}_r = \{p_r(n)\}_{n=1}^{N}$, respectively, where $p_t(n)$ and $p_r(n)$ denote the energy used by the transmitter and receiver, respectively, in the $n^{\text{th}}$ slot. The power control policy at the receiver, $p_r(n)$, is binary valued, i.e., if it decides to turn *on* in a slot, it always consumes $R$ units of energy; and it does not incur any energy cost in the sleep mode [1, 26, 45]. On the other hand, the transmit power control policy is continuous valued. Without loss of generality, we assume that each slot is of unit duration; hence, we use the terms power and energy interchangeably. By the principle of energy conservation, the battery at the transmitter evolves as

$$B_{n+1}^t = \min\left\{\max\{0, B_n^t + \mathcal{E}_t(n) - p_t(n)\}, B_{\max}^t\right\}. \tag{6.1}$$

In the above, $B_n^t$ denotes the battery at the transmitter at the start of the $n^{\text{th}}$ slot, and $B_{\max}^t < \infty$ denotes the size of the battery at the transmitter. The battery at the receiver is of size $B_{\max}^r$, and its state $B_n^r$ evolves in a similar fashion. We also consider the use of super capacitor at the transmitter, for temporarily holding energy budgeted for transmission. Its role in the operation of the transmitter will be elaborated on later.

We assume that the rate achieved corresponding to power $p_t(n)$ is well approximated by the capacity expression, i.e., $\mathcal{R}(p_t(n)) \triangleq \log(1 + p_t(n))$ [80, 81], which is an upper bound on the actual rate. For simplicity, we assume that the power spectral density of the additive white Gaussian noise at the receiver is unity. Our aim in this chapter is to devise a distributed power control strategy for the transmitter and the receiver, i.e., $\mathcal{P}_t$ and $\mathcal{P}_r$, such that the long-term time-averaged throughput is maximized. That is, our goal is to maximize

$$\mathcal{T} \triangleq \frac{1}{N} \sum_{n=1}^{N} \mathbb{1}_{\{p_r(n) \neq 0\}} \log(1 + p_t(n)). \tag{6.2}$$

In the above, $\mathbb{1}_{\{p_r(n) \neq 0\}}$ is an indicator function which takes value one if $p_r(n)$ is nonzero, otherwise it is equal to zero. Thus, $\mathbb{1}_{\{p_r(n) \neq 0\}} \log(1 + p_t(n))$ denotes the rate achieved in the $n^{\text{th}}$ slot, which is nonzero if and only if both the EHNs are on in the $n^{\text{th}}$ slot, i.e., $p_t(n) \neq 0$ and $p_r(n) \neq 0$.

Mathematically, the problem of maximizing the long-term time-averaged throughput can be written as

$$\max_{\{p_t(n), p_r(n), n \geq 1\}} \liminf_{N \to \infty} \mathcal{T} \tag{6.3a}$$

$$\text{subject to: } 0 \leq p_t(n) \leq B_t^n, \tag{6.3b}$$

$$p_r(n) \in \{0, R\}, \text{ and } p_r(n) \leq B_r^n. \tag{6.3c}$$

In (6.3c), the constraint $p_r(n) \in \{0, R\}$ denotes the fact that the power control policy at the receiver is binary-valued, i.e., it consumes $0$ or $R$ units of energy, depending on whether it is off or on, respectively. Note that, for a given sample path of the harvesting processes and deterministic policies conditioned on the sample path, $\liminf_{N \to \infty} \mathcal{T}$ is a well defined deterministic quantity. We seek to obtain the power control policy for the transmitter and receiver such that they can operate without requiring knowledge of each other's battery state, while achieving near-optimal performance. First, in order to benchmark the performance of any policy, we derive an upper bound on the throughput in (6.3).

## 6.2   Upper Bound on the Throughput

In this section, we derive an upper bound on the achievable long-term time-averaged throughput by considering a system in which both the EHNs are equipped with infinite size batteries, and have noncausal information about the energy arrivals. The following Lemma provides the upper bounds.

**Lemma 14.** *The long-term time-averaged throughput of a dual EH link satisfies:*

1. $\liminf_{N \to \infty} \mathcal{T} \leq \log(1 + \mu_t)$ *if* $\frac{\mu_r}{R} > 1$,

2. $\liminf_{N \to \infty} \mathcal{T} \leq \left(\frac{\mu_r}{R}\right) \log\left(1 + \frac{R\mu_t}{\mu_r}\right)$ *if* $\frac{\mu_r}{R} \leq 1$.

*Proof.* See Appendix E.1.                                                                      □

In the above Lemma, the first scenario *(1)* corresponds to the setting where the average harvesting rate at the receiver exceeds $R$, the energy consumed by it per slot when it

is *on*. Thus, the battery state at the receiver has a positive drift even if it remains on in all slots, i.e., the receiver is energy unconstrained. This case is equivalent to having only the transmitter as an EHN. Case *(2)* corresponds to a scenario when the receiver is energy-constrained, i.e., the average energy harvested in a slot is less than the energy consumed in one slot. Consequently, the receiver can only turn on intermittently. To avoid loss of energy, the transmitter must avoid sending data when the receiver is off. However, this requires the transmitter to know the state of the battery at the receiver. In the next section, we present near-optimal policies for both the scenarios.

## 6.3 Asymptotically Optimal Policies

In the following, we first consider Case *(1)* and present a policy which asymptotically achieves the upper bound given in Lemma 1, and does not require any feedback about the battery state at the receiver.

### 6.3.1 Energy Unconstrained Receiver, $\frac{\mu_r}{R} > 1$

First, when the battery state has a positive drift, it is known that the probability that the receiver does not have sufficient energy to turn on decays exponentially with the size of the battery (see Theorem 1). Consequently, with high probability, the receiver can always remain on, making this case equivalent to the scenario where only the transmitter is EH. The optimal policy in this scenario, denoted by $\mathcal{P}^u$, is the same as the one proposed in [33], which is as follows:

$$p^u(n) = \begin{cases} \mu_t + \delta_t^+, & B_n^t \geq \frac{B_{max}^t}{2}, \\ \min\{B_n^t, \mu_t - \delta_t^-\}, & B_n^t < \frac{B_{max}^t}{2}, \end{cases} \tag{6.4}$$

where $\delta_t^+ = \delta_t^- = \beta_t \sigma_t^2 \frac{\log B_{\max}^t}{B_{\max}^t}$. Here, $\sigma_t^2$ denotes the asymptotic variance of the harvesting process at the transmitter, and $\beta_t \geq 2$ is a constant. It is shown in [33] that the policy $\mathcal{P}^u \triangleq \{p^u(n)\}_{n=1}^N$ converges to the optimal utility at the rate $\Theta\left(\left(\frac{\log B_{\max}^t}{B_{\max}^t}\right)^2\right)$ while the transmitter battery discharge probability simultaneously goes to zero at the rate $\Theta\left(B_{\max}^t{}^{-\beta_t}\right)$. The transmitter battery discharge probability is defined as $p_d^t \triangleq \lim_{N\to\infty} \frac{1}{N}\sum_{n=1}^N \mathbb{1}_{\{B_n^t=0\}}$. The receiver battery discharge probability is defined similarly. Thus, in the scenario described in the Case *(1)*, $\mathcal{P}^u$ is asymptotically optimal as the battery size gets large.

Next, we consider Case *(2)*, and present a policy which achieves within one bit of the upper bound, using an occasional one bit feedback about the receiver's battery state.

## 6.3.2 Energy Constrained Receiver, $\frac{\mu_r}{R} < 1$

In this section, we present a policy that requires *occasional* one bit feedback. Qualitatively, the policy operates as follows. The receiver sends a one bit feedback whenever the battery level crosses the half-full mark. We assume that the feedback is received without error and delay, and ignore the energy and time overhead in sending it. The one bit feedback enables the transmitter to track whether the receiver's battery is more than or less than half full. Further, the receiver executes a deterministic policy in either half of the battery state; and the transmitter follows the receiver's policy and transmits only in slots where the receiver is also on. In the slots when the receiver is off, the transmitter accumulates the energy prescribed by its own policy in a super capacitor and uses the accumulated energy for transmission in the next slot when the receiver turns on. The consequence of using a super capacitor to temporarily store energy is

that the battery energy discharge at the transmitter depends only on its own battery state; specifically, it is independent of the policy at the receiver.

We now describe the policy in mathematical terms. The energy accumulated in the super capacitor by the end of $n^{\text{th}}$ slot, given that the transmitter does *not* transmit in that slot, is given by

$$\mathcal{C}_e(n) = \begin{cases} \mathcal{C}_e(n-1) + \mu_t + \delta_t^+, & \text{if } B_n^t \geq \frac{B_{\max}^t}{2}, \\ \mathcal{C}_e(n-1) + \min\{\mu_t - \delta_t^-, B_n^t\}, & \text{if } B_n^t < \frac{B_{\max}^t}{2}, \end{cases} \tag{6.5}$$

and $\mathcal{C}_e(n) = 0$, if data is transmitted in the $n^{\text{th}}$ slot, and $\delta_t^+ = \delta_t^- = \beta_t \sigma_t^2 \frac{\log B_{\max}^t}{B_{\max}^t}$. Here, we assume that the capacity of the super capacitor is sufficient to store the energy accumulated between two consecutive data transmissions. Let $\mathbb{1}_{\mathcal{R}^+}$ denote an indicator function which takes the value one if $B_n^r \geq \frac{B_{\max}^r}{2}$ and zero otherwise. Also, let $N_r^+ \triangleq \lfloor \frac{R}{\mu_r} \rfloor$, and $N_r^- \triangleq \lceil \frac{R}{\mu_r} \rceil$. In the $n^{\text{th}}$ slot, the transmitter follows the policy $\mathcal{P}_t^c$ given by

$$p_t^c(n) = \begin{cases} \mathcal{C}_e(n-1) + \mu_t + \delta_t^+, & \text{if } B_n^t \geq \frac{B_{\max}^t}{2}, \\ & n = N_{\text{on}} + N_r^+ \mathbb{1}_{\mathcal{R}^+} + N_r^-(1 - \mathbb{1}_{\mathcal{R}^+}), \\ \mathcal{C}_e(n-1) + \min\{\mu_t - \delta_t^-, B_n^t\}, & B_n^t < \frac{B_{\max}^t}{2}, \\ & n = N_{\text{on}} + N_r^+ \mathbb{1}_{\mathcal{R}^+} + N_r^-(1 - \mathbb{1}_{\mathcal{R}^+}), \\ 0 & \text{otherwise.} \end{cases} \tag{6.6}$$

In the above, $N_{\text{on}}$ denotes the previous slot when the transmitter and receiver were scheduled to turn on. It is initialized to zero at the first slot ($N_{\text{on}} = 0$ when $n = 0$), and at any slot index $n$ satisfying $n = N_{\text{on}} + N_r^+ \mathbb{1}_{\mathcal{R}^+} + N_r^-(1 - \mathbb{1}_{\mathcal{R}^+})$, the transmitter and receiver make an attempt if they have energy, and $N_{\text{on}}$ is set to $N_{\text{on}} = n$, i.e., it is updated to the current slot index. The policy (6.6) is derived using the policy given in

(6.4), i.e., in each slot, the transmitter computes the energy prescribed by $p^u(n)$ for that slot, and transfers the energy from the battery to the super capacitor. In a slot when the receiver is on, the transmitter uses all the energy accumulated in the super capacitor till that slot to transmit its data.

The policy at the receiver is given as

$$
p_r^c(n) = \begin{cases} R, & B_n^r \geq \frac{B_{\max}^r}{2}, n = N_{\text{on}} + N_r^+ \\ R, & R \leq B_n^r < \frac{B_{\max}^r}{2}, n = N_{\text{on}} + N_r^-, \\ 0 & \text{otherwise.} \end{cases} \tag{6.7}
$$

The receiver's policy $\mathcal{P}_r^c \triangleq \{p_r^c(n)\}_{n=1}^N$ also emulates the policy $\mathcal{P}^u$ given in (6.4). Specifically, the receiver executes a policy similar to $\mathcal{P}^u$ by turning on after $N_r^+ \triangleq \lfloor \frac{R}{\mu_r} \rfloor$ slots (resulting in a negative drift in the battery state) if battery is more than half full, otherwise it turns on after $N_r^- \triangleq \lceil \frac{R}{\mu_r} \rceil$ slots (resulting in a positive drift in the battery state).

This ensures that its battery has a positive drift when it is less than half full and a negative drift when it is more than half full.

In the discussion to follow, let $\mathcal{P}^c$ denote the joint power management policy proposed above, i.e., $\mathcal{P}_t^c \triangleq \{p_t^c(n)\}_{n=1}^N$ and $\mathcal{P}_r^c$ given by (6.6) and (6.7), respectively. The following Lemma asserts that the throughput achieved by the policy $\mathcal{P}^c$ is within 1 bit of the upper bound, when the battery capacity is large. In addition, the probability of battery discharge decays polynomially with the battery size at the transmitter, and it decays exponentially fast with the battery size at the receiver.

**Lemma 15.** *Let $\mathcal{T}^c$ denote the time-average throughput achieved by the policy $\mathcal{P}^c$. For policy $\mathcal{P}^c$, the battery discharge probability at the transmitter and receiver are $p_d^t = \Theta \left( B_{\max}^t \right.^{-\beta_t} \left. \right)$ and $p_d^r = \Theta \left( \exp \left( -\frac{B_{\max}^r \mu_r \delta_r^-}{\sigma_r^2} \right) \right)$, respectively, where $\beta_t \geq 2$ and $\delta_r^- \triangleq N_r^- - N_r$, with $N_r \triangleq \frac{R}{\mu_r}$. In*

*addition,* $\left(\frac{\mu_r}{R}\right) \log \left(1 + \frac{R\mu_t}{\mu_r}\right) - \mathcal{T}^c - 1 = O\left(\frac{\log B^t_{\max}}{B^t_{\max}}\right).$

*Proof.* See Appendix E.2. □

A careful examination of the proof of Lemma 15 reveals that the one bit gap in the throughput arises because of the receiver's policy. From (6.7), the receiver's policy is to wake up once in $N^+_r$ slots if its battery is more than half full, and to wake up once in $N^-_r$ slots if its battery is less than half full. Due to this, the drift in the receiver's battery remains fixed at $\delta^-_r = N^-_r - N_r$ when $B^r_n < B^r_{\max}/2$ and $\delta^+_r \triangleq N_r - N^+_r$ when $B^r_n \geq B^r_{\max}/2$, irrespective of the value of $B^r_{\max}$. In order to close the gap, we need finer control over the battery drift at the receiver. We need it to be of the order $o(1/B^r_{\max})$, similar to that at the transmitter. This can be achieved using time dilation, as described next. In fact, for policy $\mathcal{P}^c$, the drift at the receiver cannot be controlled, which leads to the the loss of one bit in the throughput. In the following section, we present a time-dilated version of the policy $\mathcal{P}^c$ which provides a finer control over $\delta^+_r = N_r - N^+_r$ and $\delta^-_r$.

## 6.4 Optimal Throughput via Time-dilation

The key idea behind time dilation is to spread the drift $\delta^+_r$ and $\delta^-_r$ at the receiver over a larger number of slots, resulting in a smaller per-slot drift. That is, instead of (6.7), which operates in batches of $\lfloor \frac{R}{\mu_r} \rfloor$ or $\lceil \frac{R}{\mu_r} \rceil$ slots, we consider a policy that operates in batches of $\lfloor \frac{Rf(B^r_{\max})}{\mu_r} \rfloor$ and $\lceil \frac{Rf(B^r_{\max})}{\mu_r} \rceil$ slots, where $f(\cdot) > 1$ is a time dilation function. For example, if $f(B^r_{\max})$ is an integer, the time dilated policy turns the receiver on for $f(B^r_{\max})$ slots out of $\lfloor \frac{Rf(B^r_{\max})}{\mu_r} \rfloor$ slots if the battery at the receiver is more than half full, and it turns the receiver on for $f(B^r_{\max})$ slots out of $\lceil \frac{Rf(B^r_{\max})}{\mu_r} \rceil$ if the battery is less than

half full. This results in a drift of

$$\delta_{r,f}^+(B_{\mathrm{max}}^r) = f(B_{\mathrm{max}}^r)N_r - \left\lfloor \frac{Rf(B_{\mathrm{max}}^r)}{\mu_r} \right\rfloor \tag{6.8}$$

$$\delta_{r,f}^-(B_{\mathrm{max}}^r) = \left\lceil \frac{Rf(B_{\mathrm{max}}^r)}{\mu_r} \right\rceil - f(B_{\mathrm{max}}^r)N_r \tag{6.9}$$

over $\left\lfloor \frac{Rf(B_{\mathrm{max}}^r)}{\mu_r} \right\rfloor$ and $\left\lceil \frac{Rf(B_{\mathrm{max}}^r)}{\mu_r} \right\rceil$ slots, respectively. Hence, the per-slot drift is given by

$$\delta_{\mathrm{eff}}^+ = \frac{\delta_{r,f}^+(B_{\mathrm{max}}^r)}{\left\lfloor \frac{Rf(B_{\mathrm{max}}^r)}{\mu_r} \right\rfloor} \quad \text{and} \quad \delta_{\mathrm{eff}}^- = \frac{\delta_{r,f}^+(B_{\mathrm{max}}^r)}{\left\lceil \frac{Rf(B_{\mathrm{max}}^r)}{\mu_r} \right\rceil}. \tag{6.10}$$

The transmit policy is still determined according to (6.6). Furthermore, with the help

of the one bit feedback, the transmitter can ensure that it transmits only in the $f(B_{\mathrm{max}}^r)$

slots when the receiver is 'on'. It can be shown that the dynamics of the policy under

time dilation is similar to the dynamics of the policy $\mathcal{P}^c$, as long as the dilation func-

tion $f(B_{\mathrm{max}}^r)$ is sub-linear in $B_{\mathrm{max}}^r$. As a consequence, the proof of Lemma 15 can be

extended to the time dilated policy as well, and the gap from the upper bound in this

case can be made to approach zero as the battery size at the receiver gets large. Also,

the policy operates over a longer time-window, has a smaller per-slot drift and lower

rate of crossing the half-full mark, resulting in a smaller feedback overhead.

In the next section, we propose a near-optimal policy which operates without any

feedback from the receiver, and yet achieves a throughput close to the policy $\mathcal{P}^c$.

## 6.5 A Policy for Fully Uncoordinated Links

In this section, we propose an uncoordinated policy which prescribes a deterministic

pattern for the receiver to turn on, and does not require any feedback from the receiver.

At the transmitter, the policy $\mathcal{P}^{uc}$ follows the same strategy as $\mathcal{P}_t^c$ given by (6.6). However, the indicator variable $\mathbb{1}_{\mathcal{R}^+}$ is not available at the transmitter. Hence, it keeps the *frequency* with which it transmits after $N_r^+$ and $N_r^-$ slots the same as for policy $\mathcal{P}^c$, but executes it in a deterministic pattern. The receiver also turns on in the same deterministic pattern, provided it has the energy to do so. To derive the deterministic pattern according to which the receiver turns on for the policy $\mathcal{P}^{uc}$, we first compute the empirical distribution of the battery states at the receiver in which it turns on after $N_r^+$ slots, denoted as $\pi_r^+$, under the policy $\mathcal{P}^c$. Then, starting from the first slot, under the policy $\mathcal{P}^{uc}$, the receiver turns on after $N_r^+$ and $N_r^-$ slots in the same ratio as the policy $\mathcal{P}^c$. That is:

- We compute $\frac{n^+}{n^-} = \frac{\sum_{n=1}^{N} \mathbb{1}_{\{B_n^t \geq B_{\max}^r\}}}{\sum_{n=1}^{N} \mathbb{1}_{\{B_n^t < B_{\max}^r\}}}$, for policy $\mathcal{P}^c$.

- The receiver turns on at the last slot of every batch of $N_r^+$ slots for $n^+$ consecutive batches, after that it turns on at the last slot of every batch of $N_r^-$ slots for $n^-$ consecutive batches, and so on.

Note that, in the above, $n^+$ and $n^-$ are integers, which can result in an approximation of the stationary probabilities with which the receiver turns on after $N_r^+$ and $N_r^-$ slots. Using larger integers results in a smaller approximation error, leading to the same empirical distribution in the battery states as for policy $\mathcal{P}^c$. This, in turn, results in the two policies attaining roughly the same average throughput. On the other hand, if $n^+$ and $n^-$ are large, the receiver is essentially executing a policy with a negative and positive drift (respectively) for a large number of consecutive slots, which could increase the battery discharge/overflow probability, leading to a loss of throughput.

The following Lemma characterizes the difference between the throughput achieved by the policy $\mathcal{P}^c$ and $\mathcal{P}^{uc}$, in terms of battery discharge probability of policy $\mathcal{P}^{uc}$.

**Lemma 16.** *The throughput achieved by the policy $\mathcal{P}^{uc}$, denoted by $\mathcal{T}^{uc}$, satisfies*

$$\mathcal{T}^c - \mathcal{T}^{uc} = O(\pi_0^{uc}), \tag{6.11}$$

*where $\pi_0^{uc}$ denotes the stationary probability that battery at the transmitter or receiver (or both) is empty, while operating under policy $\mathcal{P}^{uc}$.*

*Proof.* See Appendix E.3. □

The utility of the above result is that the battery discharge probability, $\pi_0^{uc}$, can be made to decrease rapidly with the battery size, for a well designed policy. Due to this, the gap between the throughput achieved by $\mathcal{P}^{uc}$ and $\mathcal{P}^c$ can be made small.

## 6.6 Simulation Results

We evaluate the performance of the proposed policies by evaluating the time-averaged throughput using Monte Carlo simulations of the system over $10^7$ slots. The harvesting processes at the transmitter and receiver are assumed to be spatially and temporally independent and identically distributed according to the Bernoulli distribution with harvesting probabilities $\rho_t$ and $\rho_r$, respectively.

Fig. 6.1 shows the average per slot throughput when the receiver is energy unconstrained. We note that the policy given in (6.4) achieves the upper bound derived in Lemma 14. In this case, the harvesting rate at the transmitter completely determines the average throughput performance.
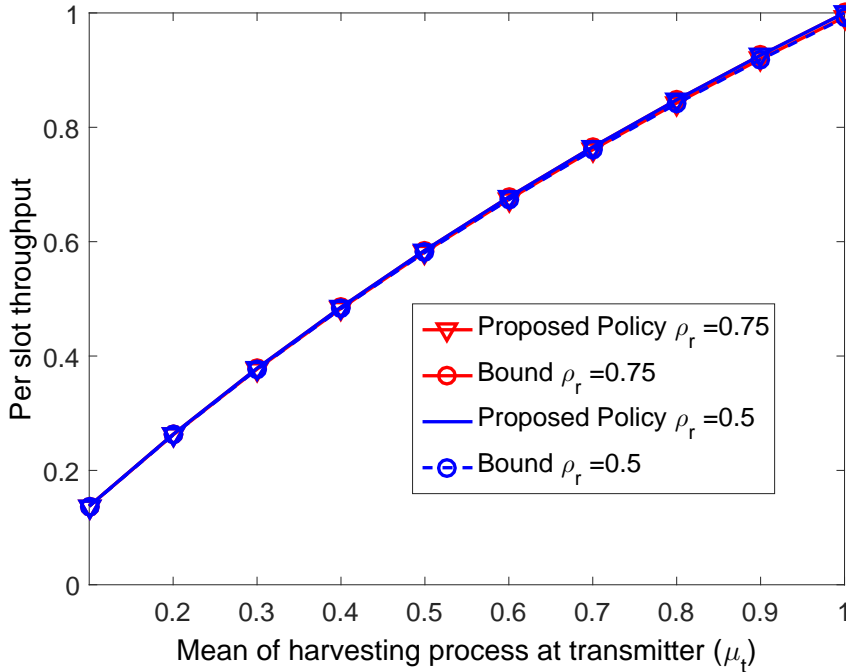
Figure 6.1: Energy unconstrained receiver: The policy presented in (6.4) achieves the bound. Parameters chosen are $R = 0.5$ and $B^t_{\max} = B^r_{\max} = 50$.

In Fig. 6.2, we show the average per slot throughput when the receiver is energy constrained. The performance of policy $\mathcal{P}^c$ given in (6.6) and (6.7), which requires an occasional one bit feedback, is benchmarked against the upper bound. We see that the throughput of $\mathcal{P}^c$ is very close to the upper bound. The figure also shows the the time-dilated policy discussed in Sec. 6.4 further closes the gap to the upper bound. In Fig. 6.3, we study the impact of time-dilation factor $f(\cdot)$ on the achieved thoroughput. Also, we compare the performance of time-dilated policy against a policy, labeled as `unconstrained policy`, under which the receiver turns on in $f(\cdot)$ out of $\lceil \frac{Rf(\cdot)}{\mu_r} \rceil$ slots, i.e., the energy consumption rate at the receiver is strictly less than the average harvesting rate. We note that, at the transmitter, both the unconstrained policy and
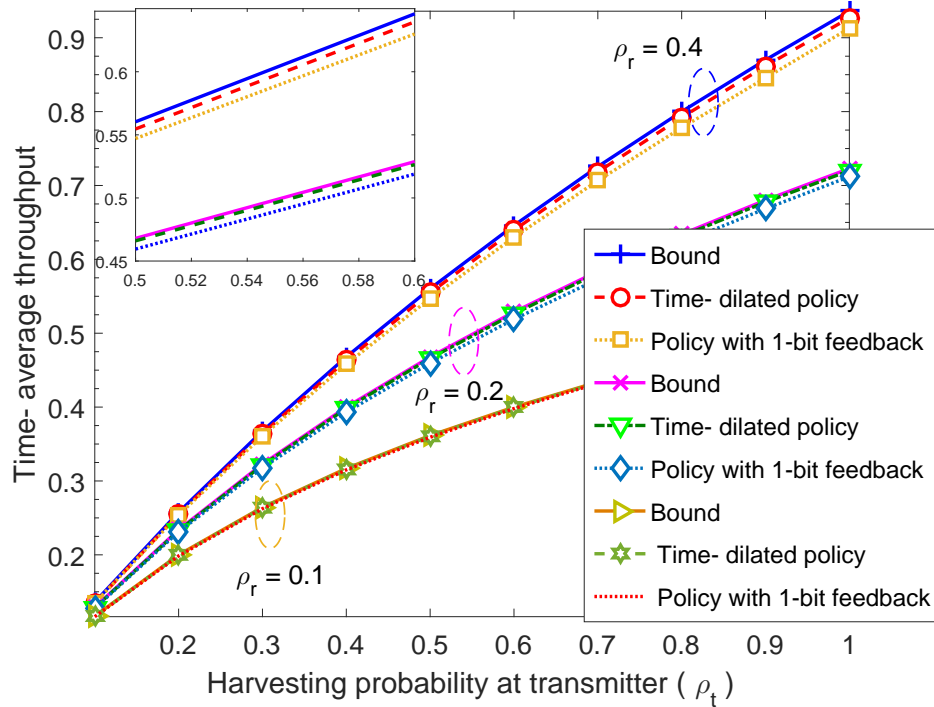
Figure 6.2: Energy constrained receiver: The policy $\mathcal{P}^c$ with occasional one bit feedback, achieves a throughput close to upper bound. The time-dilation further improves its performance. The result corresponds to time dilation $f(\cdot) = 100$. Other parameters are $R = 0.5$ and $B^t_{\max} = B^r_{\max} = 1000$.

time-dilated policy are exactly same. For the unconstrained policy, $\mathcal{P}_{\mathrm{ucr}}$, the throughput achieved with $f = 10$ is better than that achieved with $f = 5$. This indicates that the choosing a larger $f$ will result in a better throughput, because this facilitates a finer control over the per slot drift at the receiver. However, for a given battery size at the receiver, choosing a very large $f$ will result in a larger battery discharge probability. Hence, increasing $f$ without correspondingly increasing the battery size brings only limited benefits. For example, when $B^r_{\max} = 15$, the time-dilation based policy achieves a better throughput with $f = 5$ in comparison of $f = 10$. This suggests that $f$ must be judiciously chosen based on the battery size at the receiver.
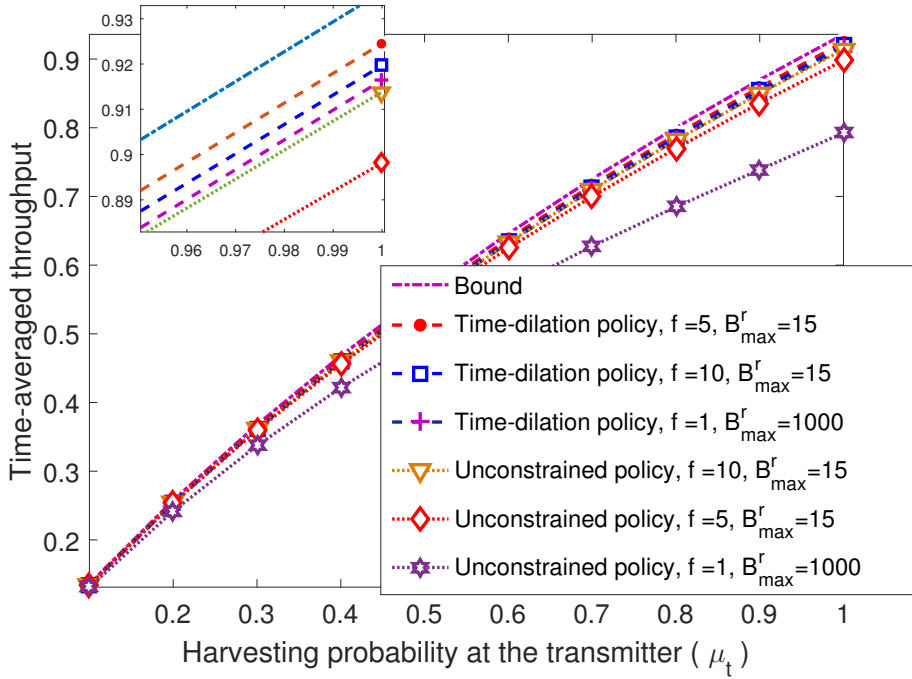
Figure 6.3: Effect of time-dilation factor $f$: compared to unconstrained policy $\mathcal{P}_{\text{ucr}}$, the time-dilation based policy $\mathcal{P}_{\text{td}}$ achieves the throughput close to upper bound with a smaller size battery at the receiver. The unconstrained policy performs better with large time-dilation factor $f(\cdot)$. Simulation parameters are $\mu_r = 0.4$ and $B^t_{\max} = 1000$.

In Fig. 6.4, we study the impact of the battery size at the two nodes on the performance of the policy $\mathcal{P}^c$ for a system with an energy constrained receiver. The per slot throughput achieved by the policy is near-optimal even with small capacity batteries. Finally, in Fig. 6.5, we compare the performance of the policy $\mathcal{P}^{uc}$ against the throughput of the policy $\mathcal{P}^c$. We note that the throughput achieved by $\mathcal{P}^{uc}$ is only marginally lower than that achieved by $\mathcal{P}^c$. Thus, the price paid for fully uncoordinated operation is quite small.
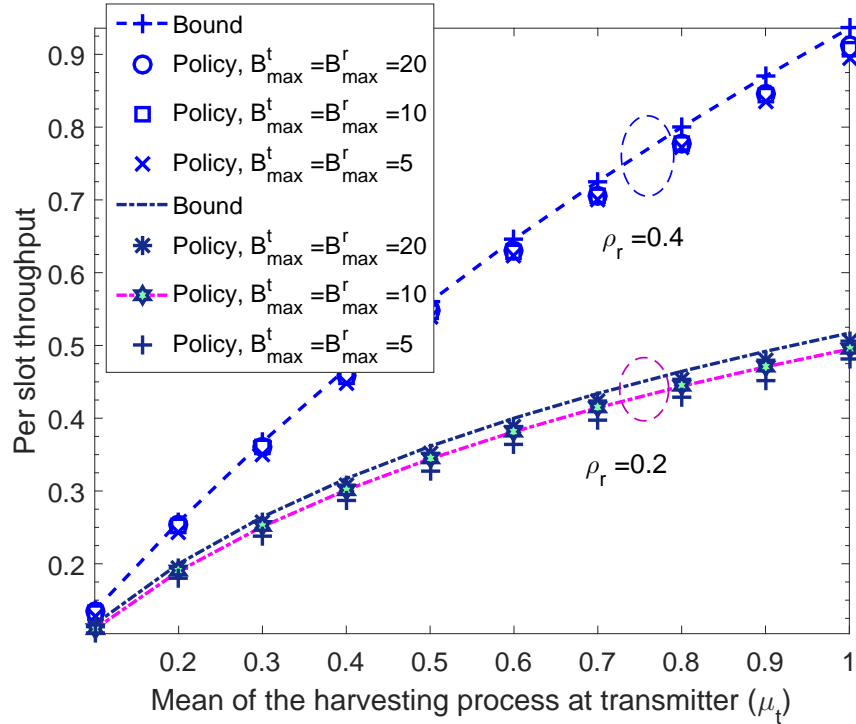
Figure 6.4: Impact of battery size on the throughput of policy $\mathcal{P}^c$, for $R = 0.5$.

## 6.7 Conclusions

In this chapter, we considered the problem of designing power control policies for un-coordinated dual EH links, where both the transmitter and receiver are unaware of the energy availability at their counterparts. First, we derived an upper bound on the achievable throughput with the help of a genie-aided system that has non-causal knowledge of the energy arrivals. Then, we considered a scenario where the receiver is energy unconstrained, and presented a policy which achieves the upper bound. Next, we considered the case of an energy constrained receiver, and presented a policy which achieves the upper bound asymptotically through time dilation and requires occasional one bit feedback . We also presented a fully uncoordinated policy in which the nodes
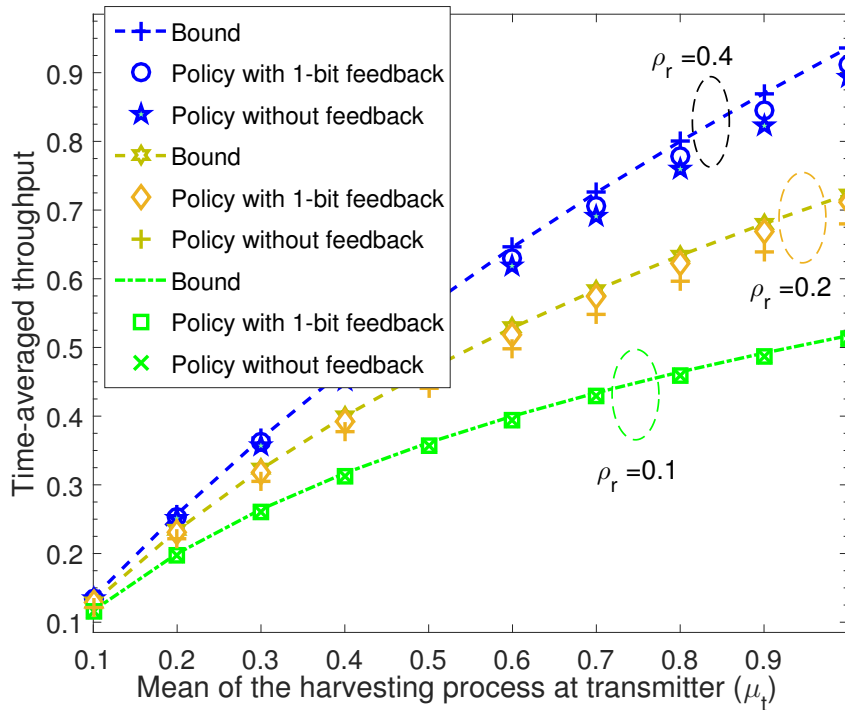
Figure 6.5: The fully uncoordinated policy $\mathcal{P}^{uc}$ achieves a throughput close to that of the policy $\mathcal{P}^{c}$. For $\mathcal{P}^{uc}$, the values of $(n^{+}, n^{-})$ are $(5, 1)$, $(1, 1)$ and $(2, 1)$ for $\rho_r = 0.1, 0.2$ and $0.4$, respectively. Other parameters: $B^{t}_{\max} = B^{r}_{\max} = 50$, $R = 0.5$.

deterministically make their data transmission attempts, and empirically showed that

it achieves near-optimal throughput without requiring any feedback.

# Chapter 7

# Conclusions and Future Work

In this thesis, the design and analysis of EH communication systems where both transmitters and receivers are EHNs was investigated under different settings, with and without coordination. We theoretically analyzed the performance of these networks, and using the analytical expressions, derived policies that achieve optimal performance. The main contributions of this thesis are summarized below.

## 7.1 Summary of contributions

Chapter 2 proposed a general framework to analyze the PDP of retransmission based point-to-point links, where both transmitter and receiver are EHNs. The developed framework was used to obtain approximate closed-form expressions for the PDP of ARQ as well as HARQ-CC, and for both slow and fast fading channels. The expressions for the PDP of mono EH links were derived as a special case of the framework. The accuracy of PDP expressions is illustrated through simulations. It was shown that

the obtained closed-form expressions are accurate over a wide range of system param-
eters. Furthermore, the presented framework was extended to account for the spatio-
temporal correlation of the EH processes across the nodes. The closed-form expressions
provided insights into the trade-offs between various system parameters. In addition,
the closed-form PDP expressions are amenable for formulating and solving the prob-
lem of designing optimal RIPs.

In Chapter 3, for dual EH links with finite size batteries, the penalty incurred by using
the policies designed under EUR constraints was characterized. It was shown that the
penalty can be expressed as a sum of two terms, each of which decays exponentially
with the size of the battery at the transmitter and receiver. This result established that
for links with sufficiently large, but finite sized batteries, it is near-optimal to design the
policies under EUR constraints. In addition, from a practitioner's viewpoint, this result
provides the order of the battery size required to achieve near-optimal performance,
using policies designed under the EUR constraint. Using this result, the PDP optimiza-
tion problem was formulated under EUR constraints. Near-optimal policies for both
ARQ and HARQ-CC based dual EH links, with both slow and fast fading channels,
were obtained by solving the PDP optimization problem using tools from geometric
programming. It was analytically shown that the presented design procedure naturally
extends to the scenarios when the harvesting processes are spatially and/or temporally
correlated. The efficacy of the designed policies is illustrated through simulations. It is
observed that the designed RIPs outperform policies obtained using MDPs.

The focus of Chapters 4 and 5 was multi-hop EH links. In Chapter 4, the framework
presented in Chapter 2 was generalized to obtain closed-form expressions for the PDP

of ARQ based multi-hop EH links. The accuracy of closed-form expressions was illustrated through simulations. Chapter 5 generalized the result in Chapter 3 by showing that in the multi-hop case also, the penalty due to use of policies operating in EUR decays exponentially with the battery size at each node. An optimization problem to find a distributed energy management policy for multi-hop EH links was formulated. Near-optimal policies were obtained in two scenarios. In the first scenario, namely, when the energy cost to receive a packet is negligible, closed-form expressions for the transmit energy levels of the optimal policy were obtained, in both slow and fast fading cases. For the slow fading channel, the transmit energy is geometrically increasing in the transmission attempt index. In contrast, for the fast fading channel, it increases exponentially. In the second case, when the energy cost to receive a data packet is non-negligible, a near-optimal policy is obtained using a CGP based iterative procedure. The obtained policies provided significant gains over existing policies.

Chapters 2-5 considered energy state coordination between transmitter and receiver, achieved through CSWP protocol or through delayed ACK/NACK messages. The rest of the thesis investigated the impact of lack of coordination between the transmitter and receiver, and proposed long-term average throughput optimal policies for uncoordinated dual EH links.

In Chapter 6, an upper bound was derived the long-term time-averaged throughput of uncoordinated dual EH links. For an energy unconstrained receiver, the upper bound is the same as that for the mono-T links, where only the transmitter is EHN. An asymptotically optimal fully uncoordinated policy was presented. The effect of lack of coordination is more prominent when the receiver is also energy constrained, as the receiver

can only turn on intermittently. In this scenario, we presented a policy which uses 1-bit feedback occasionally and achieves the throughput within 1-bit of upper bound. Next, to further close the gap from the upper bound, a policy based on time-dilation at the receiver was proposed. We argued that the time-dilation based policy achieves the upper bound and requires no feedback asymptotically as the battery size gets large. Finally, we presented a fully uncoordinated policy, which does not need any feedback for its operation and achieves near-optimal throughput. For the their operation, the proposed policies need at most 1-bit SoC information, and knowledge about the mean and variance of the EH processes.

## 7.2   Future work

Future work could study the following issues:

1. In Chapter 2-5, the channel is assumed to be block fading. It will be interesting to generalize the framework presented in Chapter 2 and 4 to time-correlated channels, and find the optimal policies in this scenario.

2. In Chapter 5, the slot allocation among the sub-frames was assumed to be fixed. Lower PDP can be achieved in the scenario where the slot allocation among the sub-frames changes dynamically; this option remains to be studied.

3. A generalization of multi-hop link design problem could be to develop a PDP-optimal joint routing and power control for an energy harvesting ad-hoc network with retransmissions.

4. It is important to study the impact of lack of coordination in multi-node networks

as well as for fading channels. Further, when the energy harvesting processes at the nodes are spatially correlated, the correlation can be exploited to achieve coordinated transmission and reception. This can be investigated further.

5. Further, for EH-based next-generation wireless communications, it would be interesting to study the uncoordinated non-orthogonal multiple access in EH networks.

6. Throughout the thesis, the energy required for receiving the data is assumed to remain fixed, regardless of transmit power and incoming rate. More sophisticated models for energy consumption at the receiver can be developed, and study their impact on the design of the optimal policies could be analyzed.

7. The framework presented in Chapters 2-5 can be easily extended to study the "age of information" in retransmission-based networks.

# Appendix A

# Appendix for Chapter 2

## A.1   Transition Probability Matrix, G, for dual EH links

The probability of transition from state $(i_1, j_1, \ell_1)$ to $(i_2, j_2, \ell_2)$ is $G^{i_2,j_2,\ell_2}_{i_1,j_1,\ell_1} = \Pr\left(B^t_{n+1} = i_2, B^r_{n+1}\right.$

$= j_2, U_{n+1} = \ell_2 \left| B^t_n = i_1, B^r_n = j_1, U_n = \ell_1 \right)$, where $i_1, i_2, j_1, j_2 \in \{0, 1, \ldots, \infty\}$, and

$\ell_1, \ell_2 \in \{-1, 1, \ldots, K\}$. For $\ell_1 \in \{1, \ldots, K\}$, $i_1 \geq L_{\ell_1}$ and $j_1 \geq R$, the $G^{i_2,j_2,\ell_2}_{i_1,j_1,\ell_1}$ is written as

in the following equation.

$$
G^{i_2,j_2,\ell_2}_{i_1,j_1,\ell_1} =
\begin{cases}
\rho_t \rho_r \Pr\left[\gamma_n < \gamma_0\right], & i_2 = i_1 - L_{\ell_1} + 1, j_2 = j_1 - R + 1, \ell_2 = \ell_1 + 1, \\[4pt]
\rho_t \rho_r \Pr\left[\gamma_n \geq \gamma_0\right], & i_2 = i_1 - L_{\ell_1} + 1, j_2 = j_1 - R + 1, \ell_2 = -1, \\[4pt]
(1 - \rho_t)\rho_r \Pr\left[\gamma_n < \gamma_0\right], & i_2 = i_1 - L_{\ell_1}, j_2 = j_1 - R + 1, \ell_2 = \ell_1 + 1, \\[4pt]
(1 - \rho_t)\rho_r \Pr\left[\gamma_n \geq \gamma_0\right], & i_2 = i_1 - L_{\ell_1}, j_2 = j_1 - R + 1, \ell_2 = -1, \\[4pt]
\rho_t(1 - \rho_r)\Pr\left[\gamma_n < \gamma_0\right], & i_2 = i_1 - L_{\ell_1} + 1, j_2 = j_1 - R, \ell_2 = \ell_1 + 1, \\[4pt]
\rho_t(1 - \rho_r)\Pr\left[\gamma_n \geq \gamma_0\right], & i_2 = i_1 - L_{\ell_1} + 1, j_2 = j_1 - R, \ell_2 = -1, \\[4pt]
(1 - \rho_t)(1 - \rho_r)\Pr\left[\gamma_n < \gamma_0\right], & i_2 = i_1 - L_{\ell_1}, j_2 = j_1 - R, \ell_2 = \ell_1 + 1, \\[4pt]
(1 - \rho_t)(1 - \rho_r)\Pr\left[\gamma_n \geq \gamma_0\right], & i_2 = i_1 - L_{\ell_1}, j_2 = j_1 - R, \ell_2 = -1, \\[4pt]
0, & \text{otherwise.}
\end{cases}
$$

$$\text{(A.1)}$$

In (A.1), $\Pr[\gamma_n < \gamma_0]$ for both slow and fast fading channels and ARQ is given by (2.2), while for HARQ-CC with slow and fast fading channels it is obtained using $\Psi_1 = n$ in (2.17) and (2.19), respectively. The terms in the above transition probability expression are obtained by considering the events that need to occur for the particular transition to happen. For example, the transition in the first case happens if both transmitter and receiver harvest the energy in the current slot, and a decoding failure occurs in the current attempt. Note that, in (A.1), for simplicity, the transition probabilities are written for infinite buffer size at both transmitter and receiver. However, as shown in Appendix A.3 for the mono EH case, the expression can be easily modified for the finite capacity battery case. The transition probabilities for the other cases, e.g., $i_1 \leq L_{\ell_1}$ and $j_1 \geq R$, are obtained similarly, and details are provided in [58].

## A.2   Proof of Lemma 4

During a frame, the transmitter has at most $i + m_t$ units of energy for its use. If $i + m_t \leq B_{\max}^t$, then $E_{\mathrm{avl}}^t = i + m_t$, while if $i + m_t > B_{\max}^t$, then $E_{\mathrm{avl}}^t \leq i + m_t$, i.e., the EHN may not be able to use the entire energy, $i + m_t$, depending on the order in which energy arrivals and departures occur. Furthermore, for the case when $i + m_t > B_{\max}^t$, $E_{\mathrm{avl}}^t = B_{\max}^t + \xi$ where $0 \leq \xi \leq K$ is a random variable which is equal to the number of slots where energy is harvested *and* $B_n^t < B_{\max}^t$. For $i + m_t > B_{\max}^t$, we approximate the available energy as $E_{\mathrm{avl}}^t \approx B_{\max}^t$, and ignore $\xi$. For policies such that $\sum_{\ell=1}^{K} L_\ell \leq B_{\max}^t$, ignoring $\xi$ for $i + m_t > B_{\max}^t$ will also result in $K$ feasible attempts. Using a similar argument, we can approximate $E_{\mathrm{avl}}^r$. Hence, when $\sum_{\ell=1}^{K} L_\ell \leq B_{\max}^t$ and $KR \leq B_{\max}^r$, the available energy can be well approximated as $E_{\mathrm{avl}}^t \approx \min\{i + m_t, B_{\max}^t\}$ and $E_{\mathrm{avl}}^r \approx$

$\min\{j + m_r, B^r_{\max}\}$.

The proof of statement $(ii)$ in the Lemma follows from the observation that a node that employs a policy that uses more than one unit of energy in each attempt (i.e., $L_\ell \geq 1$ for all $1 \leq \ell \leq K$) always has the space to accommodate one unit of energy. Hence, if the transmitter harvests energy in $m_t$ slots and has $i$ units of energy in the battery at the beginning of the frame, then the total available energy at the transmitter is given by $E^t_{\text{avl}} = i + m_t$. Similarly, $E^r_{\text{avl}} = j + m_r$ when $R \geq 1$.

## A.3   Transition Probability Matrix $\mathbf{G}_m$ for mono EH links

For mono-T EH links, the probability of transition from state $(i, \ell_1)$ to $(j, \ell_2)$ is $G^{j,\ell_2}_{(m)i,\ell_1} = \Pr(B_n = j, U_{n+1} = \ell_2 | B_n = i, U_n = \ell_1)$, where $i, j \in \{0, 1, \ldots, B^t_{\max}\}$ and $\ell_1, \ell_2 \in \{-1, 1, \ldots, K\}$. For $\ell_1 \in \{1, \ldots, K\}$ and $i \geq L_{\ell_1}$

$$G^{j,\ell_2}_{(m)i,\ell_1} = \begin{cases} \rho_t \Pr[\gamma_n < \gamma_0], & j = \min\{i - L_{\ell_1} + 1, B^t_{\max}\}, \ell_2 = \ell_1 + 1, \\ \rho_t \Pr[\gamma_n \geq \gamma_0], & j = \min\{i - L_{\ell_1} + 1, B^t_{\max}\}, \ell_2 = -1, \\ (1 - \rho_t)\Pr[\gamma_n < \gamma_0], & j = i - L_{\ell_1}, \ell_2 = \ell_1 + 1, \\ (1 - \rho_t)\Pr[\gamma_n > \gamma_0], & j = i - L_{\ell_1}, \ell_2 = -1, \\ 0, & \text{otherwise.} \end{cases} \tag{A.2}$$

In the above, $\Pr[\gamma_n < \gamma_0]$ for ARQ is written using (2.2), while for HARQ-CC with slow and fast fading channels, it can be computed using (2.17) and (2.19), respectively, with $\Psi_1 = n$.

# Appendix B

# Appendix for Chapter 3

## B.1  Proof of Lemma 7

The PDP can be written as

$$
P_{\mathrm{D}} = \min_{\mathcal{P}} \left[ \sum_{(i_1,j_1)\in\mathcal{I}_1} \pi(i_1,j_1) P_{\mathrm{D}}(K|i_1,j_1,U_n=1) + \sum_{(i_2,j_2)\in\mathcal{I}_2} \pi(i_2,j_2) P_{\mathrm{D}}(K|i_2,j_2,U_n=1) \right],
$$

(B.1)

Now, for all $(i,j) \in \mathcal{I}_2$, $P_{\mathrm{D}}(K|i,j,U_n=1) = c$, where $c \in [0,1]$ is some constant. Recall

that, in $\mathcal{I}_2$, the EHNs can make all $K$ attempts regardless of number of slots ($m_t$ and

$m_r$) in which the transmitter and receiver harvest the energy. Also, in $\mathcal{I}_1$, the packet

cannot be guaranteed to be attempted all $K$ times, and $\mathcal{I}_1 \cup \mathcal{I}_2 = \mathcal{I}$. Without loss

of generality, $\forall\ (i_1,j_1) \in \mathcal{I}_1$, we can write $P_{\mathrm{D}}(K|i_1,j_1,U_n=1) = c + \epsilon(i_1,j_1)$, where

$\epsilon(i_1,j_1) \triangleq P_{\mathrm{D}}(K|i_1,j_1,U_n=1) - c \in [0,1]$. Hence, for $(i,j) \in \mathcal{I}_2$, (B.1) can be written as

$$
\begin{aligned}
P_{\mathrm{D}} &= \min_{\mathcal{P}} \left[ P_{\mathrm{D}}(K|i,j,U_n=1) + \sum_{(i_1,j_1)\in\mathcal{I}_1} \pi(i_1,j_1)\epsilon(i_1,j_1) \right], \\
&\leq P_{\mathrm{D}}(K|i,j,U_n=1)\Big|_{\mathcal{P}^*} + \sum_{(i_1,j_1)\in\mathcal{I}_1} \pi(i_1,j_1)\Big|_{\mathcal{P}^*},
\end{aligned}
$$

(B.2)

151
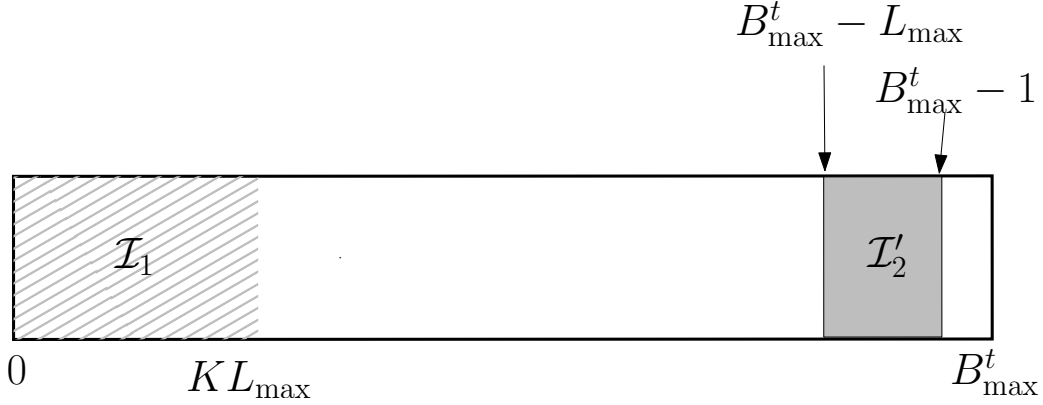
Figure B.1: Different sets of battery states used for proof of Lemma 8. Set $\mathcal{I}_1$ contains the battery states $\{0, 1, \ldots, KL_{\max}\}$, while set $\mathcal{I}'_2$ contains the battery states $\{B^t_{\max} - L_{\max}, \ldots, B^t_{\max} - 1\}$.

where $\mathcal{P}^* = \arg\min_{\mathcal{P}} P_D(K|i, j, U_n = 1)$ for any $(i, j) \in \mathcal{I}_2$. This establishes the upper bound.

Using (B.1), and the fact that $\epsilon(i_1, j_1) \geq 0$ for all $(i_1, j_1) \in \mathcal{I}_1$, $P_D(K|i, j, U_n = 1)\big|_{\mathcal{P}^*} \leq \min_{\mathcal{P}} \left[ P_D(K|i, j, U_n = 1) + \sum_{(i_1, j_1) \in \mathcal{I}_1} \pi(i_1, j_1)\epsilon(i_1, j_1) \right]$, for all $(i, j) \in \mathcal{I}_2$, which establishes the lower bound.

## B.2 Proof of Lemma 8

In this proof, we omit the superscript $t$ on battery state sets such as $\mathcal{I}_1$ and $\mathcal{I}_2$, as well as on the battery state at the stopping time $T_i$, denoted by $B_{T_i}$, since the result pertains only to the transmitter of the dual EH link. To prove the result, we compute the stationary probability of the set $\mathcal{I}_1$, in terms of the mean time to return to the set $\mathcal{I}_1$, denoted as $\mathbb{E}(T_{\mathcal{I}_1})$. Now, $\mathbb{E}(T_{\mathcal{I}_1}) = \mathbb{E}(T_1) + \mathbb{E}(T_2)$, where $\mathbb{E}(T_1)$ denotes the expected time when the DTMC first hits either the set $\mathcal{I}_1$ or the set $\mathcal{I}'_2$ once it leaves $\mathcal{I}_1$, and $\mathbb{E}(T_2)$ is the mean time required to visit the set $\mathcal{I}_1$ starting from the set $\mathcal{I}'_2$ (see Fig. B.1). The proof proceeds

by further decomposing $\mathbb{E}(T_2)$ in terms of other hitting times.

The battery evolution at the transmitter, given by (2.1), can be rewritten as follows:

$$
B_{n+1}^t = \begin{cases} \left\{ B_n^t + \mathbb{1}_{\{E_n^t \neq 0\}} - \mathcal{L}(B_n^t, B_n^r, U_n) \right\}^+ & \text{if } B_n^t \neq B_{\max}^t, \\ B_n^t - \mathcal{L}(B_n^t, B_n^r, U_n), & \text{otherwise}, \end{cases}
$$

where $\{x\}^+ \triangleq \max\{0, x\}$. Here, $\mathbb{1}_{\{E_n^t \neq 0\}}$ and $\mathcal{L}(B_n^t, B_n^r, U_n)$ are as defined in the statement of the Lemma. For a dual EH link operating in the EUR, the process $\mathbb{1}_{\{E_n^t \neq 0\}} - \mathcal{L}(B_n^t, B_n^r, U_n)$ has a positive mean drift. From renewal theory, the stationary probability of the set $\mathcal{I}_1$ is $\pi_{\mathcal{I}_1} = 1/\mathbb{E}(T_{\mathcal{I}_1})$, where $T_{\mathcal{I}_1}$ is the return time to the set $\mathcal{I}_1$. Now,

$$
\mathbb{E}(T_{\mathcal{I}_1}) = \mathbb{E}\left(T_1 | B_0 \in \mathcal{I}_1\right) + \sum_{i=1}^{L_{\max}} \mathbb{E}(T_2 | B_{T_1} = B_{\max}^t - i) \Pr\left(B_{T_1} = B_{\max}^t - i | B_0 \in \mathcal{I}_1\right),
$$

$$
\tag{B.3}
$$

where $T_1$ denotes the first time, starting from the set $\mathcal{I}_1$, when the DTMC returns to the set $\mathcal{I}_1$ or hits the set $\mathcal{I}_2'$ (see Fig. B.1) and $B_{T_i}$ denotes the battery state at time $T_i$ for all $i \in \mathbb{N}$, while $B_0$ denotes the battery state at the start. Also, $T_2$ denotes the time taken by the DTMC to return to the set $\mathcal{I}_1$, starting from a state in the set $\mathcal{I}_2'$, and is given as

$$
\mathbb{E}\left(T_2 | B_{T_1} = B_{\max}^t - i\right) = \mathbb{E}\left(T_3 | B_{T_1} = B_{\max}^t - i\right) + \Pr\left(B_{T_3} = B_{\max}^t | B_{T_1} = B_{\max}^t - i\right)
$$

$$
\times \quad \mathbb{E}\left(T_5 | B_{T_3} = B_{\max}^t\right). \tag{B.4}
$$

Here, $T_3$ denotes the first time the DTMC hits the set $\mathcal{I}_1$ or $B_{\max}^t$, starting from state $B_{\max}^t - i \in \mathcal{I}_2'$. Also, $T_5$ denotes the time taken by the DTMC, starting from $B_{\max}^t$, to return to the set $\mathcal{I}_1$. Next, $\mathbb{E}\left(T_5 | B_{T_3} = B_{\max}^t\right)$ can be written in terms of $T_4$, which is defined as the first time the DTMC hits the set $\mathcal{I}_2'$ starting from $B_{\max}^t$, as follows: $\mathbb{E}(T_5 | B_{T_3} =$

$B^t_{\max}) = \mathbb{E}\left(T_4|B_{T_3} = B^t_{\max}\right) + \sum_{j=1}^{L_{\max}} \Pr\left(B_{T_4} = B^t_{\max} - j|B_{T_3} = B^t_{\max}\right)\mathbb{E}(T_2|B_{T_4} = B^t_{\max} - j)$. Since $\sum_{j=1}^{L_{\max}} \Pr\left(B_{T_4} = B^t_{\max} - j|B_{T_3} = B^t_{\max}\right) = 1$, this can be bounded as

$$\mathbb{E}(T_5|B_{T_3} = B^t_{\max}) \leq \mathbb{E}\left(T_4|B_{T_3} = B^t_{\max}\right) + \max_{1 \leq j \leq L_{\max}} \mathbb{E}(T_2|B_{T_4} = B^t_{\max} - j). \quad \text{(B.5)}$$

Substituting the above upper bound on $\mathbb{E}(T_5|B_{T_3} = B^t_{\max})$ in (B.4), maximizing both sides over all $i$ and simplifying, we get

$$\max_{1 \leq i \leq L_{\max}} \mathbb{E}\left(T_2|B_{T_1} = B^t_{\max} - i\right) \leq \frac{\max_{1 \leq i \leq L_{\max}} \mathbb{E}\left(T_3|B_{T_1} = B^t_{\max} - i\right)}{\min_{1 \leq i \leq L_{\max}} \Pr\left(B_{T_3} \in \mathcal{I}_1|B_{T_1} = B^t_{\max} - i\right)}$$
$$+ \frac{\max_{1 \leq i \leq L_{\max}} \Pr\left(B_{T_3} = B^t_{\max}|B_{T_1} = B^t_{\max} - i\right)}{\min_{1 \leq i \leq L_{\max}} \Pr\left(B_{T_3} \in \mathcal{I}_1|B_{T_1} = B^t_{\max} - i\right)}$$
$$\times \quad \mathbb{E}\left(T_4|B_{T_3} = B^t_{\max}\right). \quad \text{(B.6)}$$

The denominator in the above uses the fact that hitting $B^t_{\max}$ and hitting a state in the set $\mathcal{I}_1$ starting from state $B^t_{\max} - i \in \mathcal{I}'_2$ are complementary events. Similar to (B.5), we can obtain a lower bound on $\mathbb{E}(T_5|B_{T_3} = B^t_{\max})$ by considering the minimum of $\mathbb{E}(T_2|B_{T_4} = B^t_{\max} - j)$ over $1 \leq j \leq L_{\max}$. Substituting the resulting inequality in (B.4) and minimizing over $i$, we get

$$\min_{1 \leq i \leq L_{\max}} \mathbb{E}\left(T_2|B_{T_1} = B^t_{\max} - i\right) \geq \frac{\min_{1 \leq i \leq L_{\max}} \mathbb{E}\left(T_3|B_{T_1} = B^t_{\max} - i\right)}{\max_{1 \leq i \leq L_{\max}} \Pr\left(B_{T_3} \in \mathcal{I}_1|B_{T_1} = B^t_{\max} - i\right)}$$
$$+ \frac{\min_{1 \leq i \leq L_{\max}} \Pr\left(B_{T_3} = B^t_{\max}|B_{T_1} = B^t_{\max} - i\right)}{\max_{1 \leq i \leq L_{\max}} \Pr\left(B_{T_3} \in \mathcal{I}_1|B_{T_1} = B^t_{\max} - i\right)}$$
$$\times \quad \mathbb{E}\left(T_4|B_{T_3} = B^t_{\max}\right).$$

$$\text{(B.7)}$$

To compute the hitting times and probabilities in (B.3), (B.6) and (B.7), we need the following Lemma.

**Lemma 17.** *The probability that, starting from a state in the set $\mathcal{I}_2'$, the DTMC hits the set $\mathcal{I}_1$ before hitting $B_{\max}^t$ at the stopping time $T_3$ decays exponentially with $B_{\max}^t$. That is,*

$Pr\left(B_{T_3} \in \mathcal{I}_1 | B_{T_1} = B_{\max}^t - i\right) = \Theta(e^{r_*^t B_{\max}^t})$, *where $r_*^t$ is as defined in Lemma 8.*

*Proof.* See Appendix B.3. $\square$

Now, using Lemma 17 and following a procedure similar to its proof in Appendix B.3, we get the following results (we omit the details to avoid repetition): we replace the following in (B.7), (B.6) and (B.3),

$$
\begin{aligned}
\Pr\left(B_{T_3} \in \mathcal{I}_1 | B_{T_1} = B_{\max}^t - i\right) &= \Theta(e^{r_*^t B_{\max}^t}), \\
\Pr\left(B_{T_1} = B_{\max}^t - i | B_0 \in \mathcal{I}_1\right) &= \Theta(1), \\
\Pr\left(B_{T_3} = B_{\max}^t | B_{T_1} = B_{\max}^t - i\right) &= \Theta(1), \\
\Pr\left(B_{T_4} = B_{\max}^t - j | B_{T_3} = B_{\max}^t\right) &= \Theta(1), \\
\mathbb{E}(T_1 | B_0 \in \mathcal{I}_1) &= \Theta(B_{\max}^t), \\
\mathbb{E}(T_3 | B_{T_1} = B_{\max}^t - i) &= \Theta(1), \\
\mathbb{E}(T_4 | B_{T_3} = B_{\max}^t) &= \Theta(1), \quad \text{(B.8)}
\end{aligned}
$$

Substituting (B.8) in (B.7), (B.6) and (B.3), we obtain $\mathbb{E}(T_{\mathcal{I}_1}) = \Theta(e^{-r_*^t B_{\max}^t})$, where $r_*^t$ is a negative root of the asymptotic log MGF of the drift process $X_n^t$. Hence, $\pi_{\mathcal{I}_1} = \Theta(e^{r_*^t B_{\max}^t})$. To close out the proof, we need to establish Lemma 17, which is presented in the following subsection.

## B.3 Computing the hitting times and hitting probabilities

*Proof.* For convenience, let $n = 0$ denote the time at which the DTMC first exits the set $\mathcal{I}'_2$. Also, let $X_n^t \triangleq \mathbb{1}_{\{E_n^t \neq 0\}} - \mathcal{L}(B_n^t, B_n^r, U_n)$. Note that, evolution of $X_n^t$ depends on the DTMC with its state denoted by $(B_n^t, B_n^r, U_n)$. In the following analysis, to simplify the notation, we do not explicitly show the dependence of $X_n^t$ on the battery state at the receiver $B_n^r$ and the retransmission index $U_n$. We are interested in analyzing the probability that, at the stopping time $T_3$, the DTMC is in a state in the set $\mathcal{I}_1$. To this end, we use Wald's identity for Markov modulated random walks [82, Chapter 9], written for our problem as follows

$$\mathbb{E}\left[\frac{\exp\left(r \sum_{n=1}^{T_3} X_n^t\right)}{\xi(r)^{T_3}} \frac{\pi_r(B_{T_3})}{\pi_r(B_0)}\right] = 1, \tag{B.9}$$

where $\xi(r)$ denotes the spectral radius of the matrix $A(r)$ whose $(i, j)^{\text{th}}$ entry is $a_{ij}(r) = p_{ij} g_i(r)$ with $p_{ij}$ being the transition probability of the battery from state $i$ to state $j$ (strictly speaking, $(i_1, j_1, u_1)$ to $(i_2, j_2, u_2)$), while $g_i(r)$ denotes the generating function of the conditional distribution of $X_n^t$, given that $B_n^t = i$, for some $i \in \mathcal{I}'_2$, and $r$ is any point on the real line for which $g_i(r)$ exists. In (B.9), $\pi_r$ denotes the right eigenvector corresponding to $\xi(r)$, and $\pi_r(B)$ denotes its $B^{\text{th}}$ element, which, strictly speaking, is a tuple $(B^t, B^r, U_n)$. However, with abuse of notation, we only show its dependence on the transmitter's battery. Also, the expectation is over $X_n^t$. Since the process $X_n^t$ has positive drift, there exists an $r_*^t < 0$ such that $\xi(-r_*^t) = 1$ [83]. Let $q$ denote the

probability of hitting $\mathcal{I}_1$ before hitting $B_{\max}^t$. Using (B.9) with $r_{*'}^t = -r_*^t$, we get

$$(1-q)\mathbb{E}\left[\exp\left(r_*^t \sum_{n=1}^{T_3} X_n^t\right) \frac{\pi_{r_{*'}^t}(B_{T_3})}{\pi_{r_{*'}^t}(B_0)}\middle| B_{T_3} = B_{\max}^t\right]$$

$$+ q\mathbb{E}\left[\exp\left(r_*^t \sum_{n=1}^{T_3} X_n^t\right) \frac{\pi_{r_{*'}^t}(B_{T_3})}{\pi_{r_{*'}^t}(B_0)}\middle| B_{T_3} \in \mathcal{I}_1\right] = 1.$$

Since, for a large battery, the overshoots are negligible [82], the above can be simplified

as

$$\mathbb{E}\left[\frac{\pi_{r_{*'}^t}(B_{T_3})}{\pi_{r_{*'}^t}(B_0)}\right] \left(q \exp\left(-r_*^t B_{\max}^t\right) + (1-q) \exp\left(r_*^t L_{\max}\right)\right) = 1. \tag{B.10}$$

Further, replacing the two expectation terms with their upper bounds, we get

$$q \exp\left(-r_*^t B_{\max}^t\right) + (1-q) \exp\left(r_*^t L_{\max}\right) \geq C_1', \tag{B.11}$$

where $C_1' \triangleq \frac{\min_{B_0} \pi_{r_{*'}^t}(B_0)}{\max_{B_{T_3}} \pi_{r_{*'}^t}(B_{T_3})}$. Thus, $q \geq C_1'' \exp\left(r_*^t B_{\max}^t\right)$. By similarly lower bounding

the expectation terms in (B.10), it can shown that $q \leq C_2'' \exp\left(r_*^t B_{\max}^t\right)$. Hence, $q = \Theta(\exp\left(r_*^t B_{\max}^t\right))$. This completes the proof. $\qquad\square$

## B.4 Proof of Theorem 1

*Proof.* In this section, we denote the stationary distribution of dual EH link by $\boldsymbol{\pi_d}$, to distinguish it from stationary distribution of mono EH links. To derive the result for the stationary distribution of a dual EH link, $\boldsymbol{\pi_d}$, we need to compute the probability of the set $\mathcal{I}_1$. From Lemma 8, $\sum_{i \in \mathcal{I}_1^t} \pi_t(i) = \Theta(e^{r_*^t B_{\max}^t})$, where $\mathcal{I}_1^t = \mathcal{I}^t \backslash \mathcal{I}_2^t$. Here, $\mathcal{I}^t$ is the set of all the battery states at the transmitter, and can be written as $\mathcal{I}^t = \mathcal{I}_1^t \cup \mathcal{I}_2^t$, where $\mathcal{I}_2^t$ denotes the set of battery states in which all $K$ attempts can be supported by

the transmitter, irrespective of the number of slots, $m_t$, in which energy is harvested. Similarly, at the receiver, $\sum_{j \in \mathcal{I}_1^r} \pi_r(j) = \Theta(e^{r_*^r B_{\max}^r})$, where $\mathcal{I}^r = \mathcal{I}_1^r \cup \mathcal{I}_2^r$, and $\mathcal{I}_1^r = \mathcal{I}^r \backslash \mathcal{I}_2^r$. The stationary distribution $\pi_r$ and the sets $I_1^r$, $I_2^r$ and $I_r$ are defined in a similar fashion as for transmitter.

Now, the stationary probability of the sets $\mathcal{I}_1^t$ and $\mathcal{I}_1^r$ can be written as

$$\sum_{i \in \mathcal{I}_1^t} \pi_t(i) = \sum_{i \in \mathcal{I}_1^t, j \in \mathcal{I}_1^r} \pi_d(i,j) + \sum_{i \in \mathcal{I}_1^t, j \in \mathcal{I}_2^r} \pi_d(i,j), \tag{B.12}$$

$$\sum_{j \in \mathcal{I}_1^r} \pi_r(j) = \sum_{i \in \mathcal{I}_1^t, j \in \mathcal{I}_1^r} \pi_d(i,j) + \sum_{i \in \mathcal{I}_2^t, j \in \mathcal{I}_1^r} \pi_d(i,j). \tag{B.13}$$

Thus, the stationary probability of the set $\mathcal{I}_1$ is given as

$$\pi_d\left((i,j) \in \mathcal{I}_1\right) = \pi_d\left(i \in \mathcal{I}_1^t, j \in \mathcal{I}_1^r\right) + \pi_d\left(i \in \mathcal{I}_2^t, j \in \mathcal{I}_1^r\right) + \pi_d\left(i \in \mathcal{I}_1^t, j \in \mathcal{I}_2^r\right),$$

Adding (B.12) and (B.13) and using Lemma 8, we get

$$2\pi_d\left(i \in \mathcal{I}_1^t, j \in \mathcal{I}_1^r\right) + \pi_d\left(i \in \mathcal{I}_2^t, j \in \mathcal{I}_1^r\right) + \pi_d\left(i \in \mathcal{I}_1^t, j \in \mathcal{I}_2^r\right) = \Theta(e^{r_*^t B_{\max}^t}) + \Theta(e^{r_*^r B_{\max}^r}). \tag{B.14}$$

The proof completes by observing that each term in the L.H.S. in (B.14) is nonnegative. Hence, one can upper and lower bound the L.H.S. in (B.14) in terms of $\pi_d\left((i,j) \in \mathcal{I}_1\right)$.

□

## B.5 Dual EH Links with ARQ/HARQ-CC and Slow Fading

For a dual EH link with ARQ and slow fading channels, using Lemma 3 and EUR conditions, the subproblem corresponding to $\chi = K'$ is written as

$$\min_{\bar{\mathbf{L}}=\{L_1,\dots,L_{K'}\}} 1 - e^{-\left(\frac{\gamma_0 \mathcal{N}_0 T_p}{L_{K'} E_s \sigma_c^2}\right)}, \tag{B.15a}$$

$$\text{subject to} \quad \sum_{\ell=1}^{K'} L_\ell \left(1 - e^{-\left(\frac{\gamma_0 \mathcal{N}_0 T_p}{L_{\ell-1} E_s \sigma_c^2}\right)}\right) \le K\rho_t, \tag{B.15b}$$

$$\sum_{\ell=1}^{K'} \left(1 - e^{-\left(\frac{\gamma_0 \mathcal{N}_0 T_p}{L_{\ell-1} E_s \sigma_c^2}\right)}\right) \le \frac{K\rho_r}{R}, \tag{B.15c}$$

and $0 \le L_1 \le L_2 \le \dots \le L_{K'} \le L_{\max}$. The objective function above is written using the fact that, for slow fading channels with ARQ, the optimal policy is a strictly non-decreasing policy (from Lemma 3). The constraints in (B.15b) and (B.15c) ensure that both the transmitter and receiver operate in the EUR. Similar to the previous case, using the Taylor series expansion of $e^{-x}$ and $Z_\ell \triangleq \frac{s}{L_\ell}$, and approximating the infinite series summations by summations of finite order, (B.15) can be converted to CGP, which can be solved using Algorithm 2.

For HARQ-CC, using (2.17) and EUR conditions, the subproblem corresponding to $\chi = K'$ is written as

$$\min_{\bar{\mathbf{L}}=\{L_1,\dots,L_{K'}\}} 1 - e^{-\frac{s}{\Sigma_{\ell=1}^{K'} L_\ell}}, \tag{B.16a}$$

$$\text{subject to} \quad \sum_{\ell=1}^{K'} L_\ell \left(1 - e^{-\frac{s}{\Sigma_{i=1}^{\ell-1} L_i}}\right) \le K\rho_t, \tag{B.16b}$$

$$\sum_{\ell=1}^{K'} \chi^\ell \left( 1 - e^{-\frac{s}{\Sigma_{i=1}^{\ell-1} L_i}} \right) \leq \frac{K\rho_r}{R}, \tag{B.16c}$$

and $0 \leq L_i \leq L_{\max}$, $1 \leq i \leq K'$. The constraints in (B.16b) and (B.16c) ensure that the dual EH link operates in the EUR. Similar to the previous cases, we solve (B.16) using Algorithm 2. To use Algorithm 2, (B.16) is converted into a CGP using the Taylor series expansion of $e^{-x}$ and defining $Z_{K'} \triangleq \frac{s}{\sum_{i=1}^{K'} L_i}$. Next, we present a method to find the optimal policies for a dual EH link with HARQ-CC and fast fading channels.

## B.6 Dual EH Links with HARQ-CC and Fast Fading

The optimization problem for finding near-optimal RIPs for dual EH links with HARQ-CC and fast fading channels can be written in a similar manner as in previous cases, with $p_{o,\ell-1}$ replaced with $p_{\text{out},1\to\ell-1}$. The $p_{\text{out},1\to\ell-1}$ is the same as $p_D(i,j,m_t,m_r)$ and is given by (2.19), with $\Psi_1 = \ell - 1$. Specifically, the optimization problem is written as

$$\min_{\bar{\mathbf{L}}=\{L_1,\dots,L_K\}} 1 - F_K \tag{B.17a}$$

$$\text{subject to} \quad \sum_{\ell=1}^{K} L_\ell (1 - F_{\ell-1}) \leq K\rho_t, \tag{B.17b}$$

$$\sum_{\ell=1}^{K} \chi^\ell (1 - F_{\ell-1}) \leq \frac{K\rho_r}{R}, \tag{B.17c}$$

and $0 \leq L_i \leq L_{\max}$, $\chi^i \in \{0,1\}$, $1 \leq i \leq K$, where $F_{\ell-1} \triangleq \sum_{i=1}^{M_{\ell-1}} \sum_{j=1}^{\tau_{i,\ell-1}} \sum_{k=0}^{j-1} \frac{\chi_{i,j}(\mathbf{L}_{\ell-1})}{k!} \left( \frac{X}{L_{\{i\}}} \right)^k e^{-\frac{X}{L_{\{i\}}}}$ with $X \triangleq \frac{\gamma_0 \mathcal{N}_0 T_p}{E_s}$, $\mathbf{L}_K \triangleq \text{diag}(\frac{L_1}{\sigma_c^2}, \frac{L_2}{\sigma_c^2}, \dots, \frac{L_K}{\sigma_c^2})$, and $L_{\{1\}}, L_{\{2\}}, \cdots, L_{\{M_K\}}$ denote the distinct nonzero elements of $\mathbf{L}_K$. $\tau_{i,\ell-1}$ denotes the multiplicity of $L_{\{i\}}$, and $\chi_{i,j}(\mathbf{L}_K)$ denotes the $(i,j)$th characteristic coefficient of $\mathbf{L}_K$ defined in (2.20). Note that, to find a solution for a given $\{\chi^\ell\}_{\ell=1}^{K}$, we need to solve $2^\chi - \chi$ subproblems, where $\chi = \sum_{\ell=1}^{L} \chi_\ell$.

Hence, to solve (B.17), since $\chi$ can take values $1, 2, \ldots, K$, we need to solve $(2^{K+2} - K(K+1) - 4)/2$ subproblems, and pick the solution corresponding to the subproblem which yields the minimum PDP among them, which is computationally expensive.

Alternatively, using a result from [38, Theorem 1], we can approximate the $p_{\text{out},1\to\ell}$ as $p_{\text{out},1\to\ell} \approx \frac{X^\ell}{\ell! L_1 L_2 \cdots L_\ell}$. Using this approximation, for a given $\{\chi^\ell\}_{\ell=1}^K$, the optimization problem in (B.17) reduces to a GP. Thus to solve (B.17), we need to solve $K$ GPs and pick the best solution.

## B.7 Proof of Theorem 1 for Markov Energy Harvesting Models

In this section, we present the proof of Theorem 1 when the EH process at the transmitter and receiver are temporally correlated. Note that, for the Markov model, the result in Theorem 1 is valid, provided Lemma 8 holds true in this scenario also. Thus, in the following, we discuss the proof of Lemma 8 for the Markov model.

In the Markov case, the drift process, defined in Lemma 8, modifies as $X_n^t \triangleq e_n^t - \mathcal{L}(B_n^t, B_n^r, U_n)$, where $e_n^t$ denotes the amount of energy harvested in the $n^{\text{th}}$ slot. For a dual EH link operating in the EUR, the process $e_n^t - \mathcal{L}(B_n^t, B_n^r, U_n)$ has a positive mean drift. From renewal theory, the stationary probability of the set $\mathcal{I}_1^t$ is $\pi_{\mathcal{I}_1^t} = 1/\mathbb{E}(T_{\mathcal{I}_1^t})$. Next, since the battery at the node still evolves in a Markovian fashion in this scenario, $\mathbb{E}(T_{\mathcal{I}_1^t})$ is given by (B.3). Further, to compute (B.3), we use the expressions given in (B.4), (B.5), (B.6) and (B.7), which are in turn computed using the results in Lemma 17. The proof completes by noting that the result in Lemma 17 is also applicable to this scenario. This is because, $X_n^t$ is a Markov modulated random walk, with its underlying

Markov chain being the one described in the beginning of Section 3.5. ∎

# Appendix C

# Appendix for Chapter 4

## C.1   Transition probabilities

For a slow fading channel, the probability of transitioning from state $\boldsymbol{a} \triangleq (\boldsymbol{B}_a, \boldsymbol{U}_a, s)$ to

$\boldsymbol{b} \triangleq (\boldsymbol{B}_b, \boldsymbol{U}_b, s+1)$ is $G_{a,b} \triangleq \Pr\left(\left(\boldsymbol{B}_{s+1} = \boldsymbol{B}_b,\ \boldsymbol{U}_{s+1} = \boldsymbol{U}_b, s+1\right) \mid \left(\boldsymbol{B}_s = \boldsymbol{B}_a, \boldsymbol{U}_s = \boldsymbol{U}_a, s\right), \gamma\right)$,

where $B_a^n, B_b^n \in \{0, 1, \ldots, B_n^{\max}\}$ and $U_a^n, U_b^n \in \{-1, 0, 1, \ldots, K_n\}$. For $B_a^n \geq E_\ell^n$ and

$B_a^{n+1} \geq R$, and $\boldsymbol{U}_a$ such that $\{U_a^i = -1\}_{i=1}^{n-1}$, $\{U_a^i = 0\}_{i=n+1}^{N}$ and $U_a^n = \ell - 1$, we can write

$G_{a,b}$ as

$$
G_{a,b}(\gamma) = \begin{cases} p(\boldsymbol{I}_s)P_e(E_\ell^n, \gamma), & \boldsymbol{B}_b = \tilde{\boldsymbol{B}}, \tilde{\boldsymbol{U}}_b^{-n} = \tilde{\boldsymbol{U}}_a^{-n}, U_b^n = U_a^n + 1, \\ p(\boldsymbol{I}_s)(1 - P_e(E_\ell^n, \gamma)), & \boldsymbol{B}_b = \tilde{\boldsymbol{B}}, \tilde{\boldsymbol{U}}_b^{-n} = \tilde{\boldsymbol{U}}_a^{-n}, U_b^n = -1, \\ 0, & \text{otherwise.} \end{cases} \tag{C.1}
$$

where $p(\boldsymbol{I}_s) \triangleq \prod_{k=1}^{N+1} \rho_k^{I_k}(1-\rho_k)^{1-I_k}$, $\tilde{\boldsymbol{B}} \triangleq \left(\min\{B_a^k + I_k - \mathbb{1}_{\{k=n\}}E_\ell^n - R\mathbb{1}_{\{k=n+1\}}, B_k^{\max}\}\right)_{k=1}^{N+1}$,

and $\tilde{\boldsymbol{U}}_a^{-n}$ and $\tilde{\boldsymbol{U}}_b^{-n}$ denote $(N-1)$-length vectors obtained by removing the $n^{\text{th}}$ compo-

nent of $\boldsymbol{U}_a$ and $\boldsymbol{U}_b$, respectively. Also, $I_k$ is the $k^{\text{th}}$ component of $\boldsymbol{I}_s \in \{0, 1\}^{N+1}$, and is

equal to one if the $k^{\text{th}}$ node harvests the energy in the current slot, otherwise it is equal

to zero. Also, $\mathbb{1}_{\{.\}}$ denotes an indicator function which takes the value $1$ if its argument

is true, and takes the value $0$ otherwise. In (C.1), $P_e(E_\ell^n, \gamma)$ is given by (4.3) for both slow and fast fading channels. The terms in the above transition probability expression are obtained by considering the events that need to occur for the particular transition to happen. For instance, (C.1) is written for the case when the transmissions of all the previous nodes were successful, i.e., $\{U_a^i = -1\}_{i=1}^{n-1}$ and the $n^{\text{th}}$ node has to make the $\ell^{\text{th}}$ attempt in $s^{\text{th}}$ slot. In this case, the transition described in the first case happens if all the nodes harvest energy according to the pattern described by $\boldsymbol{I_s}$, a decoding failure occurs in the current attempt, and the channel in the $n^{\text{th}}$ sub-frame is $\gamma$. Note that, during such an event, the battery of a node is incremented by one if it harvests energy in the current slot and its battery is not full. Further, the energy in the battery of the $n^{\text{th}}$ and $n + 1^{\text{th}}$ nodes are decreased by the amount of energy used to make the $\ell^{\text{th}}$ attempt, i.e., $E_\ell^n$ and $R$, respectively. Since only the $n^{\text{th}}$ node transmits during the $s^{\text{th}}$ slot, the local transmission index of all nodes except the $n^{\text{th}}$ node remain unchanged. The transition probabilities for the other cases, e.g., $B_a^n \leq E_{\ell_1}$ and $B_a^{n+1} \geq R$, can be written similarly.

In the fast fading case, $\boldsymbol{G}$ contains the channel-averaged entries, i.e., $P_e(E_\ell^n, \gamma)$ in (C.1) is replaced by $\mathbb{E}_\gamma(P_e(E_\ell^n, \gamma))$. We omit the details to avoid repetition.

## C.2 Procedure to compute number of feasible attempts $\Psi_n$

Recall that a packet transmission attempt is made if and only if both the transmitter and receiver have sufficient energy to make the next attempt. This implies, for a given RIP $\mathcal{P}$, the battery states at the start of the frame $B^n$ and $B^{n+1}$, the harvesting patterns of $n^{\text{th}}$ and $n + 1^{\text{th}}$ node, namely, $(m_{r,n}, m_{t,n})$ and $(m_{r,n+1}, m_{t,n+1})$, respectively, determine

the number of feasible attempts $\Psi_n$. To determine $\Psi_n$, we use the notion of *energy available for transmission and reception*, denoted as $E^n_{\text{avl},t}$ and $E^n_{\text{avl},r}$, respectively, at the $n^{\text{th}}$ node, which are random variables determined by the order of energy arrivals and consumption. To obtain closed form expressions, we approximate $E^n_{\text{avl},r}$ and $E^n_{\text{avl},t}$ as $E^n_{\text{avl},r} \approx \min\{B^n + m_{r,n}, B^{\max}_n\}$ and $E^n_{\text{avl},t} \approx \min\{E^n_{\text{avl},r} + m_{t,n} - \Psi_{n-1}R, B^{\max}_n\}$, respectively. Based on this, $\Psi_n$ can be approximated as $\Psi_n = \min\{\kappa^t_n, \kappa^r_{n+1}\}$, where $\kappa^t_n \triangleq \max\{\kappa : E^n_{\text{avl},t} - \sum_{\ell=1}^{\kappa} E^n_\ell \geq 0\}$ and $\kappa^r_{n+1} \triangleq \max\{\kappa : E^{n+1}_{\text{avl},r} - \kappa R \geq 0\}$ denote the number of feasible attempts at the transmitting and receiving EHN of the $n^{\text{th}}$ hop, respectively. Thus, we have obtained a recursive equation to compute the number of feasible attempts.

# Appendix D

# Appendix for Chapter 5

## D.1 Proof of Lemma 13

*Proof.* We define $g_2(t^*) = f_2(t^*) - t^*$ and $g_2\left(F^{-1}(K_n \rho_n E)\right) < 0$. Now, let $t^*_{\min} = \sum_{\ell=1}^{K'} E^*_\ell$ is the sum of first $K'$ components of the solution of $K_n$ dimensional problem (5.9). Since, $\frac{K_n \rho_n E}{\Pr[n]} - F(t^*) \geq t^*_{\min}$, we can write

$$
\begin{aligned}
g(t^*_{\min}) &= \left[1 + \frac{K_n}{(K_n - K')N_0}\left(\frac{\rho_n E}{\Pr[n]} - \frac{F(t^*_{\min})}{K_n}\right)\right]^{K_n - K'} - 1 - t^*_{\min}, \\
&\geq \left[1 + \frac{1}{(K_n - K')N_0}t^*_{\min}\right]^{K_n - K'} - 1 - t^*_{\min}, \\
&= \left[1 + \frac{t^*_{\min}}{N_0} + \left(\frac{t^*_{\min}}{N_0}\right)^2 \frac{n(n-1)}{2} + \cdots\right] - 1 - t^*_{\min}, \\
&> 0,
\end{aligned}
$$

where the last inequality follows from the fact that $N_0 \leq 1$. This shows that $g_2(t^*)$ has a zero, and the proof completes. $\square$

## D.2   Proof of Theorem 4

To prove the Theorem, we need the following Lemma, which asserts that the optimal RIP allocates nonzero power to all packet attempts. Its proof is similar to the proof of a corresponding Lemma in the slow fading case in [78].

**Lemma 18.** *The optimal RIP solution to (5.15), denoted by* $\mathbf{E}^{n^*} = \left\{ E_1^{n^*}, \ldots, E_{K_n}^{n^*} \right\}$, *satisfies* $E_\ell^{n^*} > 0$ *for all* $1 \le \ell \le K_n$.

Next, we make the substitution $x_k \triangleq \frac{E_k^n}{\prod_{i=1}^{k-1}(1+E_i^n)}$. Thus, $E_1^n = x_1$, $E_2^n = x_2(1 + x_1)$, $E_3^n = x_3(1 + x_1)(1 + x_2(1 + x_1))$, and so on. Hence, we can rewrite (5.15) as

$$\max_{x_1,\ldots,x_{K_n}} f_{K_n-1}(1 + x_{K_n} f_{K_n-1}), \text{ subject to } \sum_{\ell=1}^{K_n} x_\ell \le \frac{K\rho_n}{\Pr[n]}, \tag{D.1}$$

where $f_\ell \triangleq f_{\ell-1}(1 + x_\ell f_{\ell-1})$ for $1 \le \ell \le K_n$ and $f_0 \triangleq 1$. We claim that the solution to the transformed problem obeys the following recursive relationship

$$x_{\ell+1} = \frac{x_\ell}{2}\left(\frac{2 + x_\ell f_{\ell-1}}{1 + x_\ell f_{\ell-1}}\right) = \frac{x_\ell}{2}\left(\frac{f_{\ell-1} + f_\ell}{f_\ell}\right), \quad 1 \le \ell \le K_n - 1. \tag{D.2}$$

The proof follows by induction. When $K_n = 2$, using the constraint in (D.1), the objective function can be written as $f_1\left(1 + \left(\frac{K\rho_n}{\Pr[n]} - x_1\right)f_1\right)$. Let $f_1' \triangleq \mathrm{d}f_1/\mathrm{d}x_1$. Now, because of Lemma 18, and since the domain of optimization is the positive orthant, $f_1' = 0$ at the optimal solution of the unconstrained problem [84, Chapter 4]. Hence, we have

$$f_1'\left(1 + \left(\frac{K\rho_n}{\Pr[n]} - x_1\right)f_1\right) + f_1\left(f_1'\left(\frac{K\rho_n}{\Pr[n]} - x_1\right) - f_1\right) = 0$$

Rearranging the above, we get

$$x_2 = \frac{f_1}{2f_1'} - \frac{1}{2f_1} = \frac{x_1}{2}\left(\frac{2 + x_1 f_0}{1 + x_1 f_0}\right).$$

This establishes (D.2) when $K_n = 2$. Suppose (D.2) holds for $K_n = k$. We proceed to show that it holds for $K_n = k + 1$ as well. Towards this end, we derive an alternative induction hypothesis. From the constraint in (D.1), we substitute $x_k = \frac{K\rho_n}{\Pr[n]} - \sum_{\ell=1}^{k-1} x_\ell$ in the objective function, and differentiate it with respect to $x_1$ and set equal to zero to obtain

$$x_k = \frac{f_{k-1}}{2f_{k-1}'}\left(1 + \sum_{i=2}^{k-1} \frac{\partial x_i}{\partial x_1}\right) - \frac{1}{2f_{k-1}}, \tag{D.3}$$

where $f_{k-1}' = f_{k-2}' + 2x_{k-1}f_{k-2}f_{k-2}' + f_{k-2}^2 \frac{\partial x_{k-1}}{\partial x_1}$. Equating the right hand sides of the expression for $x_k$ above with the one given by the induction hypothesis in (D.2) and rearranging, we get

$$f_{k-1}' = f_{k-2}^2 \left(1 + \sum_{i=2}^{k-1} \frac{\partial x_i}{\partial x_1}\right). \tag{D.4}$$

To complete the proof, we need to show that the solution of $k+1$-dimensional optimization problem also follows the relation in (D.2). For the $(k + 1)$-dimensional problem, solving for $x_{k+1}$ from the constraint, substituting into the objective function, and differentiating with respect to $x_1$ and setting equal to zero, we obtain

$$x_{k+1} = \frac{f_k}{2f_k'}\left(1 + \sum_{i=2}^{k} \frac{\partial x_i}{\partial x_1}\right) - \frac{1}{2f_k}, \tag{D.5}$$

where $f_k' = f_{k-1}' + 2x_k f_{k-1}f_{k-1}' + f_{k-1}^2 \frac{\partial x_k}{\partial x_1}$. Now, in the $(k + 1)$-dimensional problem, if we fix $x_{k+1}$, it reduces to a $k$-dimensional problem, for which the relation (D.4) holds.

Since it holds at any value of $x_{k+1}$, it also holds at the optimal solution to the $(k+1)$-dimensional problem. In the expression for $f'_k$, substituting for $f'_{k-1}$ from the new induction hypothesis in (D.4), we get

$$f'_k = f^2_{k-2}\left(1 + \sum_{i=2}^{k-1}\frac{\partial x_i}{\partial x_1}\right)(1 + x_{k-1}(f_{k-2} + f_{k-1})) + f^2_{k-1}\frac{\partial x_k}{\partial x_1} = f^2_{k-1}\left(1 + \sum_{i=2}^{k}\frac{\partial x_i}{\partial x_1}\right)$$

The first equality above uses (D.2) and (D.4); the second equality uses the definition of $f_k$. Substituting the above expression for $f'_k$ in (D.5) results in

$$x_{k+1} = \frac{f_k}{2f^2_{k-1}} - \frac{1}{f_k} = \frac{x_k}{2}\left(\frac{f_{k-1} + f_k}{f_k}\right),$$

which is precisely the induction step for the $(k+1)$-dimensional problem. This, along with the observation that (D.2) is equivalent to (5.16), completes the proof.

## D.3 Optimal Power Allocation for the Fast Fading Multi-hop EH Links

For fast fading multi-hop EH links, using (5.3) and (4.14), the problem of finding the optimal power vector can be written as

$$\min_{\{\mathcal{P}^n\}_{n=1}^N} 1 - \Pr[N+1], \tag{D.6a}$$

$$\text{s. t.: } \Pr[n-1]\left(\sum_{\ell=1}^{K_{n-1}}\frac{\mathbb{1}_{\{E^{n-1}_\ell > 0\}}R}{\prod_{i=1}^{\ell-1}(1 + E^{n-1}_i)}\right) + \Pr[n]\left(\sum_{\ell=1}^{K_n}\frac{E^n_\ell}{\prod_{i=1}^{\ell-1}(1 + E^n_i)}\right) \le K\rho_n E \quad \text{for all } n$$

$$\tag{D.6b}$$

$$0 \le E^n_\ell \le E_{\max} \text{ for all } 1 \le \ell \le K_n \text{ and } 1 \le n \le N+1,$$

where $\Pr[m] = 1 - \prod_{n=1}^{m-1}\left(1 - \frac{1}{\prod_{\ell=1}^{K_n}(1 + E^n_\ell)}\right)$.

Similar to the slow fading case, the above problem can be converted into a CGP and solved using Algorithm 2. To convert it into a CGP we make the substitution $L_\ell^n = \prod_{i=1}^{\ell}(1 + E_\ell^n)$.

# Appendix E

# Appendix for Chapter 6

## E.1 Proof of Lemma 14

First, we derive the upper bound in the scenario when $\frac{\mu_r}{R} \geq 1$.

*Case 1).* From (6.2), the time-averaged throughput of a dual EH link can be upper bounded as

$$
\begin{aligned}
\mathcal{T} &= \frac{1}{N} \sum_{n=1}^{N} \mathbb{1}_{\{p_r(n) \neq 0\}} \log(1 + p_t(n)), \\
&\leq \frac{1}{N} \sum_{n=1}^{N} \log(1 + p_t(n)) \leq \log\left(1 + \frac{1}{N} \sum_{n=1}^{N} p_t(n)\right).
\end{aligned}
$$

$$
\begin{aligned}
\mathcal{T} &= \frac{1}{N} \sum_{n=1}^{N} \mathbb{1}_{\{p_r(n) \neq 0\}} \log(1 + p_t(n)), \\
&\overset{(a)}{\leq} \frac{1}{N} \sum_{n=1}^{N} \log(1 + p_t(n)) \overset{(b)}{\leq} \log\left(1 + \frac{1}{N} \sum_{n=1}^{N} p_t(n)\right).
\end{aligned}
$$

In the above, (a) follows from the fact that an energy unconstrained receiver with infinite sized battery can remain on in all slots, and (b) The last inequality above follows

from Jensen's inequality. Next, taking the limit $N \to \infty$, we get

$$
\begin{aligned}
\liminf_{N\to\infty} \mathcal{T} &\leq \liminf_{N\to\infty} \log\left(1 + \frac{1}{N}\sum_{n=1}^{N} p_t(n)\right), \\
&\overset{(c)}{=} \log\left(1 + \liminf_{N\to\infty} \frac{1}{N}\sum_{n=1}^{N} p_t(n)\right), \\
&\overset{(d)}{\leq} \log\left(1 + \liminf_{N\to\infty} \frac{1}{N}\sum_{n=1}^{N} \mathcal{E}_t(n)\right), \\
&\overset{(e)}{=} \log(1 + \mu_t),
\end{aligned}
$$

where (c) follows because the logarithm is a continuous function, (d) follows from the fact that the total energy consumed can not exceed the total energy harvested, and (e) follows from the ergodicity of the harvesting process. This completes the proof in Case (1). □

*Case 2).* In this scenario, the receiver can only turn on intermittently, and the lack of information about the battery state of the other node can lead to energy loss at the nodes. To obtain an upper bound, we consider a genie-aided system where the transmitter and receiver are equipped with infinite sized batteries, and the entire energy harvested over $N$ slots is made available in the first slot itself, at both the nodes. In this case, there is no energy loss due to lack of coordination, as both the transmitter and receiver know the number of slots when the receiver can turn on. Hence, the throughput of this system is an upper bound on (6.3a).

From the strong law of large numbers, for large $N$, the energy at the transmitter and the receiver at the beginning of communication is $N\mu_t$ and $N\mu_r$, respectively. Thus, the total number of slots the receiver can remain on is $N' = \lfloor \frac{N\mu_r}{R} \rfloor$. The long-term

time-averaged throughput, $\mathcal{T}_g$, of this genie-aided system is

$$\liminf_{N\to\infty} \mathcal{T}_g \leq \liminf_{N\to\infty} \frac{1}{N} \sum_{n=1}^{N'} \log(1 + p_t(n)),$$

$$\leq \liminf_{N\to\infty} \frac{N'}{N} \log\left(1 + \frac{N\mu_t}{N'}\right). \tag{E.1}$$

The last inequality above is based on the fact that it is optimal to equally allocate the energy available over the $N'$ slots, since the logarithm is a concave function. Noting that $\lim_{N\to\infty} \frac{N'}{N} = \frac{\mu_r}{R}$ completes the proof. $\square$

## E.2 Proof of Lemma 15

*Proof.* The proof of this Lemma is adapted from [33]. At the transmitter, we choose $\delta_t^+ = \delta_t^- = \beta_t \sigma_t^2 \frac{\log B_{\max}^t}{B_{\max}^t}$. On the other hand, at the receiver, $\delta_r^+ = N_r - \lfloor \frac{R}{\mu_r} \rfloor$, and $\delta_r^- = \lceil \frac{R}{\mu_r} \rceil - N_r$, where $N_r = \frac{R}{\mu_r}$. First, we analyze the battery discharge probability at the transmitter and receiver, denoted by $p_d^t$ and $p_d^r$, respectively. We use [33, Lem. 2], which was derived for the case where only the transmitter is an EHN.

Recall that the energy transferred from the battery to the super capacitor at the transmitter depends on the battery state at the transmitter, while the feedback sent by the receiver only determines the slot in which the data is transmitted, using the energy accumulated in the super capacitor. Similarly, the decision to turn on at the receiver depends only on the state of the battery at the receiver. Thus, the batteries at both the transmitter and receiver evolve independently of each other. Hence, the result in [33, Lem. 2] is applicable to our case where both the transmitter and receiver are

EHNs. Thus, the battery discharge probabilities at the transmitter and receiver decay as $\Theta\left(\exp\left(-\frac{B_{\max}^t \delta_t^-}{\sigma_t^2}\right)\right)$ and $\Theta\left(\exp\left(-\frac{B_{\max}^r \mu_r \delta_r^-}{\sigma_r^2}\right)\right)$, respectively. Since $\delta_t^+ = \delta_t^- = \beta_t \sigma_t^2 \frac{\log B_{\max}^t}{B_{\max}^t}$, $p_d^t = \Theta\left(B_{\max}^t{}^{-\beta_t}\right)$, $\beta_t > 0$. Similar results hold for the battery overflow probabilities also.

Next, to show that the policy $\mathcal{P}^c$ asymptotically achieves within one bit of the upper bound, we first characterize the rate obtained in a slot. Under policy $\mathcal{P}^c$, the receiver turns on after $N_r^+$ and $N_r^-$ slots, depending on the battery state at the receiver. Thus, the rate obtained in a slot ranges between $\mathcal{R}_{\max}^{N_r^-} \triangleq \mathcal{R}\left(N_r^-(\mu_t + \delta_t^+)\right)$ and $\mathcal{R}_{\min}^{N_r^+} \triangleq \mathcal{R}\left(N_r^+(\mu_t - \delta_t^-)\right)$. Here, $\mathcal{R}_{\max}^{N_r^-}$ denotes the maximum rate obtained in a slot, which is achieved when receiver turns on after $N_r^-$ slots and the battery at the transmitter remains more than half full during all the $N_r^-$ slots. Similarly, $\mathcal{R}_{\min}^{N_r^+}$ is the minimum rate obtained in a slot, which is achieved when the receiver turns on after $N_r^+$ slots and the battery at the transmitter is less than half full for the entire duration of $N_r^+$ slots. Since $\mathcal{R}$ is an analytic function, using Taylor's expansion, we can write

$$
\begin{aligned}
\mathcal{R}_{\max}^{N_r^-} &= \mathcal{R}\left[(N_r + \delta_r^-)(\mu_t + \delta_t^+)\right] \\
&= \mathcal{R}(N_r \mu_t) + \mathcal{R}^{(1)}(N_r \mu_t)\delta_{\max} + \mathcal{R}^{(2)}(N_r \mu_t)\delta_{\max}^2 + o(\delta_{\max}^2)
\end{aligned}
\tag{E.2}
$$

where $\delta_{\max} \triangleq \delta_r^-(\mu_t + \delta_t^+) + N_r \delta_t^+$. Similarly,

$$
\mathcal{R}_{\min}^{N_r^+} = \mathcal{R}(N_r \mu_t) + \mathcal{R}^{(1)}(N_r \mu_t)\delta_{\min} + \mathcal{R}^{(2)}(N_r \mu_t)\delta_{\min}^2 + o(\delta_{\min}^2)
$$

where $\delta_{\min} \triangleq \delta_r^+ \delta_t^- - N_r \delta_t^- - \mu_t \delta_r^+$. Now, the actual rate achieved depends by the amount of energy used for transmission, which, in turn, depends on the number of slots since

the previous transmission attempt. It also depends on the sequence of states the batteries at the two nodes go through, starting from the slot the transmitter previously made an attempt. Hence, the transmit power corresponding to an arbitrary state sequence $s$ can be written as

$$p_s = \begin{cases} N_r^- \mu_t + k_s \delta_t^+ - (N_r^- - k_s)\delta_t^-, & \text{if } s \in \mathcal{S}_{N_r^-}, \\ N_r^+ \mu_t + \ell_s \delta_t^+ - (N_r^- - \ell_s)\delta_t^-, & \text{if } s \in \mathcal{S}_{N_r^+}, \end{cases} \tag{E.3}$$

where $0 \le k_s \le N_r^-$ and $0 \le \ell_s \le N_r^-$ denote the number of slots when the battery at the transmitter is more than half full, when the communication happens in $N_r^-$ and $N_r^+$ slots, respectively. Also, $\mathcal{S}_{N_r^-}$ and $\mathcal{S}_{N_r^+}$ denote the set of sequence of states in which the receiver turns on after $N_r^-$ and $N_r^+$ slots, respectively.

The total number of bits transmitted corresponding to an arbitrary state sequence $s$ in which the transmit energy is $N_r \mu_t + \delta_s$, is written as

$$\mathcal{R}_s = \mathcal{R}(N_r \mu_t) + \mathcal{R}^{(1)}(N_r \mu_t)\delta_s + \mathcal{R}^{(2)}(N_r \mu_t)\delta_s^2 + o(\delta_s)^2. \tag{E.4}$$

In the above, since $N_r^- = N_r + \delta_r^-$ $N_r^+ = N_r - \delta_r^+$ and $\delta_t^+ = \delta_t^-$, $\delta_s$ (by comparing $p_s$ with $N_r \mu_t + \delta_s$) is given as

$$\delta_s = \begin{cases} \mu_t \delta_r^- - N_r^- \delta_t^- + 2k_s \delta_t & \text{if } s \in \mathcal{S}_{N_r^-} \\ -N_r^+ \delta_t^- - \mu_t \delta_r^+ + 2\ell_s \delta_t & \text{if } s \in \mathcal{S}_{N_r^+}. \end{cases} \tag{E.5}$$

The rates obtained for policy $\mathcal{P}^c$ can also be characterized in terms of the Markov chain described in the following. In terms of Markov reward process, the rate $\mathcal{R}_s$ can be viewed as the reward obtained when the Markov chain $\mathcal{M}$ visits the state $s$. The state of Markov chain is given by a set of tuples of battery states at the transmitter and

the receiver. Depending on the length of the sequence of tuples of the battery states, the state space of the Markov chain can be partitioned into two disjoint subsets, containing $N_r^+$ and $N_r^-$ length sequences of battery states, denoted by $\mathcal{S}_{N_r^+}$ and $\mathcal{S}_{N_r^-}$, respectively. A typical state $s \in \mathcal{S}_{N_r^+}$ is denoted as $\{(B_m^t, B_m^r)\}_{m=1}^{N_r^+}$. The transition probabilities of this Markov chain can be written in terms of the transition probabilities of the Markov chains describing the evolution of the battery at the transmitter and receiver, given by (6.1). For instance, in a scenario where the transmitter and the receiver harvest the energy according to a Bernoulli process, the probability of making a transition from an arbitrary state $s \in \mathcal{S}_{N_r^+}$ to a state $s' \in \mathcal{S}_{N_r^+}$, in which the reward obtained is $\mathcal{R}_{\min}^{N_r^+}$, can be written as follows. The probability of transition from $s$ to $s'$ is one, if the battery at the transmitter and receiver in the last tuple of the state $s$ is such that $B_{N_r^+}^t < \frac{B_{\max}^r}{2} - N_r^+$ and $B_{N_r^+}^r \geq \frac{B_{\max}^r}{2} + R$, and for state $s'$, $B_m^t < \frac{B_{\max}^t}{2}$ as well as $B_m^r > \frac{B_{\max}^r}{2}$ for all $1 \leq m \leq N_r^+$; otherwise it is zero. Note that, the rate $\mathcal{R}_{\min}^{N_r^+}$ is the reward corresponding to the state which is given by the set of tuples of battery states in which the battery at the transmitter is always less than half full while the battery at the receiver is more than half full.

Under the above Markov chain formulation, the time-averaged throughput is

$$\mathcal{T}^c = \sum_{s \in \mathcal{S}} \pi_s \frac{\mathcal{R}_s}{N_s}, \tag{E.6}$$

where $\pi_s$ denotes the steady state probability of the system being in a state $s$ such that the rate $\mathcal{R}_s$ is obtained in $N$ slots. Note that, the existence of the steady state distribution is ensured by the fact that the Markov chain $\mathcal{M}$ has a finite number of states. Also, in the above, $N_s$ takes the value $N_r^+$ and $N_r^-$ depending on the state s. Next, using (E.4),

time-averaged throughput in (E.6) can be rewritten as

$$
\mathcal{T}^c = \sum_{s \in \mathcal{S}_{N_r^-}} \pi_s \frac{\mathcal{R}_s}{N_r + \delta_r^+} + \sum_{s \in \mathcal{S}_{N_r^+}} \pi_s \frac{\mathcal{R}_s}{N_r - \delta_r^+}, \tag{E.7}
$$

$$
= \mathcal{R}(N_r \mu_t) \left[ \frac{1}{N_r + \delta_r^+} \sum_{s \in \mathcal{S}_{N_r^-}} \pi_s + \frac{1}{N_r - \delta_r^+} \sum_{s \in \mathcal{S}_{N_r^+}} \pi_s \right]
$$

$$
+ \mathcal{R}^{(1)}(N_r \mu_t) \left[ \frac{1}{N_r^-} \sum_{s \in \mathcal{S}_{N_r^-}} \pi_s \delta_s + \frac{1}{N_r^+} \sum_{s \in \mathcal{S}_{N_r^+}} \pi_s \delta_s \right]
$$

$$
+ \mathcal{R}^{(2)}(N_r \mu_t) \left[ \frac{1}{N_r^-} \sum_{s \in \mathcal{S}_{N_r^-}} \pi_s \delta_s^2 + \frac{1}{N_r^+} \sum_{s \in \mathcal{S}_{N_r^+}} \pi_s \delta_s^2 \right] + \sum_{s \in \mathcal{S}_{N_r^+}} \pi_s o(\delta_s^2) + \sum_{s \in \mathcal{S}_{N_r^-}} \pi_s o(\delta_s^2).
$$

$$
\tag{E.8}
$$

In the following, we study the behavior of each of the terms in RHS of (E.8). The first term in (E.8) can we rewritten as

$$
\frac{\mathcal{R}(N_r \mu_t)}{N_r \left(1 + \frac{\delta_r^-}{N_r}\right) \left(1 - \frac{\delta_r^+}{N_r}\right)} \left[ 1 + \frac{\delta_r^-}{N_r} \sum_{s \in \mathcal{S}_{N_r^+}} \pi_s - \frac{\delta_r^+}{N_r} \sum_{s \in \mathcal{S}_{N_r^-}} \pi_s \right]
$$

$$
= \frac{\mathcal{R}(N_r \mu_t)}{N_r \left(1 + \frac{\delta_r^-}{N_r}\right) \left(1 - \frac{\delta_r^+}{N_r}\right)} \left[ 1 + \frac{\delta_r^- \pi_r^+}{N_r} - \frac{\delta_r^+ \pi_r^-}{N_r} \right], \tag{E.9}
$$

where $\pi_r^+ \triangleq \sum_{s \in \mathcal{S}_{N_r^+}} \pi_s$ and $\pi_r^- \triangleq \sum_{s \in \mathcal{S}_{N_r^-}} \pi_s$ denote the stationary probability of being in a state such that the receiver turns on after $N_r^+$ and $N_r^-$ slots, respectively. Next, using the energy conservation principle at the receiver

$$
\pi_r^+ \left( \frac{R}{N_r - \delta_r^+} \right) + (\pi_r^- - p_d^r) \left( \frac{R}{N_r + \delta_r^-} \right) = \mu_r (1 - p_o^r), \tag{E.10}
$$

where $p_d^r$ and $p_o^r$ denote the probability of battery discharge and overflow, respectively.

Simplifying the above equation, and using the result for discharge and overflow probability, $p_d^r$ and $p_o^r$, derived at the start of this section, we get

$$\pi_r^+ \delta_r^- - \pi_r^- \delta_r^+ = O(\delta_r^-) \tag{E.11}$$

On the other hand, the second term in (E.8) is written as

$$\mathcal{R}^{(1)}(N_r \mu_t) \left[ \frac{1}{N_r^-} \sum_{s \in \mathcal{S}_{N_r^-}} \pi_s \left( \mu_t \delta_r^- - N_r^- \delta_t^- + 2k_s \delta_t \right) + \frac{1}{N_r^+} \sum_{s \in \mathcal{S}_{N_r^+}} \pi_s \left( -N_r^+ \delta_t^- - \mu_t \delta_r^+ + 2\ell_s \delta_t \right) \right]$$

$$= \mathcal{R}^{(1)}(N_r \mu_t) \left( -\delta_t^- + \frac{\mu_t \delta_r^- \pi_r^-}{N_r^-} + \frac{\mu_t \delta_r^+ \pi_r^+}{N_r^+} + \frac{2\delta_t}{N_r^-} \sum_{s \in \mathcal{S}_{N_r^-}} \pi_s k_s + \frac{2\delta_t}{N_r^+} \sum_{s \in \mathcal{S}_{N_r^+}} \pi_s \ell_s \right)$$

$$= \mathcal{R}^{(1)}(N_r \mu_t) \left( -\delta_t^- - \frac{\mu_t \delta_r^+ \delta_r^-}{(N_r + \delta_r^-)(N_r - \delta_r^+)} + \frac{\mu_t N_r}{(N_r + \delta_r^-)(N_r - \delta_r^+)} [\pi_r^- \delta_r^- - \pi_r^+ \delta_r^+] + A \right), \tag{E.12}$$

where $A \triangleq \frac{2\delta_t}{N_r} \sum_{s \in \mathcal{S}_{N_r^-}} \pi_s k_s + \frac{2\delta_t}{N_r^+} \sum_{s \in \mathcal{S}_{N_r^+}} \pi_s \ell_s$. Using (E.11), we have

$$\pi_r^- \delta_r^- - \pi_r^+ \delta_r^+ = \delta_r^- - \delta_r^+ + (\pi_r^- \delta_r^+ - \pi_r^+ \delta_r^-). \tag{E.13}$$

Note that the quantity in (E.12) converges to zero as $O(\delta_r^+) + O(\delta_r^-) + O(\delta_t^+)$, and $\sum_{s \in \mathcal{S}_{N_r^+}} \pi_s o(\delta_s^2)$, $\sum_{s \in \mathcal{S}_{N_r^-}} \pi_s o(\delta_s^2)$ and the last but one term in (E.8), goes to zero as $O(\delta_r^{+2}) + O(\delta_t^{-2})$ and $O(\delta_r^{-2}) + O(\delta_t^{-2})$, respectively. The proof completes by noting that the right-hand side in (E.9) converges to $\frac{\mathcal{R}(\mu_t N_r)}{N_r}$, and $N_r = \frac{N}{\lfloor \frac{N \mu_r}{R} \rfloor}$. $\square$

## E.3 Proof of Lemma 16

*Proof.* To prove the result, we consider a Markov chain $\mathcal{M}'$ which has the same state space as the Markov chain $\mathcal{M}$, described in the proof of Lemma 15, and its transition probabilities are governed by the policy and the harvesting statistics at both the nodes.

The average throughput achieved by the policy $P^{uc}$ can be written as

$$\mathcal{T}^{uc} = \sum_{s \in \mathcal{S}} \pi_s^{uc} \frac{\mathcal{R}_s^{uc}}{N_s},$$

where $\pi_s^{uc}$ denote the stationary probability of Markov chain $\mathcal{M}'$ being in the state $s \in \mathcal{S}$. Thus, the difference between the time-average throughput achieved by two policies, using (E.6), can be written as

$$
\begin{aligned}
\mathcal{T}^c - \mathcal{T}^{uc} &= \sum_{s \in \mathcal{S}} \pi_s \frac{\mathcal{R}_s}{N_s} - \sum_{s \in \mathcal{S}} \pi_s^{uc} \frac{\mathcal{R}_s^{uc}}{N_s}, \\
&\overset{(a)}{=} \sum_{s \in \mathcal{S}} \frac{\mathcal{R}_s}{N_s} \left( \pi_s - \pi_s^{uc} \right), \\
&\overset{(b)}{<} \frac{\mathcal{R}_{\max}^{N_r^-}}{N_r^+} \left( \pi_0^{uc} - \pi_0 \right) < \frac{\mathcal{R}_{\max}^{N_r^-}}{N_r^+} \pi_0^{uc},
\end{aligned}
$$

where $(a)$ follows from the fact the rate obtained in state $s$ is the same for both $\mathcal{P}^c$ and $\mathcal{P}^{uc}$, and (b) uses the fact that the stationary distribution sums to one, and the maximum achieved rate is $\mathcal{R}_{\max}^{N_r^+}$. This completes the proof. $\qquad\square$

# Bibliography

[1] S. Zhou, T. Chen, W. Chen, and Z. Niu, "Outage minimization for a fading wireless link with energy harvesting transmitter and receiver," *IEEE J. Sel. Areas Commun.*, vol. 33, no. 3, pp. 496–511, Mar. 2015.

[2] A. Aprem, C. R. Murthy, and N. B. Mehta, "Transmit power control policies for energy harvesting sensors with retransmissions," *IEEE J. Sel. Topics Signal Process.*, vol. 7, no. 5, pp. 895–906, Oct. 2013.

[3] S. Rao and N. B. Mehta, "Hybrid energy harvesting wireless systems: Performance evaluation and benchmarking," *IEEE Trans. Wireless Commun.*, vol. 13, no. 9, pp. 4782–4793, Sept. 2014.

[4] S. Ulukus, A. Yener, E. Erkip, O. Simeone, M. Zorzi, P. Grover, and K. Huang, "Energy harvesting wireless communications: A review of recent advances," *IEEE J. Sel. Areas Commun.*, vol. 33, no. 3, pp. 360–381, Mar. 2015.

[5] C. Yuen, M. Elkashlan, Y. Qian, T. Duong, L. Shu, and F. Schmidt, "Energy harvesting communications: Part 1 [guest editorial]," *IEEE Commun. Mag.*, vol. 53, no. 4, pp. 68–69, Apr. 2015.

[6] O. Ozel and S. Ulukus, "Achieving AWGN capacity under stochastic energy harvesting," *IEEE Trans. Inf. Theory*, vol. 58, no. 10, pp. 6471–6483, Oct. 2012.

[7] V. Jog and V. Anantharam, "A geometric analysis of the AWGN channel with a $(\sigma, \rho)$ -power constraint," *IEEE Trans. Inf. Theory*, vol. 62, no. 8, pp. 4413–4438, Aug. 2016.

[8] D. Shaviv, P. M. Nguyen, and A. Özgür, "Capacity of the energy-harvesting channel with a finite battery," *IEEE Trans. Inf. Theory*, vol. 62, no. 11, pp. 6436–6458, Nov. 2016.

[9] K. Tutuncuoglu, O. Ozel, A. Yener, and S. Ulukus, "The binary energy harvesting channel with a unit-sized battery," *IEEE Trans. Inf. Theory*, vol. 63, no. 7, pp. 4240–4256, Jul. 2017.

[10] V. Sharma, U. Mukherji, V. Josheph, and S. Gupta, "Optimal energy management policies for energy harvesting sensor nodes," *IEEE Trans. Wireless Commun.*, vol. 9, no. 4, pp. 1326–1336, Apr. 2010.

[11] C. Huang, R. Zhang, and S. Cui, "Optimal power allocation for outage probability minimization in fading channels with energy harvesting constraints," *IEEE Trans. Wireless Commun.*, vol. 13, no. 2, pp. 1074–1087, Feb. 2014.

[12] O. Ozel, K. Tutuncuoglu, J. Yang, S. Ulukus, and A. Yener, "Transmission with energy harvesting nodes in fading wireless channels: Optimal policies," *IEEE J. Sel. Areas Commun.*, vol. 29, no. 8, pp. 1732–1743, Sep. 2011.

[13] M. A. Antepli, E. Uysal-Biyikoglu, and H. Erkal, "Optimal packet scheduling on

an energy harvesting broadcast link," *IEEE J. Sel. Areas Commun.*, vol. 29, no. 8, pp. 1721–1731, Sep. 2011.

[14] J. Yang and S. Ulukus, "Optimal packet scheduling in an energy harvesting communication system," *IEEE Trans. Commun.*, vol. 60, no. 1, pp. 220–230, Jan. 2012.

[15] K. Tutuncuoglu and A. Yener, "Optimum transmission policies for battery limited energy harvesting nodes," *IEEE Trans. Wireless Commun.*, vol. 11, no. 3, pp. 1180–1189, Mar. 2012.

[16] A. Baknina and S. Ulukus, "Optimal and near-optimal online strategies for energy harvesting broadcast channels," *IEEE J. Sel. Areas Commun.*, vol. 34, no. 12, pp. 3696–3708, Dec. 2016.

[17] D. Shaviv and A. Özgür, "Universally near optimal online power control for energy harvesting nodes," *IEEE J. Sel. Areas Commun.*, vol. 34, no. 12, pp. 3620–3631, Dec. 2016.

[18] H. A. Inan and A. Ozgur, "Online power control for the energy harvesting multiple access channel," in *Proc. 14th Int. Symp. on Modeling and Optim. in Mobile, Ad Hoc, and Wireless Networks (WiOpt)*, May 2016, pp. 1–6.

[19] R. Vaze, R. Garg, and N. Pathak, "Dynamic power allocation for maximizing throughput in energy-harvesting communication system," *IEEE/ACM Trans. Netw.*, vol. 22, no. 5, pp. 1621–1630, Oct. 2014.

[20] S. Wei, W. Guan, and K. Liu, "Power scheduling for energy harvesting wireless

communications with battery capacity constraint," *IEEE Trans. Wireless Commun.*, vol. 14, no. 8, pp. 4640–4653, Aug. 2015.

[21] O. Orhan, D. Gündüz, and E. Erkip, "Energy harvesting broadband communication systems with processing energy cost," *IEEE Trans. Wireless Commun.*, vol. 13, no. 11, pp. 6095–6107, Nov. 2014.

[22] C. K. Ho and R. Zhang, "Optimal energy allocation for wireless communication with energy harvesting constraints," *IEEE Trans. Signal Process.*, vol. 60, no. 9, pp. 4808–4818, Sep. 2012.

[23] P. Grover, K. Woyach, and A. Sahai, "Towards a communication-theoretic understanding of system-level power consumption," *IEEE J. Sel. Areas Commun.*, vol. 29, no. 8, pp. 1744–1755, Sep. 2011.

[24] R. Yates and H. Mahdavi-Doost, "Energy harvesting receivers: Packet sampling and decoding policies," *IEEE J. Sel. Areas Commun.*, vol. 33, no. 3, pp. 558–570, Mar. 2015.

[25] A. Arafa and S. Ulukus, "Optimal policies for wireless networks with energy harvesting transmitters and receivers: Effects of decoding costs," *IEEE J. Sel. Areas Commun.*, vol. 33, no. 12, pp. 2611–2625, Dec. 2015.

[26] S. Satpathi, R. Nagda, and R. Vaze, "Optimal offline and competitive online strategies for transmitter-receiver energy harvesting," *IEEE Trans. Inf. Theory*, vol. 62, no. 8, pp. 4674–4695, Aug. 2016.

[27] L. Chen *et al.*, "Range extension of passive wake-up radio systems through energy harvesting," in *Proc. IEEE Int. Conf. on Communications*, Jun. 2013, pp. 1549–1554.

[28] J. Doshi and R. Vaze, "Long term throughput and approximate capacity of transmitter-receiver energy harvesting channel with fading," in *Proc. IEEE ICCS*, Nov 2014, pp. 46–50.

[29] I.-S. Kim, "Nonlinear state of charge estimator for hybrid electric vehicle battery," *IEEE Trans. Power Electron.*, vol. 23, no. 4, pp. 2027–2034, Jul. 2008.

[30] R. Xiong, H. He, F. Sun, and K. Zhao, "Evaluation on state of charge estimation of batteries with adaptive extended Kalman filter by experiment approach," *IEEE Trans. Veh. Technol.*, vol. 62, no. 1, pp. 108–117, Jan. 2013.

[31] N. Michelusi, L. Badia, R. Carli, K. Stamatiou, and M. Zorzi, "Correlated energy generation and imperfect state-of-charge knowledge in energy harvesting devices," Aug. 2012, pp. 401–406.

[32] D. D. Testa and M. Zorzi, "Optimal policies for two-user energy harvesting device networks with imperfect state-of-charge knowledge," in *Proc. IEEE Inf. Theory and Applications Workshop*, Feb. 2014, pp. 1–5.

[33] R. Srivastava and C. E. Koksal, "Basic performance limits and tradeoffs in energy-harvesting sensor nodes with finite data and energy storage," *IEEE/ACM Trans. Netw.*, vol. 21, no. 4, pp. 1049–1062, Aug. 2013.

[34] B. Medepally, N. B. Mehta, and C. R. Murthy, "Implications of energy profile and

storage on energy harvesting sensor link performance," in *Proc. IEEE Globecom*, Dec. 2009, pp. 1–6.

[35] "IEEE standard for local and metropolitan area networks–part 15.4: Low-rate wireless personal area networks (LR-WPANs)," *IEEE Std 802.15.4-2011 (Revision. of IEEE Std 802.15.4-2006)*, pp. 1–314, Sep. 2011.

[36] [Online]. Available: https://www.bluetooth.com/specifications/adopted-specifications

[37] I. Stanojev, O. Simeone, Y. Bar-Ness, and D. Kim, "On the energy efficiency of Hybrid-ARQ protocols in fading channels," in *Proc. IEEE Int. Conf. on Communications*, June 2007, pp. 3173–3177.

[38] T. Chaitanya and E. G. Larrson, "Optimal power allocation for Hybrid ARQ with chase combining in i.i.d. Rayleigh fading channels," *IEEE Trans. Commun.*, vol. 61, no. 5, pp. 1835–1846, May 2013.

[39] P. Frenger, S. Parkvall, and E. Dahlman, "Performance comparison of HARQ with chase combining and incremental redundancy for HSDPA," in *Proc. 54th IEEE Veh. Tech. Conf.*, vol. 3, Fall 2001, pp. 1829–1833.

[40] W. Su, S. Lee, D. A. Pados, and J. D. Matyjas, "Optimal power assignment for minimizing the average total transmission power in hybrid-ARQ Rayleigh fading links," *IEEE Trans. Commun.*, vol. 59, no. 7, pp. 1867–1877, Jul. 2011.

[41] T. Chaitanya and E. Larsson, "Outage-optimal power allocation for Hybrid ARQ

with incremental redundancy," *IEEE Trans. Wireless Commun.*, vol. 10, no. 7, pp. 2069–2074, July 2011.

[42] D. Tuninetti, "Transmitter channel state information and repetition protocols in block fading channels," in *Proc. IEEE Inf. Theory Workshop*, Sep. 2007, pp. 505–510.

[43] G. Caire and D. Tuninetti, "The throughput of hybrid-ARQ protocols for the Gaussian collision channel," *IEEE Trans. Inf. Theory*, vol. 47, no. 5, pp. 1971–1988, Jul. 2001.

[44] P. Wu and N. Jindal, "Coding versus ARQ in fading channels: How reliable should the PHY be?" *IEEE Trans. Commun.*, vol. 59, no. 12, pp. 3363–3374, Dec. 2011.

[45] A. Yadav, M. Goonewardena, W. Ajib, and H. Elbiaze, "Novel retransmission scheme for energy harvesting transmitter and receiver," in *Proc. IEEE ICC*, Jun. 2015, pp. 3198–3203.

[46] Y. Mao, J. Zhang, and K. B. Letaief, "Arq with adaptive feedback for energy harvesting receivers," in *Proc. WCNC*, 2016, pp. 1–6.

[47] [Online]. Available: http://www.impinj.com/

[48] [Online]. Available: http://www.powercastco.com/

[49] J. Lei, R. Yates, and L. Greenstein, "A generic model for optimizing single-hop transmission policy of replenishable sensors," *IEEE Trans. Wireless Commun.*, vol. 8, no. 2, pp. 547–551, Feb. 2009.

[50] C. K. Ho and R. Zhang, "Optimal energy allocation for wireless communications

powered by energy harvesters," in *Proc. IEEE Int. Symp. Inf. Theory*, Jun. 2010, pp. 2368–2372.

[51] C. K. Ho, P. D. Khoa, and P. Ming, "Markovian model for harvested energy in wireless communication," in *Proc. IEEE ICCS*, Nov. 2010, pp. 311–315.

[52] M. Coleman, C. K. Lee, C. Zhu, and W. G. Hurley, "State-of-charge determination from EMF voltage estimation: Using impedance, terminal voltage, and current for lead-acid and lithium-ion batteries," *IEEE Trans. Ind. Electron.*, vol. 54, no. 5, pp. 2550–2558, Oct. 2007.

[53] K. Tutuncuoglu and A. Yener, "Communicating with energy harvesting transmitters and receivers," in *Proc. IEEE Inf. Theory and Applications Workshop*, Feb. 2012, pp. 240–245.

[54] J. Vazifehdan, R. V. Prasad, M. Jacobsson, and I. Niemegeers, "An analytical energy consumption model for packet transfer over the wireless links," *IEEE Commun. Lett.*, vol. 1, no. 1, pp. 30–33, Jan. 2012.

[55] H. Mahdavi-Doost and R. D. Yates, "Energy harvesting receivers: Finite battery capacity," in *Proc. IEEE Int. Symp. Inf. Theory*, Jul. 2013, pp. 1799–1803.

[56] I. Krikidis, T. Charalambous, and J. Thompson, "Buffer-aided relay selection for cooperative diversity systems without delay constraints," *IEEE Trans. Wireless Commun.*, vol. 11, no. 5, pp. 1957–1967, May 2012.

[57] Y. Zhang *et al.*, "A batteryless $19\mu$W MICS/ISM-band energy harvesting body sensor node SoC for ExG applications," *IEEE J. Solid-State Circuits*, vol. 48, no. 1, pp. 199–213, Jan. 2013.

[58] M. K. Sharma and C. R. Murthy, "Transition probabilities for DTMC modeling of dual and mono energy harvesting links," Tech. Rep. [Online]. Available: http://www.ece.iisc.ernet.in/~cmurthy/SPCLab/lib/exe/fetch.php?media=dualehdetails.pdf

[59] S. Sudevalayam and P. Kulkarni, "Energy harvesting sensor nodes: Survey and implications," *IEEE Commun. Surveys Tuts.*, vol. 13, no. 3, pp. 443–461, Third Quarter 2011.

[60] M. Hasan and E. Hossain, "Distributed resource allocation for relay-aided device-to-device communication: A message passing approach," *IEEE Trans. Wireless Commun.*, vol. 13, no. 11, pp. 6326–6341, Nov. 2014.

[61] M. Chiang, C. W. Tan, D. Palomar, D. O'Neill, and D. Julian, "Power control by geometric programming," *IEEE Trans. Wireless Commun.*, vol. 6, no. 7, pp. 2640–2651, Jul. 2007.

[62] "GGPLAB: A simple MATLAB toolbox for geometric programming." [Online]. Available: http://www.stanford.edu/~boyd/ggplab/

[63] M. L. Ku, W. Li, Y. Chen, and K. J. R. Liu, "Advances in energy harvesting communications: Past, present, and future challenges," *IEEE Commun. Surveys Tuts.*, vol. 18, no. 2, pp. 1384–1412, Second Quarter 2016.

[64] A. Goldsmith, *Wireless Communications*.    Cambridge University Press, 2005, cambridge Books Online.

[65] M. Gatzianas, L. Georgiadis, and L. Tassiulas, "Control of wireless networks with rechargeable batteries," *IEEE Trans. Wireless Commun.*, vol. 9, no. 2, pp. 581–593, Feb. 2010.

[66] Q. Tan, Y. Liu, Y. Han, W. An, S. Ci, and H. Tang, "Energy harvesting aware topology control with power adaptation in wireless sensor networks," in *Proc. WCNC*, Apr. 2014, pp. 2722–2727.

[67] I. W. Lai, C. H. Lee, K. C. Chen, and E. Biglieri, "Open-loop end-to-end transmission for multihop opportunistic networks with energy-harvesting devices," *IEEE Trans. Commun.*, vol. 64, no. 7, pp. 2860–2872, Jul. 2016.

[68] C. Tapparello, O. Simeone, and M. Rossi, "Dynamic compression-transmission for energy-harvesting multihop networks with correlated sources," *IEEE/ACM Trans. Netw.*, vol. 22, no. 6, pp. 1729–1741, Dec. 2014.

[69] V. Joseph, V. Sharma, U. Mukherji, and M. Kashyap, "Joint power control, scheduling and routing for multicast in multihop energy harvesting sensor networks," in *Proc. Int. Conf. Ultra Modern Telecommun. Workshops*, Oct. 2009, pp. 1–8.

[70] L. Huang and M. J. Neely, "Utility optimal scheduling in energy-harvesting networks," *IEEE/ACM Trans. Netw.*, vol. 21, no. 4, pp. 1117–1130, Aug. 2013.

[71] S. Chen, P. Sinha, N. B. Shroff, and C. Joo, "A simple asymptotically optimal

joint energy allocation and routing scheme in rechargeable sensor networks," *IEEE/ACM Trans. Netw.*, vol. 22, no. 4, pp. 1325–1336, Aug. 2014.

[72] S. Sarkar, M. H. R. Khouzani, and K. Kar, "Optimal routing and scheduling in multihop wireless renewable energy networks," *IEEE Trans. Autom. Control*, vol. 58, no. 7, pp. 1792–1798, Jul. 2013.

[73] Z. Mao, C. E. Koksal, and N. B. Shroff, "Near optimal power and rate control of multi-hop sensor networks with energy replenishment: Basic limitations with finite energy and data storage," *IEEE Trans. Autom. Control*, vol. 57, no. 4, pp. 815–829, Apr. 2012.

[74] J. A. Paradiso and M. Feldmeier, "A compact, wireless, self-powered pushbutton controller," in *Proc. Int. Conf. Uniquitous Comput.*, 2001, pp. 299–304.

[75] H. Seo and B. G. Lee, "Optimal transmission power for single- and multi-hop links in wireless packet networks with ARQ capability," *IEEE Trans. Commun.*, vol. 55, no. 5, pp. 996–1006, May 2007.

[76] L. Song and N. B. Mandayam, "Hierarchical SIR and rate control on the forward link for CDMA data users under delay and error constraints," *IEEE J. Sel. Areas Commun.*, vol. 19, no. 10, pp. 1871–1882, Oct. 2001.

[77] Q. Liu, S. Zhou, and G. B. Giannakis, "Cross-layer combining of adaptive modulation and coding with truncated ARQ over wireless links," *IEEE Trans. Wireless Commun.*, vol. 3, no. 5, pp. 1746–1755, Sep. 2004.

[78] A. Devraj, M. Sharma, and C. Murthy, "Power allocation in energy harvesting

sensors with ARQ: A convex optimization approach," in *Proc. IEEE GlobalSIP*, Dec. 2014, pp. 208–212.

[79] P. L. Cao, T. J. Oechtering, R. F. Schaefer, and M. Skoglund, "Optimal transmit strategy for MISO channels with joint sum and per-antenna power constraints," *IEEE Trans. Signal Process.*, vol. 64, no. 16, pp. 4296–4306, Aug. 2016.

[80] Y. Dong, F. Farnia, and A. Ozgur, "Near optimal energy control and approximate capacity of energy harvesting communication," *IEEE J. Sel. Areas Commun.*, vol. 33, no. 3, pp. 540–557, Mar. 2015.

[81] J. Xu and R. Zhang, "Throughput optimal policies for energy harvesting wireless transmitters with non-ideal circuit power," *IEEE J. Sel. Areas Commun.*, vol. 32, no. 2, pp. 322–332, Feb. 2014.

[82] R. G. Gallager, *Stochastic Processes: Theory for Applications*. Cambridge University Press, 2014.

[83] D. N. C. Tse, "Variable-rate lossy compression and its effects on communication networks," Ph.D. dissertation, MIT, Cambridge, MA, Cambridge, MA, Sep. 1994. [Online]. Available: http://www.eecs.berkeley.edu/~dtse/pub.html

[84] S. Boyd and L. Vandenberghe, *Convex Optimization*. Cambridge University Press, 2004.